DYNAMICAL SYSTEMS MODELS OF ASSET PRICING

NATASHA KIRBY

Dynamical Systems Models of Asset Pricing

by

©Natasha Kirby

A Thesis Submitted to the School of Graduate Studies in partial fulfillment of the requirement for the degree of Master of Science

Department of Mathematics and Statistics
Memorial University of Newfoundland

July, 2006

St. John's, Newfoundland, Canada

Your file Votre référence
ISBN: 978-0-494-30478-5
Our file Notre référence
ISBN: 978-0-494-30478-5

Abstract

In this thesis we study asset pricing models using a dynamical systems approach. We first review the literature on current dynamical systems models of asset pricing. The foundation of these models is the fact that they incorporate heterogeneous beliefs among traders. Two main trader groups are discussed, fundamental traders and trend–chasing chartists. The theory of discrete dynamical systems, or maps, is also explored, and in depth analysis of these models is carried out. We modify a model of Chiarella, Dieci and Gardini to incorporate a third group of traders called contrarian chartists. The main idea surrounding contrarian chartists is that they not only disagree with the majority of traders, but they choose when to act on the disagreement in order to make a profit. A second case of this model is also discussed, where contrarian chartists are thought to always disagree with the majority. This case reduces to the literature model with one different parameter value. In each case, the model consists of a system of two difference equations. The first equation represents the logarithm of the asset price at any given time t, and the other represents the expectation of price change from one time period to the next. This system exhibits complicated behaviour including local behaviour such as period–doubling and Neimark–Sacker bifurcations as well as local attractors,

global bifurcations and chaos. The results in terms of asset prices are also included for these models. The thesis concludes with some limitations and suggestions for future research.

Acknowledgements

I would first like to thank my supervisor, Dr. Andrew Foster, for working with me on this project. His guidance and insight has been essential, and I appreciate the time he has devoted to leading me in the right direction. I am also grateful for his guidance as my teaching mentor. His confidence in my teaching abilities has helped me succeed in the classroom, and I am grateful to have been given the opportunity to teach during my program. I would like to thank my greatest inspiration, my grandmother, the late Doris Taylor. I thank my parents, Barry and Gloria Kirby, and my sister Trina, for their continuous support . Thank you to the faculty and staff of the Department of Mathematics and Statistics at Memorial University of Newfoundland. Special thanks go to Dwayne Hart of the Mathematics and Statistics department, and the staff at the Digital Media Center, for helping me with various computer tasks. I would like to thank the School of Business at Memorial University of Newfoundland for allowing me to attend the 2004 Northern Finance Association conference and for allowing me to take graduate courses in the Finance department. Thank you to the Atlantic Association for Research in the Mathematical Sciences (AARMS) for allowing me to take graduate courses through their summer school at Dalhousie University. I thank the School of

Graduate Studies for their financial support (George Albert Hatcher Memorial Scholarship and F.A. Aldrich Graduate Award), as well as the Department of Mathematics and Statistics, the School of Graduate Studies, the Faculty of Science and the Graduate Students' Union for travel assistance. I would finally like to thank several students at Memorial University, including Adam Burke, Peter Smith, Heather McIntosh and Jason McGraw.

List of Figures

Contents

Chapter 1

Mathematical Models of Asset Pricing

Asset pricing models are a means by which the abstract states of the world are mapped into the prices of financial assets. These prices are assumed to be endogenous. This means that they are caused by the state of the world as opposed to affecting present and future states of the world. Mathematical models have been developed over time to represent the prices of financial assets such as stocks and bonds. In this chapter, we review the models in current use and the literature on dynamical systems modeling of asset pricing.

1.1 The CAPM

The popular Capital Asset Pricing Model, or CAPM (see [2, 27, 34]) states that the expected return of the ith security, $E(r_i)$, is the sum of the risk free rate, R_f, and the excess market returns multiplied by the beta coefficient of

the ith security. More specifically,

$$E(r_i) = R_f + \beta_i[E(M) - R_f], \tag{1.1.1}$$

where

$$\beta_i = \frac{\text{Cov}[r_i, M]}{\text{V}[M]}. \tag{1.1.2}$$

The CAPM is contained within the series of theoretical propositions labeled Efficient Market Hypothesis (EMH). An efficient market is one where prices reflect all available information. Therefore, prices change only when new information is at hand.

The CAPM has several basic underlying assumptions. One of these assumptions is that investors have homogeneous expectations regarding future prices. In reality however, investors have differing opinions regarding future prices. Thus, an optimal market portfolio may not exist.

The validity of the CAPM has been questioned and tested frequently. Many of these tests concentrate on testing the EMH, while others evaluate the historical usefulness of the CAPM. Over 20 years ago, the first empirical tests on the CAPM were carried out. These tests, using data from the 1930's to the 1960's, were largely supportive of the CAPM as researchers showed that the average return on a portfolio of stocks was positively related to the beta of the portfolio [33]. This supports the CAPM since the quantity $E(M) - R_f$ is positive. Later studies have led to results which are both conflicting and inconclusive due to the nature of the testing. Fama and French [19] recently presented evidence which contradicts the CAPM. A main argument is that the CAPM is very weak over certain time frames. Counterarguments have been made, and it is unclear if their evidence is sufficient to discard the CAPM.

Some people believe it is impossible to accurately test the CAPM since more than one variable is being tested at the same time. One such paper (see [32]) states that it is impossible to accurately test the CAPM since two things are being analyzed simultaneously. The first thing tested is the proposition that the market is an efficient portfolio *a priori*, or prior to (independent of) experience [20]. The second thing being tested is the actual expression of the CAPM. Regressions are performed and certain conditions are checked to see if the CAPM is satisfied.

1.2 Stochastic Models

Stochastic processes have become increasingly important tools to describe the evolution of financial assets. These processes have great potential in describing financial uncertainty, and are able to account for the possibility of extreme events that occur in real markets. The simplest discrete–time stochastic process used to model financial assets is the random walk. This type of model predicts that prices follow random paths with price changes that are unpredictable based on past prices. For example, let us assume that the initial price of an asset is p_0. At time $t = 1$, the asset price either increases by Δp units to a price of p_1, or decreases by Δp units to a price of p_1', where each price change is equally likely to occur (*i.e.,* the probability of each price occurring is 0.5). Continuing, if the price at $t = 1$ is p_1, then at $t = 2$ the price can either increase or decrease by Δp units, each event being equally likely. The same is true if the price at $t = 1$ is p_1'. This process continues for $t = 3$ and so on. This is a standard random walk. These models are appealing due to their

simplicity, however more complicated continuous–time stochastic processes are required in order to accurately measure most asset prices.

Brownian motion is a continuous–time stochastic process. For more information on Brownian Motion, see [1]. Let us assume that the price of a risky asset follows geometric Brownian motion, that is

$$dS_t = \mu S_t dt + \sigma S_t dW_t, \tag{1.2.1}$$

where S_t is the price of the risky asset at time t and W_t is Brownian. The parameter μ is the drift term and the parameter σ is the volatility of the risky asset. Now consider a European call option on the risky asset with strike price K and maturity time T. From this, the famous Black–Scholes model can be derived. This model is used for European call options on stocks which do not pay dividends [3, 30, 35]. The value of the option, $V(S,t)$ at any time from $t = 0$ until maturity is given as

$$V(S,t) = SN(x) - KN(x - \sigma\sqrt{T-t})e^{rt}, \tag{1.2.2}$$

where V is the value of the option at time t, S is the price of the underlying asset at time t, K is the strike price and $N(x)$ is the cumulative normal distribution function with

$$x = \frac{ln(S/K) + (r + 1/2\sigma^2)(T-t)}{\sigma\sqrt{T-t}}.$$

The theory of stochastic differential equations, such as the one given in (1.2.1), is complicated, and simple trading strategies often outperform these stochastic models when they are applied to financial markets [7].

1.3 Dynamical Systems Models

When doubt was cast on the idea that prices of assets are properly modeled as a purely random process, a dynamical systems approach to asset pricing was introduced [7]. A dynamical system is a deterministic model where the value of some function changes with time according to a rule based on past values. These models are typically represented by ordinary differential equations (continuous dynamical systems) or maps (discrete dynamical systems, difference equations). The deterministic component of asset pricing arises when the interaction of different classes of investors is considered. With increased knowledge of the behavior of dynamical systems came the realization that the interaction of investor classes can be expressed as discrete dynamical systems. Despite their appearance of simplicity, these maps have the capacity to exhibit an astonishingly wide range of behavior.

Investors trade due to differences in risk aversion and beliefs about future prices. Traders can be grouped into categories of behavioral types in a number of ways. In these models usually two dominant classes are considered, fundamentalists and chartists. Fundamentalists, or "smart money" traders, base their decisions on the belief that, over time, prices tend to return to their fundamental value. Chartists use technical trading rules to predict future prices. Simple rules, past trends, and extrapolation of data are among some of the tools they use to make their predictions. Several models incorporating heterogeneity have been formulated. Some of these models consider only fundamentalists and "trend chaser" chartists [4, 5, 8, 9, 10, 15, 36] while others also include "contrarian" chartists [6, 12, 13, 14, 16]. While trend chasers make decisions that agree with prevailing wisdom, contrarians make decisions

that often contradict this wisdom.

Some recently published models will be reviewed here to illustrate the dynamical systems approach to asset pricing. The basic assumptions of these models is discussed in this section while the behavior and solution techniques are left for Chapter 3.

1.3.1 Westerhoff's Model

Westerhoff [36] developed an asset pricing model taking into account fundamentalists and trend chasing chartists. The price of an asset at time $t+1$ is dependent upon the excess demand of the speculators in the previous period. If there is indeed excess demand then the price increases.

Let P be the logarithm of the asset price. The change in P at time $t+1$ is proportional to the sum of the orders generated by fundamentalists and chartists, obtaining a map

$$P_{t+1} = P_t + N(D_t^F + D_t^C). \tag{1.3.1}$$

Here N quantifies the aggressiveness of speculators. For instance, if the number of speculators increases over time, then the parameter N will also increase. If the number of speculators decreases, then N will decrease. Note that N must realistically take only positive values.

Expressions can be given for the orders generated by each trader type, based on the beliefs of each group. Since fundamentalists trust that prices converge to their fundamental value over time, D_t^F can be expressed as

$$D_t^F = F - P_t, \tag{1.3.2}$$

where F is the logarithm of the fundamental value of the asset. This value is considered constant and known. Note that the total excess demand for the asset by fundamentalists at time t is given as ND_t^F. If the current price of the asset is larger than the perceived fundamental value then fundamentalists assume that the asset is overpriced, and hence the excess demand for the asset decreases. Likewise, if the current price is smaller than the fundamental price then fundamentalists assume that the asset is underpriced, and hence the demand for the asset increases. If this were the only group of traders present, the asset price in the next period would coincide with this increase or decrease in demand for the asset. However, there exists another group of traders called trend chasing chartists who are also considered in this model.

The orders generated for the asset by trend chasers at time t, denoted D_t^C, is given as

$$D_t^C = (P_t - F)V_{t-1} \tag{1.3.3}$$

where

$$V_{t-1} = N|D_{t-1}^F| + N|D_{t-1}^C|. \tag{1.3.4}$$

Note that the total excess demand for the asset by trend–chasers at time t is ND_t^C. Trend chasers buy when the price is high and sell when the price is low, assuming that prices will continue the upward or downward trend. Thus, if the current price is higher than the fundamental price, the excess demand for the asset increases and vice-versa. In the above equation, V_{t-1} represents the trading volume at time $t-1$. Chartists consider V_{t-1} to provide clues about how reliable their extrapolations may be. More specifically, a high trading volume when current prices exceed the fundamental price causes trend chasers to purchase more of the asset, whereas a low trading volume under the same

condition would cause chartists to purchase less of the asset.

With this, the total excess demand for the asset at time t can be written as

$$\begin{aligned} E_t &= N(D_t^F + D_t^C) \\ &= N(F - P_t + V_{t-1}(P_t - F)), \end{aligned} \tag{1.3.5}$$

and hence the asset price at time $t+1$ can be written as

$$P_{t+1} = P_t + N(F - P_t + V_{t-1}(P_t - F)). \tag{1.3.6}$$

Since the deviation from the fundamental value is of importance, and not the actual fundamental value of the asset, F can be set to zero without loss of generality. Note that since F denotes the logarithm of the fundamental asset price, we are setting the fundamental price to one (rather than zero). Thus, from the above equations we obtain the recurrence relation

$$\begin{cases} P_{t+1} = P_t\,(1 - N + NV_{t-1}) \\ V_t = N|P_t|\,(1 + |V_{t-1}|) \end{cases} \tag{1.3.7}$$

which depends on P_t and V_{t-1}.

The model presented in [36] does not contain equation (1.3.7) and his stated final model is in error (private correspondence). However, his analysis is entirely based upon the defining conditions (1.3.1 - 1.3.4).

1.3.2 Chiarella, Gardini, and Dieci's Model

Chiarella, Gardini, and Dieci [11] developed a more complex model. In addition to considering fundamental traders and trend–chasers, they also take

into account how fundamentalists and chartists adjust to mispricing and past trends, respectively. We will introduce the model by defining the excess demand equations for fundamentalists and trend–chasers, and comparing them to those given in (1.3.2) and (1.3.3).

Fundamentalist demand is defined by

$$D_t^0 = a(W_t - P_t), \tag{1.3.8}$$

where P_t is the logarithm of the asset price at time t and W_t is the logarithm of the fundamental value of the asset at time t. The difference between (1.3.1) and (1.3.8) is that the parameter a has been inserted into the above equation. This parameter represents the strength at which fundamentalists adjust to the difference between the fundamental asset value and the current price. For instance, if the current price of the asset is much higher than the fundamental price, then fundamentalists may react strongly to this price difference and the excess demand for the asset may increase substantially ($a > 1$). The perceived fundamental value is assumed known and constant, and hence W_t can simply be denoted W.

Chartist demand is defined by the following nonlinear function h:

$$d_t = h(\psi_{t,t+1} - g_t). \tag{1.3.9}$$

Here, $\psi_{t,t+1} - g_t$ is called the return differential as $\psi_{t,t+1}$ is the expectation of the price change between the current and next period and g_t is the return on the riskless asset during the same period. The return on the riskless asset is also assumed constant and can be simply denoted by g. The function h is not specific but is rather any function satisfying a set of expected properties

for the return differential. These properties, as given in [11], are listed below (where $x = \psi_{t,t+1} - g$):

1. $h'(x) > 0 \; \forall x$ (the function is increasing everywhere)
2. $h(0) = 0$ (the function passes through the origin)
3. $\exists \; x^*$ such that $h''(x) < 0 \; (> 0) \; \forall x > x^* \; (< x^*)$ (the function is purely concave up (down) when x is smaller than (larger than) some value x^*)
4. $\lim_{x \to \pm\infty} h'(x) = 0$. (the function is bounded above and below as $|x|$ approaches infinity).

The expectation of the price change between time t and $t+1$ is given as

$$\psi_{t,t+1} = \psi_{t-1,t} + c\left(P_t - P_{t-1} - \psi_{t-1,t}\right). \tag{1.3.10}$$

In other words, the expectation of price change is based on the previous expectation, and how close this is to the actual price change from time $t-1$ to time t.

Note that the above properties allow for an arbitrary value $x^* \neq 0$ (*i.e.*, the inflection point in chartist demand can occur at any arbitrary value of the return differential). In all examples and simulations in [11] however, x^* is set to zero. This is since the function being used in this model is

$$h(x) = \alpha \arctan(x).$$

To have $x^* = 0$ means that when the return differential is greater than zero, chartists will always buy up more of the risky asset. Similarly, when the return differential is less than zero, chartists will always sell some of their shares of

the risky asset. Thus, to assume that $x^* = 0$ means that chartists are always making decisions which agree with the current trend. When the expectation of price change exceeds the return on the riskless asset, a buying signal is received, and vice–versa.

The parameter c captures how fast chartists update their estimate of the trend. In reality, it makes sense that $0 < c < 1$. This is since a trend–chaser cannot adjust their estimate of the trend more often than they receive information about price change.

Instead of incorporating the parameters a and c into [36], Westerhoff chose to use only one parameter, namely N, to represent the aggressiveness of all speculators, regardless of their beliefs. Equation (1.3.2) can be rewritten such that it is identical to (1.3.8) (*i.e.*, include the parameter a) and a similar reaction coefficient could have also been incorporated into (1.3.3).

As in [36], the updated asset price is proportional to the sum of the excess demands of fundamentalists and chartists. Thus, the model is as follows:

$$\begin{cases} \psi_{t,t+1} = \psi_{t-1,t} + c\left[(P_t - P_{t-1}) - \psi_{t-1,t}\right] \\ P_{t+1} = P_t + \beta_p \left(a\left(W - P_t\right) + h(\psi_{t,t+1} - g)\right]. \end{cases} \tag{1.3.11}$$

The parameter β_p captures how fast the asset price adjusts to the excess demand. Again, comparing this to [36], it is interesting to note that the total excess demand for the asset at time t, denoted E_t, can be written as $\beta_p E_t$, such that the price adjustment speed is incorporated into (1.3.7).

The system (1.3.11) appears three–dimensional due to the dependence on P_t and P_{t-1} by $\psi_{t,t+1}$. However, it can easily be reduced to the two–dimensional

system below:

$$\begin{cases} \psi_{t,t+1} = (1-c)\psi_{t-1,t} + c\beta_p \left[a(W - P_t) + h(\psi_{t-1,t} - g)\right] \\ P_{t+1} = P_t + \beta_p \left[a(W - P_t) + h(\psi_{t-1,t} - g)\right]. \end{cases} \tag{1.3.12}$$

1.3.3 Chiarella and He's Model

Chiarella and He [12] developed a different model taking into account heterogenous beliefs, risk and learning. The model builds on the framework of [4] by relaxing several of its assumptions. They consider the influence that differing risk attitudes of fundamentalists and chartists have on asset price dynamics. The model is developed as follows.

They begin by considering an asset pricing model with one risk-free asset and one risky asset. A Walrasian scenario is used to derive the demand equation, where a hypothetical market maker matches supply and demand in an environment of perfect competition (perfect information and no transaction costs), and the market finds the price that equates the sum of these demand schedules to the supply. They let R denote the return on the risk-free asset, p_t denote the price per share of the risky asset at time t, and y_t be the stochastic dividend process of the risky asset. Investor wealth at time $t+1$ can be expressed as the sum of the wealth obtained by investing in the risky and riskless assets:

$$W_{t+1} = R(W_t - p_t z_t) + (p_{t+1} + y_{t+1})z_t \tag{1.3.13}$$

$$= RW_t + (p_{t+1} + y_{t+1} - Rp_t)z_t. \tag{1.3.14}$$

Here, z_t represents the number of shares of the risky asset purchased at time t and is required since p_t is the price *per* share. The term $p_{t+1} + y_{t+1} - Rp_t$ is the excess return at time $t+1$ and can simply be denoted R_{t+1}.

At any given time t, information is known about the prices leading up to and including this time. They let $F_t = \{p_t, p_{t-1}, ...; y_t, y_{t-1}, ...\}$ denote this set of information. The conditional expectation and variance at time t of investor wealth, given the information set F_t (typically denoted $E_{ht}[W_{t+1}|F_t]$ and $V_{ht}[W_{t+1}|F_t]$ in standard statistics texts), can be determined. Since there are two (or three) types of investors considered in this model, the authors introduce h to represent each trader type. Note that the expectation of a sum is the sum of the expectations (*i.e,* $E[aX + b] = aE[X] + b$) and $V[aX + b] = a^2V[X]$. The same rules apply to conditional expectation and variance. Thus, we get that

$$\begin{aligned} E_{ht}[W_{t+1}|F_t] &= RW_t + z_t E_{ht}[R_{t+1}|F_t] \\ V_{ht}(W_{t+1}) &= z_t^2 V_{ht}[R_{t+1}] \end{aligned} \tag{1.3.15}$$

Now, different investors have differing opinions toward risk. These differing attitudes can be characterized by a coefficient of risk aversion a_h (*i.e.,* a trader of type h has a risk aversion a_h). The number of shares of the risky asset purchased by trader type h at time t is denoted z_{ht} and is dependant upon this coefficient. It satisfies the equation

$$z_{ht} = \frac{E_{ht}[R_{t+1}|F_t]}{a_h V_{ht}[R_{t+1}|F_t]}. \tag{1.3.16}$$

An important difference between this model and the other models discussed is that the proportion of investors in this case is not fixed. Thus, at time t, a certain number of investors of type h will exist. More specifically, a fraction of the total investors will be fundamental traders, and the remaining investors will be chartists. The fraction of trader type h existing in the market at time

t is denoted n_{ht}. Certainly, $\sum_h n_{ht} = 1$. Thus, the equilibrium of supply and demand (where supply of outside shares is assumed to be zero in this case) is given as

$$\sum_h n_{h,t-1} \frac{E_{ht}[R_{t+1}|F_t]}{a_h V_{ht}[R_{t+1}|F_t]} = 0. \tag{1.3.17}$$

As in previous models, fundamentalists believe that prices eventually return to some fundamental value. In this model, this price is denoted p_t^*. Let x_t represent the difference between the price per share and the fundamental price:

$$x_t = p_t - p_t^*.$$

Following the work of Brock and Hommes [4, 5, 6], two assumptions are made about the deviation of the price per share of the risky asset at time t (p_t) from the fundamental price p_t^*.

Assumption 1.3.1. *Each group of traders predict the expectation of price in two components, with everyone agreeing on the first component, and disagreeing on the second component (an "agent specific prediction component"). Mathematically, the assumption is the following:*

$$E_{ht}[p_{t+1} + y_{t+1}] = \underbrace{E_t[p_{t+1}^* + y_{t+1}]}_{fundamental} + \underbrace{f_{h,t}}_{agent\ specific} \tag{1.3.18}$$

with $f_{h,t} = f_h(x_{t-1}, ..., x_{t-L})$, L being a positive integer.

Assumption 1.3.2. *Each group of agents predict the variance of price in two components, a fundamental component (σ^2) which everyone agrees on, and an "agent specific prediction component." Mathematically, the assumption is the*

following:

$$V_{ht}[p_{t+1} + y_{t+1}] = \underbrace{V_t[p^*_{t+1} + y_{t+1}]}_{fundamental} + \underbrace{g_{h,t}}_{agent\ specific} \quad (1.3.19)$$

$$V_t[p^*_{t+1} + y_{t+1}] = \sigma^2 \quad (1.3.20)$$

with $g_{h,t} = g_h(x_{t-1}, ..., x_{t-L})$ *[12].*

Using these assumptions and 1.3.15 the expected excess return and variance are given as

$$E_{h,t}[R_{t+1}] = f_{h,t} - Rx_t \quad (1.3.21)$$

$$V_{ht}[R_{t+1}] = \sigma^2 + g_{h,t}, \quad (1.3.22)$$

repectively. These equations can now be substituted into (1.3.17) to obtain

$$R\left[\sum_h \frac{n_{h,t-1}}{a_h(\sigma^2 + g_{h,t})}\right] x_t = \sum_h \frac{n_{h,t-1} f_{h,t}}{a_h(\sigma^2 + g_{h,t})}. \quad (1.3.23)$$

R_{t+1} can be rewritten as follows:

$$R_{t+1} = x_{t-1} - Rx_t + \delta_{t+1}. \quad (1.3.24)$$

Here, $\delta_{t+1} = p^*_{t+1} + y_{t+1} - E_t[p^*_{t+1} + y_{t+1}]$ is a Martingale Difference Sequence with respect to the information set F_t. A stochastic series (in this case δ) is a Martingale Difference Sequence if its expectation with respect to another stochastic series (in this case F_t) is zero, (*i.e.*, $E[\delta_{t+1}|F_t] = 0\ \forall\ t$).

Now, each trader type will have a realized profit $\pi_{h,t}$ at time t given by

$$\pi_{h,t} = R_{t+1} z_{ht}. \quad (1.3.25)$$

The authors consider a weighted average of realized profits at time t, U_{ht}, which depends on the weighted average and realized profit in the previous

period. In addition, the parameter η is inserted into the equation, where η represents the memory strength of traders over time. This can be written as

$$U_{ht} = \pi_{h,t} + \eta U_{h,t-1}. \tag{1.3.26}$$

The weighted average is necessary when formulating an expression for the fraction of traders of type h. The fraction of traders of type h at time t are decided using discrete choice probability (see [4] for details on this method). Basically, traders are making decisions concerning trader groups based on how attractive it is to be in a different group at a certain time. Thus, the fraction of each trader type, denoted n_{ht} is defined by

$$n_{ht} = \exp\left[\frac{\beta U_{h,t-1}}{\sum_h \exp[\beta U_{h,t-1}]}\right]. \tag{1.3.27}$$

In this equation, $\beta > 0$ represents the intensity of choice, which captures the sensitivity of agents to switch from one trading strategy to another. The larger β becomes, the more agents will choose the strategy with the highest fitness. If $\beta = 0$ then agents are indifferent and hence there is an even split among strategies. In similar models [4, 5] this is often considered the most important parameter of the model.

Rearranging equation (1.3.23), the following system is obtained:

$$\begin{cases} Rx_t = \dfrac{\sum_h \dfrac{n_{h,t-1}}{a_h(\sigma^2 + g_{h,t})}}{\sum_h \dfrac{n_{h,t-1} f_{h,t}}{a_h(\sigma^2 + g_{h,t})}} \\ n_{ht} = \exp\left[\dfrac{\beta U_{h,t-1}}{\sum_h exp[\beta U_{h,t-1}]}\right] \end{cases} \tag{1.3.28}$$

The different risk attitudes and learning schemes of investors has not yet been deeply explored. The next step in the development of the model is

to consider these aspects when there are both fundamentalists and chartists present. It is assumed that beliefs follow a linear return and nonlinear variance as shown below [12]:

$$\bar{x}_t = \frac{1}{L}\sum_{i=1}^{L} x_{t-i}, \tag{1.3.29}$$

$$\bar{\sigma}_t^2 = \frac{1}{L}\sum_{i=1}^{L}[x_{t-i} - \bar{x}_t]^2. \tag{1.3.30}$$

The two assumptions made earlier can be made more concise. The term f_{ht}, representing the agent specific component of the mean, can be written as

$$f_{ht} = d_h \bar{x}_t, \tag{1.3.31}$$

where d_h is the trend of trader type h. The agent specific component of the variance, g_{ht} can be written as

$$g_{ht} = \sigma^2 v_h(\bar{\sigma}^2), \tag{1.3.32}$$

where $v_h(\sigma^2) = \mu\left[1 - \frac{1}{(1+\sigma^2)\xi}\right]$. μ and ξ are positive constants, and this function is used in order to obtain upper and lower bounds on the variance estimate by fundamentalists [12].

When $d_h = 0$ the first assumption captures the beliefs on return of the fundamentalists. This is due to the consistency in their beliefs. Otherwise, the beliefs on return of the chartists are captured. Thus, if we assume that Type 1 investors are fundamentalists and Type 2 investors are chartists, we can set $d_2 = d$. The value of d is directly proportional to the amount in which chartists use trends to predict future prices.

The authors let $\eta = 0$, $\delta_t = 0$ and C represent the cost incurred by the fundamentalists in each period to obtain past information, including market equilibrium equations and the fractions of all other traders involved. Finally, set $a = a_2/a_1$ and $m_t = n_{1,t} - n_{2,t}$. Thus the system can be reduced to

$$\begin{cases} x_{t+1} = \dfrac{d}{R}\dfrac{(1+v_h(\bar{\sigma}_t^2))(1-m_t)}{a(1+m_t)+(1+v_h(\bar{\sigma}_t^2))(1-m_t)}\bar{x}_t \\ m_{t+1} = \tanh\left[\dfrac{\beta}{2a_1\sigma^2}(Rx_t - x_{t+1})\left(\dfrac{Rx_t}{1+v_h(\bar{\sigma}_t^2)} + \dfrac{d\bar{x}_t - Rx_t}{a}\right) - \dfrac{\beta C}{2}\right]. \end{cases} \tag{1.3.33}$$

A special case of this model occurs when $L = 1$. Thus, it follows that $\bar{x}_t = x_{t-1}$, $\bar{\sigma}_t^2 = 0$, and $v_h(\bar{\sigma}_t^2) = 0$. The model is then reduced to:

$$\begin{cases} x_{t+1} = \dfrac{d}{R}\dfrac{(1-m_t)}{a+1+(a-1)m_t}x_t \\ m_{t+1} = \tanh\left[\dfrac{\beta}{2a_1\sigma^2}(Rx_t - x_{t+1})\left(Rx_t + \dfrac{dx_{t-1} - Rx_t}{a}\right) - \dfrac{\beta C}{2}\right]. \end{cases} \tag{1.3.34}$$

This model is much more complicated than [11, 36] since it not only incorporates heterogeneous beliefs, but also incorporates risk and learning strategies. It is three dimensional due to dependance on x_t and x_{t-1} by m_{t+1}, and is hence less mathematically tractable since the theory is not as well known for three dimensional maps. The behaviour of all three maps will be discussed in Chapter 3.

Chapter 2

Dynamical Systems Theory

In this Chapter, the necessary definitions and theorems for studying maps will be reviewed. Analysis of dynamical systems models in general involves both bifurcation theory and graphical tools. The object of bifurcation theory is to study the changes that maps undergo as parameter values change. For more details concerning the basic definitions and theory of maps as dynamical systems see standard texts such as [17, 24, 31].

2.1 Fixed Points and Stability

We will first look at some basic notions concerning maps, including the definition of a fixed point, as well as the stability of a fixed point. In general, a map can be expressed as

$$\mathbf{x} \mapsto \mathbf{f}(\mathbf{x}), \tag{2.1.1}$$

where $\mathbf{x} \in \mathbb{R}^n$ is a vector, $\mathbf{f} : \mathbb{R}^n \to \mathbb{R}^n$ is a vector valued function, and $\mathbf{x}_{n+1} = \mathbf{f}(\mathbf{x}_n)$ for all n.

Definition 2.1.1. *An orbit is a sequence of vectors generated by iterating a map,* i.e., $\mathbf{x}_1, \mathbf{x}_2, \mathbf{x}_3, ..., \mathbf{x}_n, ...$.

Definition 2.1.2. *A point* $\bar{\mathbf{x}}$ *is said to be a fixed point of (2.1.1) if* $\bar{\mathbf{x}} = \mathbf{f}(\bar{\mathbf{x}})$ *[24]. In other words, fixed points are those* $\mathbf{x}$ *values which do not change with time and hence satisfy* $\mathbf{x}_{t+1} = \mathbf{x}_t$ *for all* t.

Often when analyzing maps, as we will see in Chapters 3 and 4, the fixed points corresponding to some iterate of a map is of great importance. Thus, we proceed with the definition of a periodic point.

Definition 2.1.3. *A point* $\bar{\mathbf{x}}$ *is said to be a periodic point of (2.1.1) if* $\bar{\mathbf{x}} = \mathbf{f}^n(\bar{\mathbf{x}})$. *Thus a periodic point of 2.1.1 corresponds to a fixed point of the nth iterate map* $\mathbf{x} \rightarrow \mathbf{f}^n(\mathbf{x})$. *The point* $\bar{\mathbf{x}}$ *has minimal period* n *if* n *is the least positive integer such that the above condition is satisfied. The set of all iterates of a periodic point is called a periodic orbit [24]. A periodic orbit of minimal period* n *is often called a period–*n *cycle.*

The concept of stability is the same for a fixed point or a periodic point. We will continue by defining what we mean by a stable (or unstable) fixed point.

Definition 2.1.4. *A fixed point* $\bar{\mathbf{x}}$ *is called stable if* $\forall \epsilon > 0$, $\exists \delta > 0$ *such that,* $\forall \tilde{\mathbf{x}}$ *and* $\forall n \geq 0$, *if* $||\tilde{\mathbf{x}} - \bar{\mathbf{x}}|| < \delta$ *then* $||\mathbf{f}^n(\tilde{\mathbf{x}}) - \bar{\mathbf{x}}|| < \epsilon$. *A fixed point is called asymptotically stable if, in addition to the above condition,* $\exists r > 0$ *such that* $\mathbf{f}^n(\tilde{\mathbf{x}}) \rightarrow \bar{\mathbf{x}}$ *as* $n \rightarrow \pm\infty$ $\forall \tilde{\mathbf{x}}$ *satisfying* $||\tilde{\mathbf{x}} - \bar{\mathbf{x}}|| < r$. *A fixed point is unstable if it is not stable [24].*

In most situations it is not necessary to use Definition 2.1.4 to determine the stabilities of fixed points. Instead, we use the convenient theorem which is given below.

Theorem 2.1.1. *Let* $\mathbf{f}(\mathbf{x})$ *be a* C^1 *function with fixed point* $\bar{\mathbf{x}}$ *and let* $J(\bar{\mathbf{x}})$ *be the Jacobian matrix, an* $n \times n$ *matrix of partial derivatives where* n *is the dimension of the system, corresponding to (2.1.1). In other words,*

$$J(\bar{\mathbf{x}}) = \begin{bmatrix} \partial f_1/\partial x_1 & \partial f_1/\partial x_2 & \cdots & \partial f_1/\partial x_n \\ \partial f_2/\partial x_1 & \partial f_2/\partial x_2 & \cdots & \partial f_2/\partial x_n \\ \vdots & \vdots & \vdots & \vdots \\ \partial f_n/\partial x_1 & \partial f_n/\partial x_2 & \cdots & \partial f_n/\partial x_n \end{bmatrix}, \tag{2.1.2}$$

evaluated at $\bar{\mathbf{x}}$.

1. *If the eigenvalues, denoted* λ_1, λ_2, ..., λ_n, *of the Jacobian matrix have moduli less than one, then the fixed point* $\bar{\mathbf{x}}$ *is asymptotically stable.*

2. *If at least one of the eigenvalues has modulus greater than one, then* $\bar{\mathbf{x}}$ *is unstable [24].*

The eigenvalues of $J(\bar{\mathbf{x}})$ are found by solving the following equation (called the characteristic equation) for λ:

$$\begin{vmatrix} \frac{\partial f_1}{\partial x_1}(\bar{\mathbf{x}}) - \lambda & \frac{\partial f_1}{\partial x_2}(\bar{\mathbf{x}}) & \cdots & \frac{\partial f_1}{\partial x_n}(\bar{\mathbf{x}}) \\ \frac{\partial f_2}{\partial x_1}(\bar{\mathbf{x}}) & \frac{\partial f_2}{\partial x_2}(\bar{\mathbf{x}}) - \lambda & \cdots & \frac{\partial f_2}{\partial x_n}(\bar{\mathbf{x}}) \\ \vdots & \vdots & \vdots & \vdots \\ \frac{\partial f_n}{\partial x_1}(\bar{\mathbf{x}}) & \frac{\partial f_n}{\partial x_2}(\bar{\mathbf{x}}) & \cdots & \frac{\partial f_n}{\partial x_n}(\bar{\mathbf{x}}) - \lambda \end{vmatrix} = 0. \tag{2.1.3}$$

Theorem 2.1.1 is only useful when the eigenvalues of the Jacobian matrix do not have a modulus of one. Thus, we may classify fixed points in terms of these eigenvalues, which is done in the following definition.

Definition 2.1.5. *A fixed point $\bar{\mathbf{x}}$ is said to be hyperbolic if the Jacobian matrix has no eigenvalues with modulus one. If at least one eigenvalue of the Jacobian matrix has modulus one, then the fixed point $\bar{\mathbf{x}}$ is said to be nonhyperbolic [24].*

Note that if a fixed point is nonhyperbolic, its stability cannot be determined from the eigenvalues of the Jacobian matrix.

2.2 Bifurcations

Bifurcations occur in the vicinity of nonhyperbolic fixed points. In this section, the definitions and theorems related to the bifurcations occuring in the models derived in the previous Chapter will be reviewed. First, however, a basic definition of a bifurcation is given.

Definition 2.2.1. *A bifurcation is a change in the qualitative behavior of a system that occurs due to a small change in a parameter value.*

The local bifurcations occuring in the maps discussed in this thesis are saddle–node bifurcations, transcritical bifurcations, pitchfork bifurcations, period–doubling bifurcations, and Neimark–Sacker bifurcations. They are all examples of codimension–one bifurcations. These bifurcations will now be described in more detail.

Definition 2.2.2. *In a saddle–node bifurcation, a pair of fixed points, one which is stable and the other which is unstable, are created. For parameter*

values less than the bifurcation value, no fixed points exist. As the parameter passes through the bifurcation value, two fixed points appear, one being a stable fixed point and the other an unstable fixed point.

Definition 2.2.3. *In a transcritical bifurcation, two fixed points meet and exchange stability. The stable fixed point becomes unstable, and the unstable fixed point becomes stable.*

Definition 2.2.4. *A supercritical pitchfork bifurcation is the bifurcation of a stable fixed point into two new stable fixed points. The new fixed points occur for parameter values where the original fixed point is unstable. A subcritical pitchfork bifurcation is the bifurcation of an unstable fixed point into two new unstable fixed points. The new fixed points occur for parameter values where the original fixed point is stable [24].*

Definition 2.2.5. *A supercritical period–doubling bifurcation is the bifurcation of a stable fixed point into a stable periodic orbit with period–2. The new period–2 orbit occurs for parameter values where the original fixed point is unstable. A supercritical period–doubling cascade occurs when each of the stable period–2 orbits undergo period–doubling bifurcations (to obtain a stable periodic orbit of period–4) and so on.*

Definition 2.2.6. *A supercritical Neimark–Sacker bifurcation occurs when a stable invariant circle is born as an attracting (stable) fixed point becomes repelling (unstable) [17]. The invariant circle appearing in the Neimark–Sacker bifurcation is called a limit cycle.*

The saddle–node bifurcation is sometimes referred to as a "fold" or "tangent" bifurcation. The period–doubling bifurcation is sometimes called a "flip"

bifurcation. The Neimark–Sacker bifurcation is called "Hopf" or "Neimark–Hopf" bifurcation in some literature.

The following results can be used to identify the codimension–one bifurcations occuring in the planar maps discussed in this thesis.

Theorem 2.2.1. *1. If $|\lambda_1| < 1$ and λ_2 changes from $|\lambda_2| < 1$ to $\lambda_2 > 1$ then generically a saddle–node bifurcation occurs at $\lambda_2 = 1$. If special symmetry occurs in the system, a transcritical bifurcation, or a pitchfork bifurcation may occur.*

2. If $|\lambda_1| < 1$ and λ_2 changes from $|\lambda_2| < 1$ to $\lambda_2 < -1$ then generically a period–doubling bifurcation occurs at $\lambda_2 = -1$.

3. If $\lambda_{1,2} = a \pm bi$ and $r = \sqrt{a^2 + b^2}$ changes from $r < 1$ to $r > 1$ then generically a Neimark–Sacker bifurcation occurs at $r = 1$. This is only true if there are no resonance terms, i.e., *$\lambda^k(\mu_0) \neq 1$, where μ_0 is the parameter value correponding to $r = 1$, for $k = 1, 2, 3, 4$.*

There are also global bifurcations occuring in the maps discussed in this thesis. Global bifurcations are not merely the result of changes in the stability of a fixed point.

Definition 2.2.7. *An attractor is a set of points towards which neighboring points approach as a map is iterated. Examples of simple attractors are stable fixed points, periodic orbits and limit cycles. More complicated attractors are stable quasiperiodic and chaotic sets.*

Definition 2.2.8. *The basin of attraction of an attractor is the closure of the set of initial conditions which are attracted to that particular attractor [31]. The closure of a set A is the smallest set which contains A.*

Definition 2.2.9. *A chaotic map possesses three ingredients: unpredictability (due to sensitivity of initial conditions), indecomposability (it cannot be broken down into subsystems), and an element of regularity (intermingling of periodic and aperiodic trajectories) [17].*

Definition 2.2.10. *A boundary crisis occurs when the basin boundary of a chaotic attractor collides with an unstable orbit, causing the destruction of the chaotic attractor [22].*

Definition 2.2.11. *An interior crisis occurs when there is a collision between an unstable orbit and a chaotic attractor within the basin of attraction, causing a sudden change in the size of the attractor [22].*

The global bifurcations observed in this thesis are generally "contact bifurcations" such as these, where the basin boundary of a stable attractor (or attractors) collides with an unstable orbit, causing a sudden change in the attractor. For example, in the behaviour of the model in Section 3.1, two limit cycles intersect simultaneously with an unstable fixed point at the origin. A "figure–eight" structure is formed at this bifurcation value, followed by a merging and overlapping of the limit cycles into a single chaotic attractor as the parameter value is increased. The bifurcation can be labeled a "symmetric figure–eight homoclinic bifurcation" [26].

Bifurcation theory involving maps with dimension higher than two is much more complicated, and we rely heavily on graphical tools to investigate the behaviour of these systems. The model given in (1.3.34) is three–dimensional, and hence these graphical tools are necessary in this case.

All three models discussed in Chapter 1 can be enriched by being portrayed through these special graphing techniques. They allow readers to obtain a

clearer image of the behaviour occuring in these systems as parameter values change. These graphs are discussed below, and are crucial in Chapters 3 and 4.

Definition 2.2.12. *An Orbit Diagram is a plot of a parameter (on the x-axis) and the iterates, after transients, of a map (on the y-axis). It is simply a record of the stable solutions for any choice of parameters [18].*

Definition 2.2.13. *A Bifurcation Diagram is the plot of the location of fixed points, along with their stabilities, versus a chosen parameter. Stable fixed points are shown as solid curves, and the unstable fixed points are shown as dashed curves.*

Although these are the main graphical tools we rely on when analyzing (1.3.7), (1.3.12) and (1.3.34), there are other diagrams that aid the analysis. Before these are discussed, some important definitions are reviewed.

Definition 2.2.14. *Liapunov exponents are a measure of how fast, on average, two neighboring trajectories move away from each other. If the maximal Liapunov exponent, denoted ω, is negative, then the attractor is a stable fixed point or periodic orbit. If $\omega = 0$ then the attractor may be a quasiperiodic orbit. If ω is positive then the attractor is chaotic.*

Computer software can easily plot the maximal Liapunov exponent as a parameter is varied. From this diagram it can be determined if a system is chaotic, and it can also indicate where possible bifurcations occur (when $\omega = 0$).

Definition 2.2.15. *A basin diagram is a grid of initial conditions, where each point on the grid (*i.e., *each initial condition) is assigned a color based on an*

algorithm. First, a number of "trial" initial conditions are randomly selected, and as their trajectories converge to an attractor (or tend to infinity) points are drawn in the limit set on the grid. If more than one attractor exists, the basin for each attractor is plotted with a different color.

Programs written in C, as well as XPPAUT [18] were used in this thesis for plotting Liapunov exponents, orbit diagrams and bifurcation diagrams. MAPPER [25] and iDMC [29] were used to plot basin diagrams and orbits of planar maps (phase–diagrams) and two–parameter bifurcation diagrams.

Chapter 3

Analysis of Current Models

In this chapter, we will use the definitions and theorems from Chapter 2 in order to analyze the maps discussed in Chapter 1. The model results are then discussed in terms of asset prices.

3.1 Westerhoff's Model

Westerhoff's model (1.3.7) can also be written as the following two–dimensional map:

$$\begin{aligned} P &\mapsto P(1-N+NV) \\ V &\mapsto N|P|(1+V). \end{aligned} \tag{3.1.1}$$

To find the fixed points of the map, we solve the following system:

$$\begin{aligned} \bar{P} &= \bar{P}(1-N+N\bar{V}) \\ \bar{V} &= N|\bar{P}|(1+\bar{V}) \end{aligned} \tag{3.1.2}$$

This map has three fixed points, as indicated below:

$$(\bar{P}, \bar{V}) = (0,0) \tag{3.1.3}$$

$$(\bar{P}, \bar{V}) = \left(\frac{1}{2N}, 1\right) \tag{3.1.4}$$

$$(\bar{P}, \bar{V}) = \left(\frac{-1}{2N}, 1\right). \tag{3.1.5}$$

The stability of these fixed points can be determined from the eigenvalues of the Jacobian matrix. Since the partial derivatives of (1.3.7) involve absolute values, we must consider two cases. The first case is when $P > 0$. The Jacobian matrix corresponding to $P > 0$ is

$$J_1 = \begin{bmatrix} 1 - N + NV & NP \\ N + NV & NP \end{bmatrix}. \tag{3.1.6}$$

If $P < 0$, then the Jacobian matrix is

$$J_2 = \begin{bmatrix} 1 - N + NV & NP \\ -N - NV & -NP \end{bmatrix}. \tag{3.1.7}$$

Now we must substitute each fixed point into the proper matrix and find the corresponding eigenvalues. In the limit as $(P, V) \to (0,0)$, the Jacobian corresponding to the fixed point at the origin is

$$J(0,0) = \begin{bmatrix} 1 - N & 0 \\ \pm N & 0 \end{bmatrix}. \tag{3.1.8}$$

The eigenvalues are found by solving

$$\begin{vmatrix} 1 - N - \lambda & 0 \\ \pm N & -\lambda \end{vmatrix} = 0. \tag{3.1.9}$$

Two eigenvalues result, namely $\lambda_1 = 0$ and $\lambda_2 = 1 - N$.

Stability results can be obtained from these eigenvalues using Theorem 2.1.1. For instance, the fixed point $(0,0)$ is asymptotically stable when $|\lambda_1| < 1$ and $|\lambda_2| < 1$. Since $\lambda_1 = 0$ it is always less than one, we must determine when $|\lambda_2| < 1$. This is equivalent to solving the inequality $-1 < 1 - N < 1$. Thus, $|\lambda_2| < 1$ when $0 < N < 2$, and hence $(0,0)$ is asymptotically stable when $0 < N < 2$ and is unstable when $N > 2$.

We now set the absolute value of the eigenvalues equal to one. This is since we are interested in nonhyperbolic fixed points, as mentioned in Chapter 2. The parameter values for which the eigenvalues equal one indicate where possible changes in stability occur, and hence give the possible bifurcation values of the system. For the fixed point at the origin, the values of N which correspond to $\lambda_2 = 1 - N = \pm 1$ are $N = 0$ and $N = 2$. Thus, we possibly have bifurcations occuring at these values.

Using Theorem 2.2.1 we can identify the bifurcations occuring at these parameter values. Since $|\lambda_1| < 1$ and λ_2 changes smoothly from $|\lambda_2| < 1$ to $\lambda_2 < -1$ as N increases through 2, a period–doubling bifurcation occurs at $\lambda_2 = -1$. It can be shown that the bifurcation at $N = 0$ is a transcritical bifurcation, however this is insignificant since N is restricted to be non-negative in this model.

A similar process is carried out for the fixed point given in (3.1.4). Substituting this value into J_1 (since $P = 1/2N$ is positive) yields

$$J_1\left(\frac{1}{2N}, 1\right) = \begin{bmatrix} 1 & 1/2 \\ 2N & 1/2 \end{bmatrix}. \tag{3.1.10}$$

The eigenvalues are found by solving

$$\begin{vmatrix} 1-\lambda & 1/2 \\ 2N & 1/2-\lambda \end{vmatrix} = 0. \tag{3.1.11}$$

The eigenvalues are found to be $\lambda_{1,2} = 3/4 \pm \sqrt{1/16 + N}$.

Again, the fixed point $(1/2N, 1)$ is asymptotically stable when $|\lambda_1| < 1$ and $|\lambda_2| < 1$. It can be shown however that $\lambda_1 > 1$ for all $N > 0$. It can also be shown that $|\lambda_2| > 1$ when $N > 3$, however due to the condition on λ_1 the fixed point $(1/2N, 1)$ is unstable for all positive N. Since no changes in stability occur as the parameter N changes, no new bifurcation values result.

Finally, the fixed point given in (3.1.5) is examined. Substituting this value into J_2 (since $P = -1/2N$ is negative) yields

$$J_2\left(\frac{-1}{2N}, 1\right) = \begin{bmatrix} 1 & -1/2 \\ -2N & 1/2 \end{bmatrix}. \tag{3.1.12}$$

The eigenvalues are found by solving

$$\begin{vmatrix} 1-\lambda & -1/2 \\ -2N & -1/2-\lambda \end{vmatrix} = 0. \tag{3.1.13}$$

The characteristic equation in this case is identical to the one obtained using (3.1.4). Thus, the same eigenvalues result, and the same stability results are obtained. No new bifurcation values result due to the instability of this fixed point for all values of N.

Figure 3.1 is the orbit diagram corresponding to (1.3.7). From this figure it is evident that if $0 < N < 2$ then prices converge to their fundamental value. If $N > 2$ then prices switch between two values, one that is lower and

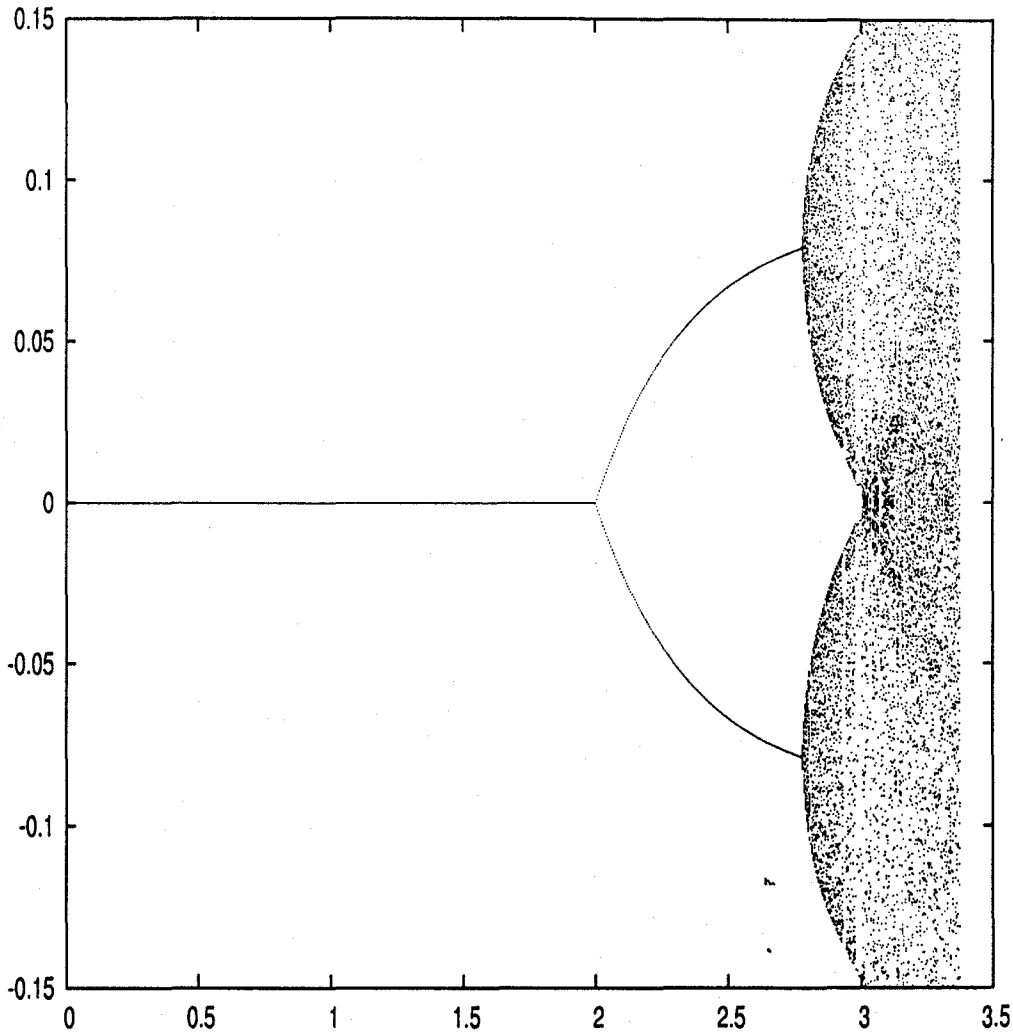

Figure 3.1: Orbit Diagram corresponding to Westerhoff's Model

another that is higher than the fundamental value. At $N \approx 2.8$, a Neimark–Sacker bifurcation occurs for each of the points of the period–2 cycle. Instead of prices switching between two points, they now switch between two limit cycles. We can prove the existence of these Neimark–Sacker bifurcations using the second iterate of the map:

$$\begin{aligned} P &\mapsto P(1-N+NV)(1-N+N^2|P|(1+V)) \\ V &\mapsto N(|P(1-N+NV)|(1+N|P|(1+V)). \end{aligned} \tag{3.1.14}$$

These fixed points of the second iterate correspond to fixed points or to components of period–2 cycles in the original map. The period–2 fixed points are found by solving the following system:

$$\begin{aligned} \bar{P} &= \bar{P}(1-N+N\bar{V})(1-N+N^2|\bar{P}|(1+\bar{V})) \\ \bar{V} &= N(|\bar{P}(1-N+N\bar{V})|(1+N|\bar{P}|(1+\bar{V})). \end{aligned} \tag{3.1.15}$$

Now, since solving this system involves absolute values, we must consider four cases. The first is the case when $P > 0$ and $1 - N + NV < 0$. Thus, rather than solve the above system, we solve the following system:

$$\begin{aligned} \bar{P} &= \bar{P}(1-N+N\bar{V})(1-N+N^2\bar{P}(1+\bar{V})) \\ \bar{V} &= -NP(1-N+N\bar{V})(1+N\bar{P}(1+\bar{V})). \end{aligned} \tag{3.1.16}$$

In other words, using the first equation in (3.1.16) we get that

$$\bar{P} = 0 \tag{3.1.17}$$

or

$$\bar{P} = \frac{2-N+N\bar{V}-\bar{V}}{N(1+\bar{V})(1-N+N\bar{V})}. \tag{3.1.18}$$

We can then put these $\bar{P}$ values into the second equation in (3.1.16), solve for $\bar{V}$, and simplify both equations. When $\bar{P} = 0$ we get $\bar{V} = 0$, *i.e.*, a period–1 fixed point. When $\bar{P}$ is the latter of the two expressions, we obtain the following period–2 fixed point:

$$(\bar{P}, \bar{V}) = \left(\frac{N-2}{2N(N-1)}, \frac{N-2}{N} \right). \tag{3.1.19}$$

This period–2 fixed point exists for $N \geq 2$.

Stability analysis of (3.1.19) is carried out in the usual way. Since the derivatives of the the second iterate of the map are more complicated, we rely on computer software to compute these derivatives and solve the characteristic equation.

The eigenvalues obtained from the characteristic equation are as follows:

$$\lambda_{1,2} = -\frac{8N^3 - 37N^2 + 52N - 24}{8(N^2 - 2N + 1)} \pm \frac{\sqrt{512 - 2048N + 3248N^2 - 2536N^3 + 969N^4 - 144N^5}}{8(N^2 - 2N + 1)}.$$

When $N \geq 2$, these eigenvalues are complex conjugate. Thus, a Neimark–Sacker bifurcation will occur if $r = \sqrt{a^2 + b^2}$ passes smoothly through $r = 1$. Solving for N when $r = 1$ gives us

$$N^* = \frac{7 + \sqrt{17}}{4} \approx 2.78. \tag{3.1.20}$$

Testing the non–resonance conditions of the Neimark–Sacker bifurcation at this value N^* yields

$$\begin{aligned} \lambda^1(N^*) &\approx -0.257 \pm 0.966i \\ \lambda^2(N^*) &\approx -0.868 \pm 0.496i \\ \lambda^3(N^*) &\approx 0.703 \pm 0.711i \\ \lambda^4(N^*) &\approx 0.507 \pm 0.862i \end{aligned}$$

so that $\lambda^k(N^*) \neq 1$, $k = 1, 2, 3, 4$. Also

$$\frac{d|\lambda(N^*)|}{dN} \approx 1.35 > 0$$

Thus, a Neimark–Sacker bifurcation occurs at N^*, which is consistent with Figure 1.

The second case we will look at is when $P > 0$ and $1 - N + NV > 0$. To find the period–2 fixed points in this case, we solve the following system:

$$\begin{aligned} \bar{P} &= \bar{P}(1 - N + N\bar{V})(1 - N + N^2\bar{P}(1 + \bar{V})) \\ \bar{V} &= N\bar{P}(1 - N + N\bar{V})(1 + N\bar{P}(1 + \bar{V})). \end{aligned} \tag{3.1.21}$$

Using (3.1.17), (3.1.18) and solving for V we obtain three fixed points. The first is the period–1 fixed point $(\bar{P}, \bar{V}) = (1/2N, 1)$. The other period–2 fixed points satisfy

$$\bar{V} = (N - 2) \pm \sqrt{\frac{(N-1)(N-2)(N-3)}{N}}, \tag{3.1.22}$$

where $\bar{P}$ can be found by substituting these values of $\bar{V}$ into (3.1.18). These fixed points exist for $N \geq 3$, and form a period–2 orbit since they map to each other. Again, the stabilities of these fixed points are determined by examining the eigenvalues of the Jacobian matrix. For all $N \geq 3$, one of these eigenvalues is greater than one. Thus, this period–2 cycle is unstable.

The third case we will look at is when $P < 0$ and $1 - N + NV < 0$. To find the period–2 fixed points in this case, we solve the following system:

$$\begin{aligned} \bar{P} &= \bar{P}(1 - N + N\bar{V})(1 - N - N^2\bar{P}(1 + \bar{V})) \\ \bar{V} &= NP(1 - N + N\bar{V})(1 - N\bar{P}(1 + \bar{V})). \end{aligned} \tag{3.1.23}$$

Solving for P in this case we obtain

$$\bar{P} = 0 \tag{3.1.24}$$

or

$$\bar{P} = -\frac{2 - N + N\bar{V} - \bar{V}}{N(1+\bar{V})(1 - N + N\bar{V})}. \tag{3.1.25}$$

Using (3.1.17), (3.1.18) and solving for V we obtain the following period–2 fixed point:

$$(\bar{P}, \bar{V}) = \left(\frac{2-N}{2N(N-1)}, \frac{N-2}{N}\right). \tag{3.1.26}$$

This fixed point exists for $N \geq 2$. The period–2 fixed point (3.1.26) and the period–2 fixed point (3.1.19) from Case 1 combine to form a period–2 cycle. Thus, a Neimark–Sacker bifurcation occurs at the value of N given in (3.1.20), consistent with Figure 1.

The final case to consider is when $P < 0$ and $1 - N + NV > 0$. To find the period–2 fixed points in this case, we solve the following system:

$$\bar{P} = \bar{P}(1 - N + N\bar{V})(1 - N - N^2\bar{P}(1+\bar{V})) \tag{3.1.27}$$

$$\bar{V} = -N\bar{P}(1 - N + N\bar{V})(1 - N\bar{P}(1+\bar{V})). \tag{3.1.28}$$

Using (3.1.24), (3.1.25) and solving for V we obtain three fixed points. The first is the period–1 fixed point $(\bar{P}, \bar{V}) = (-1/2N, 1)$. The other values that result have V coordinate the same as those obtained in Case 2, with P coordinate of opposite sign to those in Case 2. These period–2 fixed points exist for $N \geq 3$ and form a period–2 cycle since they map to each other. Again, the stability of these fixed points is determined by examining the eigenvalues of the Jacobian

matrix. For all $N \geq 3$, one of these eigenvalues is greater than one. Thus, as with the cycle of Case 2, this period–2 cycle is unstable.

The limit cycle behavior exists until $N = 3.0$. At this point a symmetric figure–eight homoclinic bifurcation occurs due to the collision of the limit cycles formed by the symmetric Neimark–Sacker bifurcations with the unstable fixed point at the origin. This is displayed in Figures 3.2 and 3.3.

As N increases past $N = 3.0$ the system enters chaos from the break-up of the limit cycles. Price dynamics are purely chaotic for $3.0 < N < 3.3$. Therefore the price of the asset cannot be accurately predicted if N is in this region. This is shown in Figure 3.4. The existence of chaos in this region is confirmed using Liapunov exponents, illustrated in Figure 3.5.

Figure 3.5 shows the maximal Liapunov exponent as a function of N. Since this exponent is positive when $N > 3$, it is evident that prices are purely chaotic when N is in this region.

At $N \approx 3.4$ the system undergoes a boundary crisis. As mentioned in Chapter 2, this occurs when the boundary of a chaotic set collides with an unstable fixed point or unstable periodic trajectory. This causes the destruction of the chaotic set. The boundary crisis is illustrated in Figure 3.6 [25], as the boundary of the chaotic set (in white) collides with the unstable fixed points $(P, V) = (1/2N, 1)$ and $(P, V) = (-1/2N, 1)$. This diagram, like other basin diagrams constructed in this thesis, is a grid of initial conditions. In this case however, each point on the grid is assigned a color dependent upon the orbit generated by the initial condition. If the orbit tends to an attractor, a dark blue dot is plotted. If orbits tend to infinity, increasingly lighter dots are plotted, depending on how quickly the orbit tends to infinity.

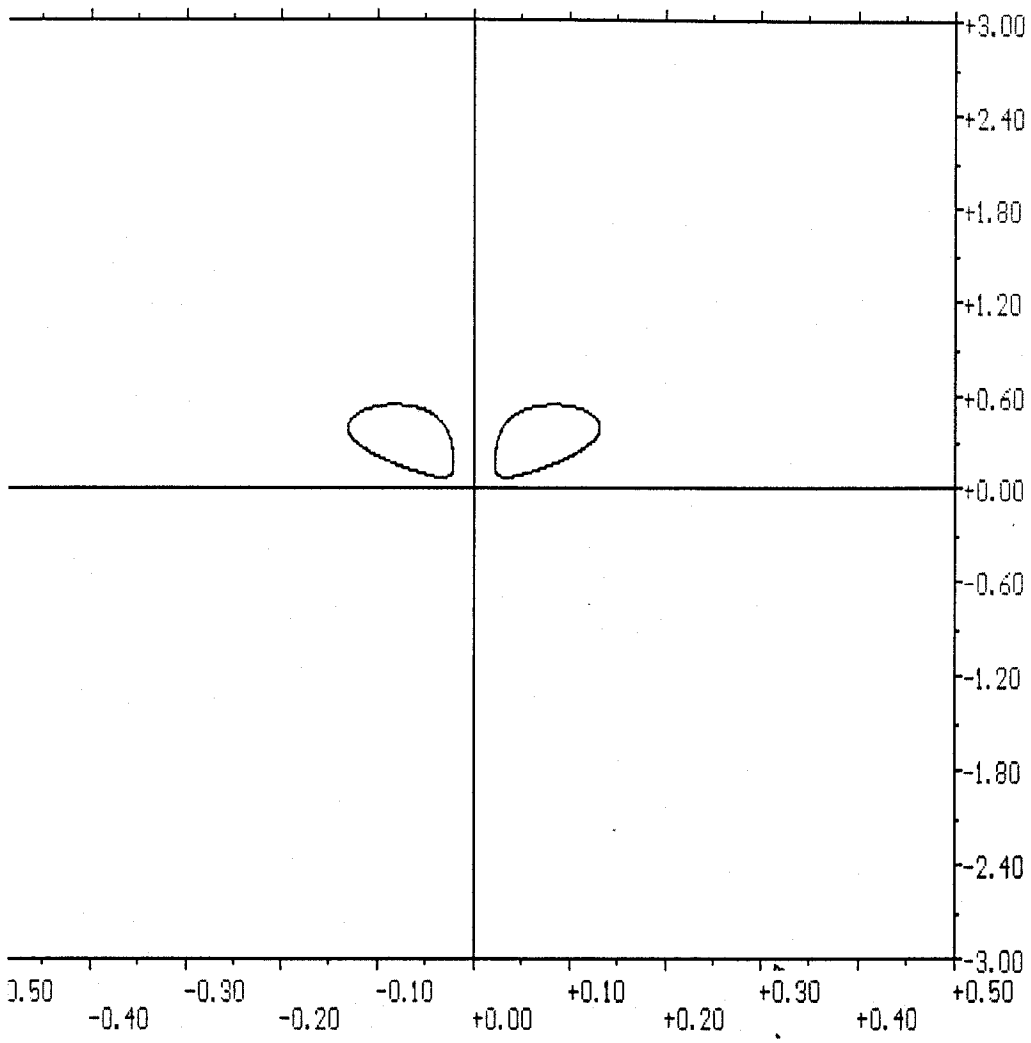

Figure 3.2: Phase diagram illustrating symmetric Neimark–Sacker bifurcations ($N = 2.9$)

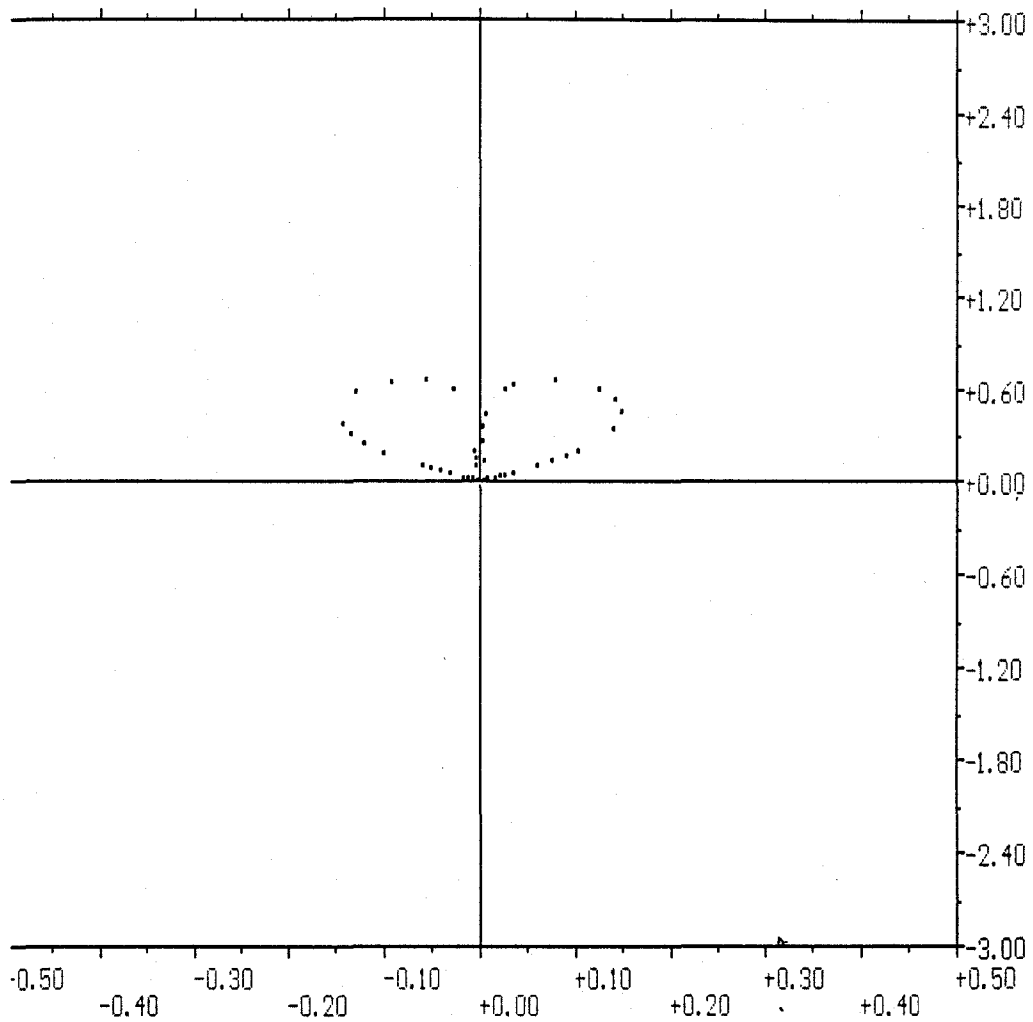

Figure 3.3: Phase Diagram at Homoclinic bifurcation ($N = 3.0$)

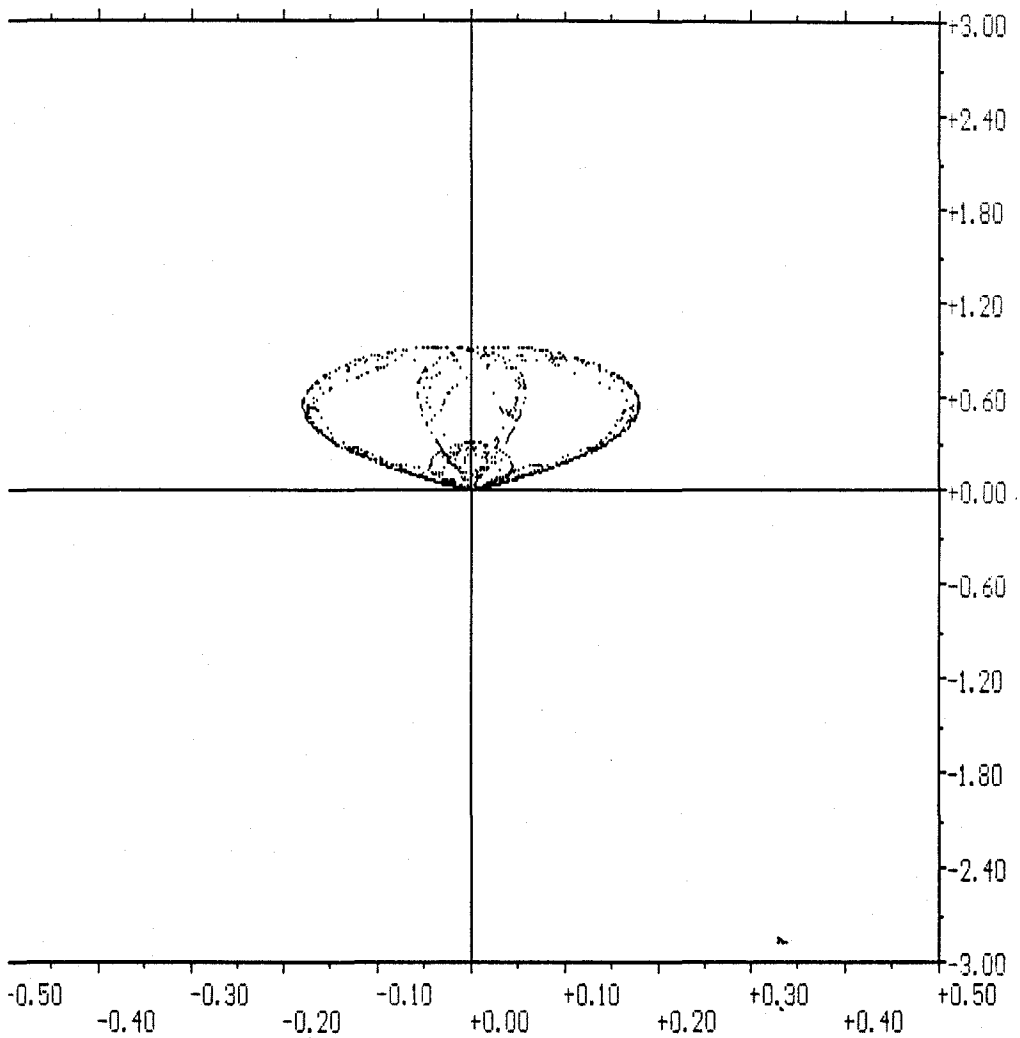

Figure 3.4: Phase diagram illustrating chaos ($N = 3.2$)

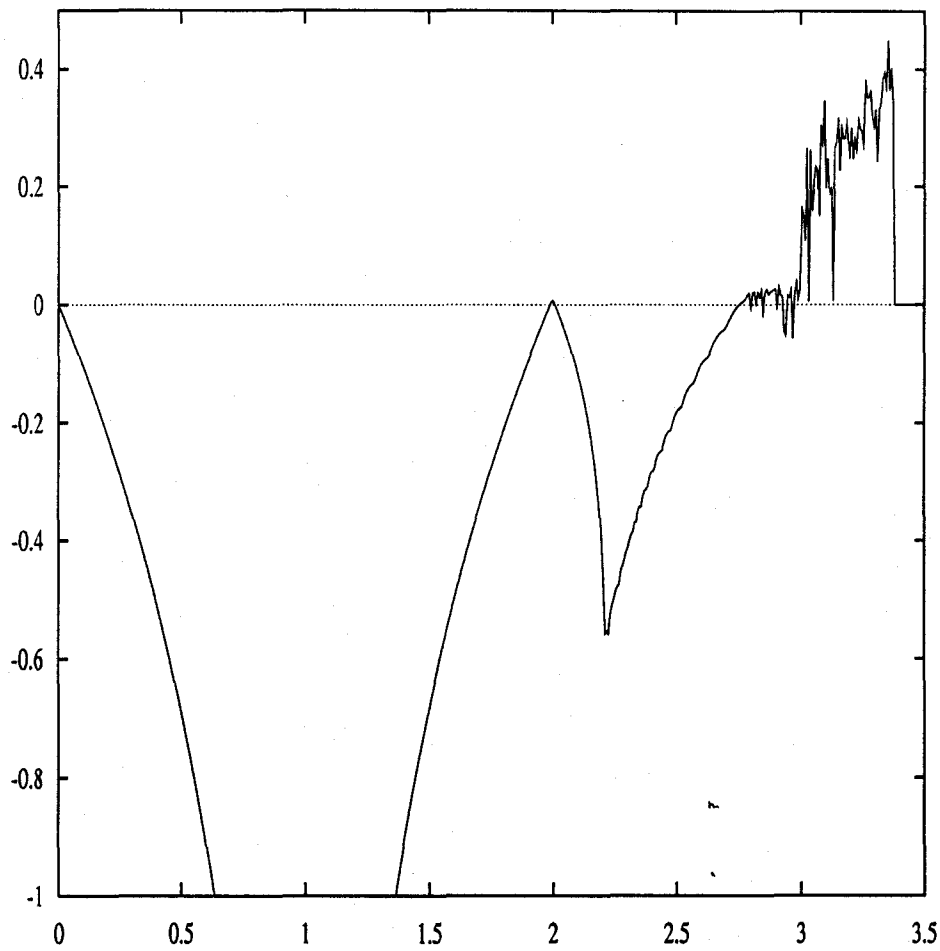

Figure 3.5: Maximal Liapunov exponent as a function of the parameter N

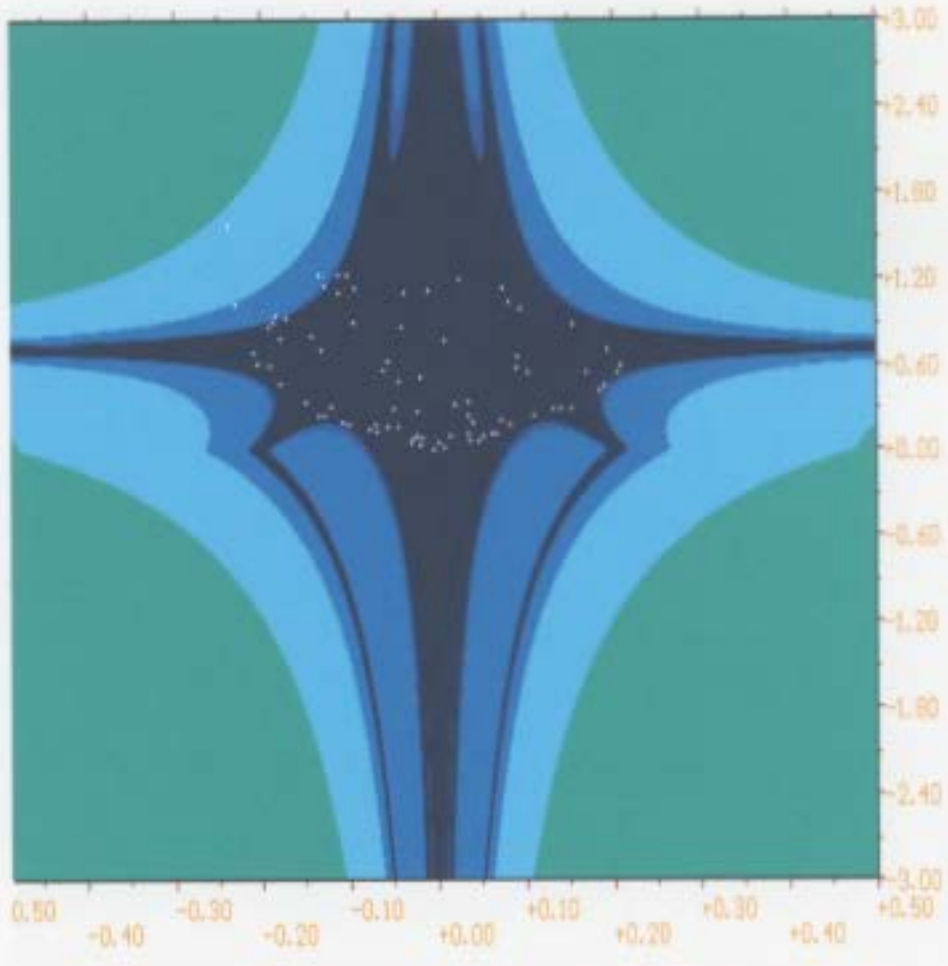

Figure 3.6: Boundary Crisis ($N = 3.4$)

3.2 Chiarella, Dieci and Gardini

The model presented in (1.3.12) can be re–written as follows:

$$\begin{aligned} P &\mapsto P + \beta_p \left[a(W - P) + h(\psi - g)\right] \\ \psi &\mapsto (1 - c)\psi + c\beta_p \left[a(W - P) + h(\psi - g)\right] \end{aligned} \tag{3.2.1}$$

To find fixed points we solve the following system:

$$\begin{aligned} \bar{P} &= \bar{P} + \beta_p \left[a(W - \bar{P}) + h(\bar{\psi} - g)\right] \\ \bar{\psi} &= (1 - c)\bar{\psi} + c\beta_p \left[a(W - \bar{P}) + h(\bar{\psi} - g)\right]. \end{aligned} \tag{3.2.2}$$

The map has one fixed point, namely $(\bar{P}, \bar{\psi}) = (W + h(-g)/a, 0)$. Introducing the price deviation, $p = P - (W + h(-g)/a)$ allows the system to be written in such a way that the unique fixed point is at the origin. The new map, T, can be written as

$$T : \begin{cases} p \mapsto p - \beta_p \left[ap - k(\psi)\right] \\ \psi \mapsto (1 - c)\psi - c\beta_p \left[ap - k(\psi)\right] \end{cases} \tag{3.2.3}$$

where $k(\psi) = h(\psi - g) - h(-g)$.

To obtain stability results, the Jacobian matrix corresponding to T is found. This matrix is given below:

$$J = \begin{bmatrix} 1 - a\beta_p & \beta_p k'(\psi) \\ -ac\beta_p & 1 - c + c\beta_p k'(\psi) \end{bmatrix}. \tag{3.2.4}$$

The Jacobian matrix is then evaluated at the unique fixed point $(0, 0)$ so that the corresponding eigenvalues can be obtained:

$$J(0,0) = \begin{bmatrix} 1 - a\beta_p & \beta_p k'(0) \\ -ac\beta_p & 1 - c + c\beta_p k'(0) \end{bmatrix}. \tag{3.2.5}$$

As before, the eigenvalues of the Jacobian matrix are obtained from the characteristic equation, $\det(J(0,0) - \lambda I) = 0$, *i.e.*,

$$\begin{vmatrix} 1 - a\beta_p - \lambda & \beta_p k'(0) \\ -ac\beta_p & 1 - c + c\beta_p k'(0) - \lambda \end{vmatrix} = 0. \tag{3.2.6}$$

Simplifying gives

$$\lambda^2 - \lambda(2 - c + c\beta_p k'(0) - a\beta_p) + 1 - c + c\beta_p k'(0) - a\beta_p + ac\beta_p = 0. \tag{3.2.7}$$

The eigenvalues which result from (3.2.7) are quite complicated and are given below:

$$\lambda_{1,2} = \frac{2 - a\beta_p - c + c\beta_p k'(0)}{2} \pm \frac{\sqrt{a^2\beta_p^2 - 2ac\beta_p(1 + \beta_p k'(0)) + c^2(1 - \beta_p k'(0) + \beta_p^2(k'(0))^2)}}{2}. \tag{3.2.8}$$

The fixed point $(p, \psi) = (0, 0)$ is stable when $|\lambda_1| < 1$ and $|\lambda_2| < 1$. In [11], three criteria are used, which are equivalent to $|\lambda_1| < 1$ and $|\lambda_2| < 1$ in planar maps. These are:

1. $1 - \mathrm{tr}[J(0,0)] + \det[J(0,0)] > 0$
2. $1 + \mathrm{tr}[J(0,0)] + \det[J(0,0)] > 0$
3. $\det[J(0,0)] < 1$.

In a general 2×2 matrix given by

$$A = \begin{bmatrix} a_{11} & a_{12} \\ a_{21} & a_{22} \end{bmatrix},$$

$\text{tr}(A) = a_{11} + a_{22}$ and $\det(A) = a_{11}a_{22} - a_{12}a_{21}$. The characteristic equation given in (3.2.6) can be expressed as $\lambda^2 - \lambda\text{tr}[J(0,0)] + \det[J(0,0)] = 0$. Using the three conditions given above, the following three inequalities are obtained in [11]:

$$\begin{aligned} a\beta_p c &> 0 \\ a\beta_p(2-c) &< 2(2-c)) + 2c\beta_p k'(0) \\ a\beta_p(1-c) &> c[\beta_p k'(0) - 1]. \end{aligned}$$

The first inequality is always true since the parameters a, β_p and c are always positive. Here we simplify the second and third inequalities to obtain the following inequality:

$$\frac{2(a\beta_p - 2)}{2\beta_p k'(0) + a\beta_p - 2} < c < \frac{a\beta_p}{\beta_p k'(0) + a\beta_p - 1} \tag{3.2.9}$$

The fixed point $(0,0)$ is stable when this inequality is satisfied, and unstable otherwise, assuming the denominators are positive.

The analysis in the original paper is carried out using two-parameter bifurcation diagrams where a and c are varied. In this thesis a one-parameter orbit diagram is used, and the parameter c is varied.

The bifurcation values are found by setting the absolute value of the eigenvalues equal to one. These values indicate where changes in stability occur, and hence give the possible bifurcation values of the system. At our fixed point $(\bar{p}, \bar{\psi}) = (0,0)$, it can be shown that two bifurcation values result. These bifurcations (in terms of the parameter c) occur when

$$c = \frac{2(a\beta_p - 2)}{2\beta_p k'(0) + a\beta_p - 2} \tag{3.2.10}$$

and

$$c = \frac{a\beta_p}{\beta_p k'(0) + a\beta_p - 1}. \tag{3.2.11}$$

Since $\lambda_1 = 0$, and λ_2 decreases through $\lambda_2 = -1$ as c decreases through the value given in (3.2.10), a period–doubling bifurcation takes place at this value. As well, since the eigenvalues are complex valued and r passes smoothly through unity as c increases through the value in (3.2.11), a Neimark–Sacker bifurcation occurs at this value. To study the dynamics, parameter values are careful chosen for four of five parameters. Using the function $h(x) = \alpha \arctan x$ the following parameter values are used in the analysis of the map T: $a = 1.8$, $\beta_p = 1.8$, $g = 0.5$, $\alpha = 2.3$.

Figure 3.7 shows the constructed orbit diagram (p vs. c) of this system. The subcritical period doubling bifurcation takes place as c increases through $c^* \approx 0.315$, consistent with that found when substituting the chosen parameters into (3.2.10). This creates a stable fixed point $(0, 0)$ and an unstable period–2 cycle when $c > c^*$. Figure 3.8 shows the basin diagram corresponding to $c = 0.32$. When initial conditions are close to zero, the map tends to the fixed point at the origin. The unstable period–2 cycle is shown, with coordinates of approximately $(-1.2, -0.5)$ and $(1.3, 0.5)$. The boundary of the basin of attraction for the origin is dependent upon the stable manifold of the unstable period–2 cycle. The period–2 cycle does not appear in Figure 3.7 since an orbit diagram shows only stable solutions for a range of parameter values.

When $c > 0.315$, prices tend to their fundamental value. A Neimark–Sacker bifurcation occurs at $c \approx 0.584$, which again is consistent with the value obtained using the chosen parameter values and (3.2.11), and prices now

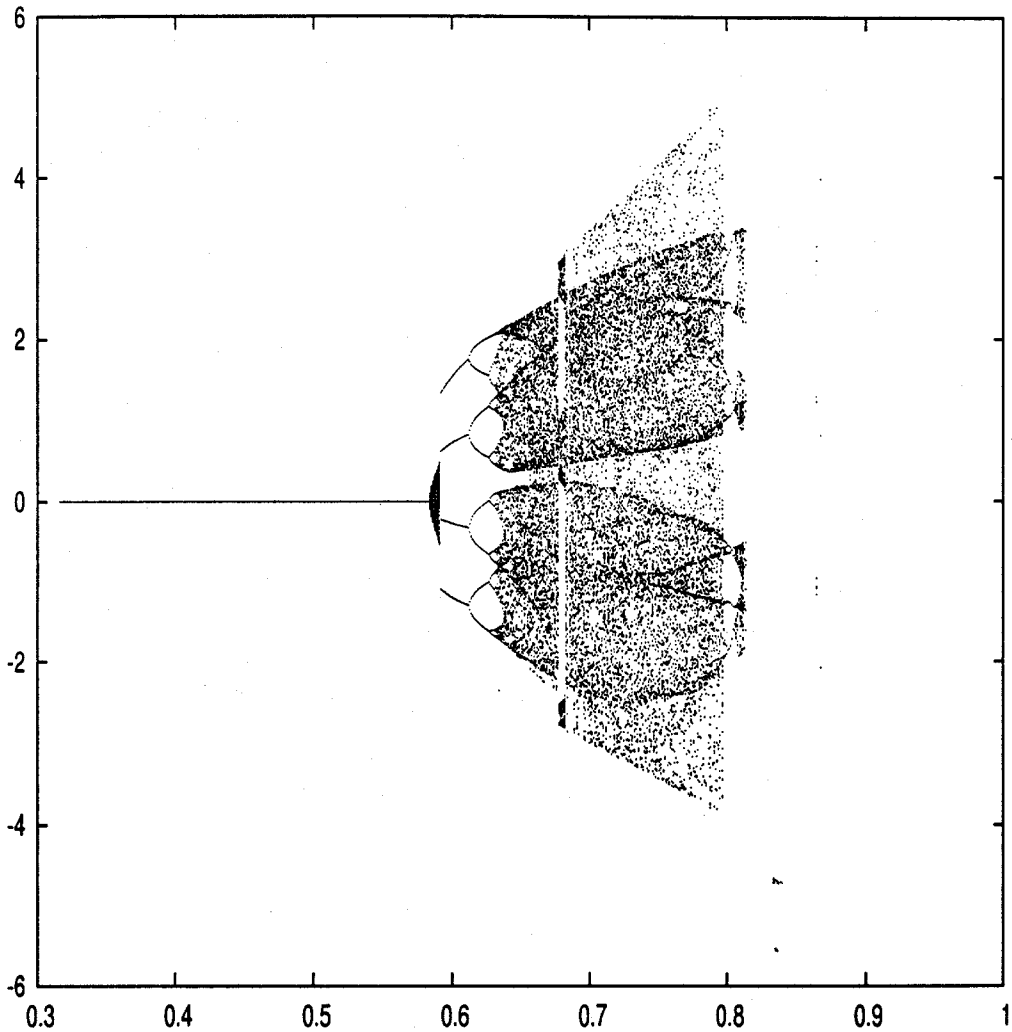

Figure 3.7: Orbit Diagram (Chiarella *et al.*)

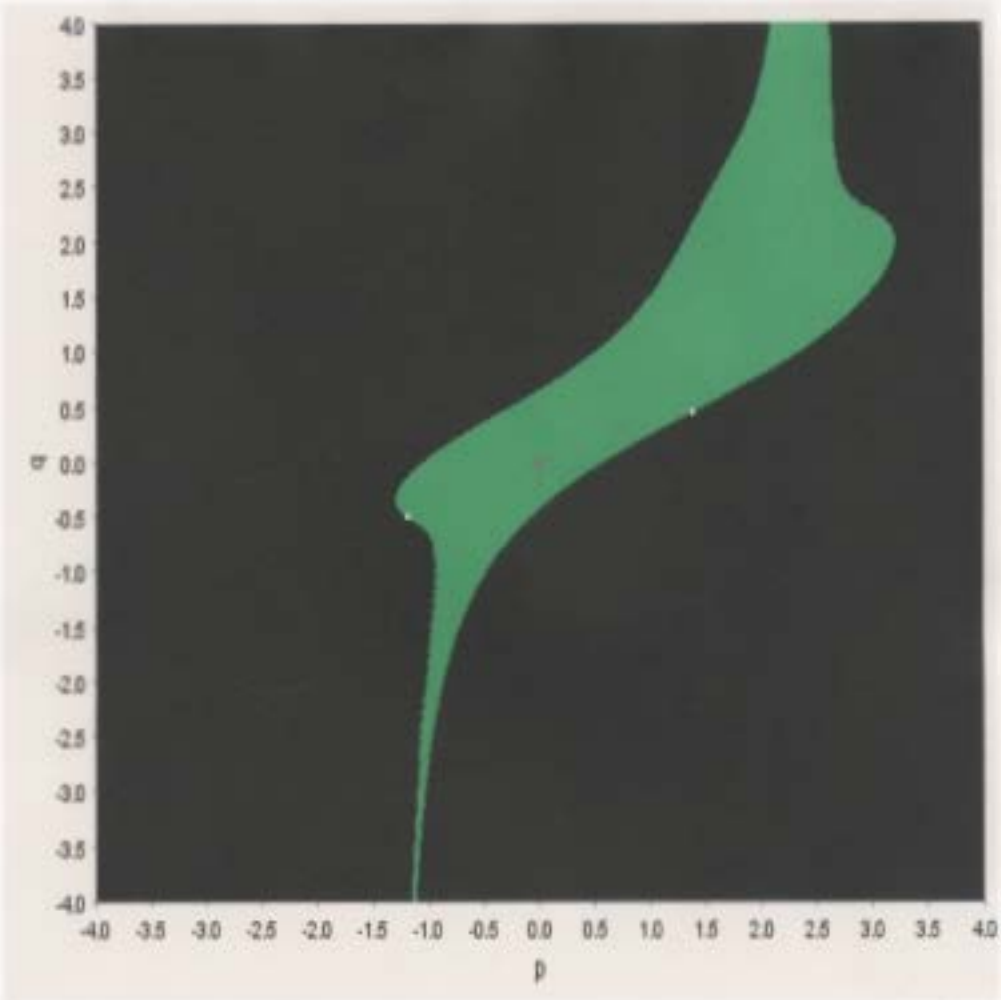

Figure 3.8: Basin Diagram ($c = 0.32$)

The basin for the origin is shown in green, the basin for infinity is shown in black, and the unstable period–2 cycle is shown in white.

tend toward values of a limit cycle rather than just two values.

For values of c greater than approximately 0.6, a complicated series of global bifurcations occur involving contact bifurcations between basin boundaries of local attractors rather than directly involving changes in the fixed points themselves. See [11] for their analysis of these basin structures. The parameter values chosen in their analysis and description of contact bifurcations differ from those used in this thesis. In this thesis the basin structures will be analyzed using computer software [29].

When c reaches $c \approx 0.5807$, a saddle–node bifurcation in period–4 occurs. The result is a locally stable period–4 cycle and an unstable period–4 cycle. These cycles are displayed in Figure 3.9.

When c increases through $c \approx 0.5836$ a Neimark–Sacker bifurcation occurs, as previously discussed and displayed in Figure 3.7. For $0.584 < c < 0.5913$ the limit cycle and stable period–4 cycle co–exist. These attractors and their corresponding local basins of attraction are given in Figure 3.10.

When $c \approx 0.5913$ a contact bifurcation occurs where the limit cycle collides with the unstable period–4 cycle. The unstable period–4 cycle thus forms a heteroclinic orbit, and a "heteroclinic bifurcation" is said to take place at this value. This causes the annihilation of the limit cycle. Hence, as c increases past this value, the period–4 cycle remains as the only attractor (except for the one at infinity). This is shown in Figure 3.11.

As is shown in Figure 3.7, the period–4 cycle period doubles to create a period–8 cycle, and we see a period–doubling cascade to chaos. We will denote the resulting chaotic attractor A_4.

At $c \approx 0.6455$, a new saddle–node bifurcation occurs, this time in period–3.

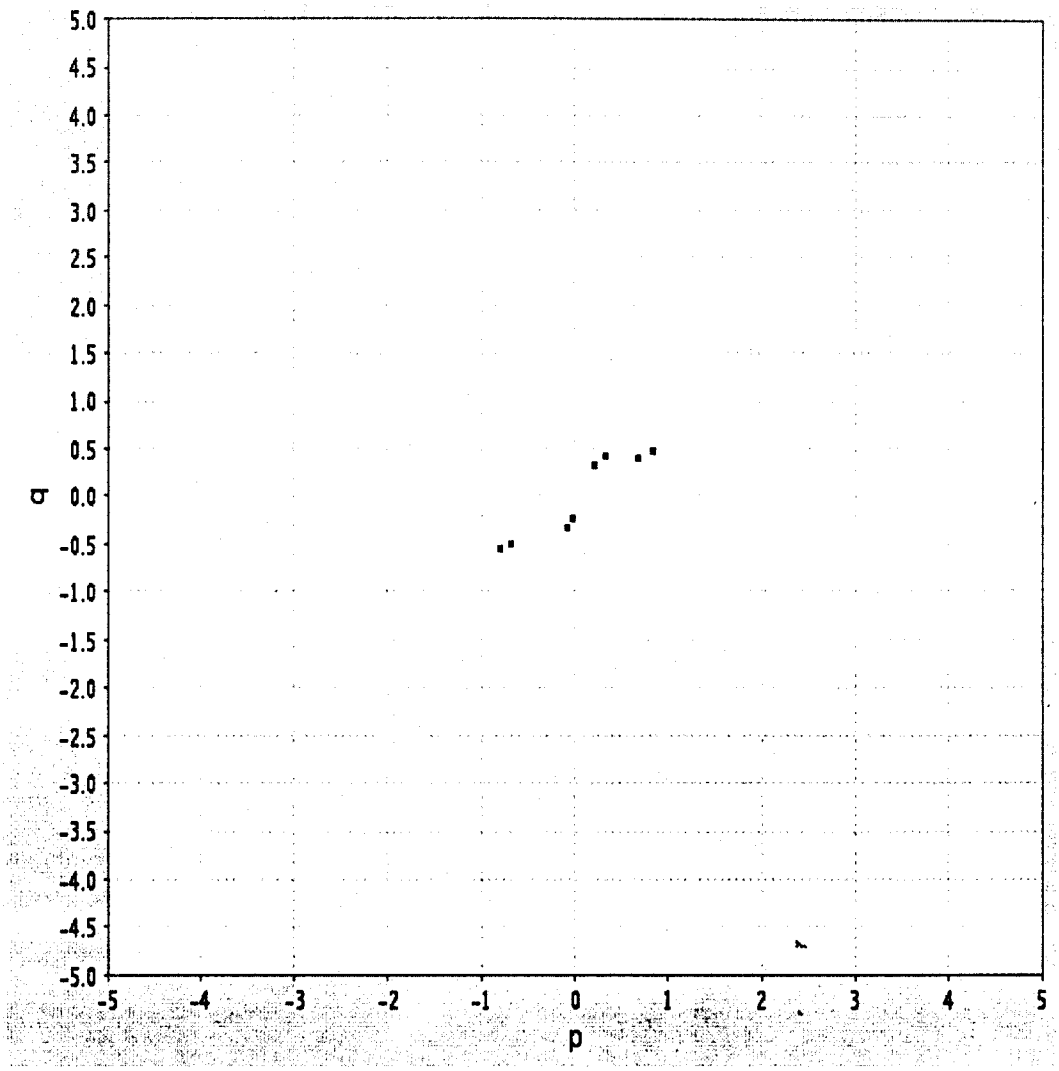

Figure 3.9: Period–4 Cycle ($c = 0.581$)

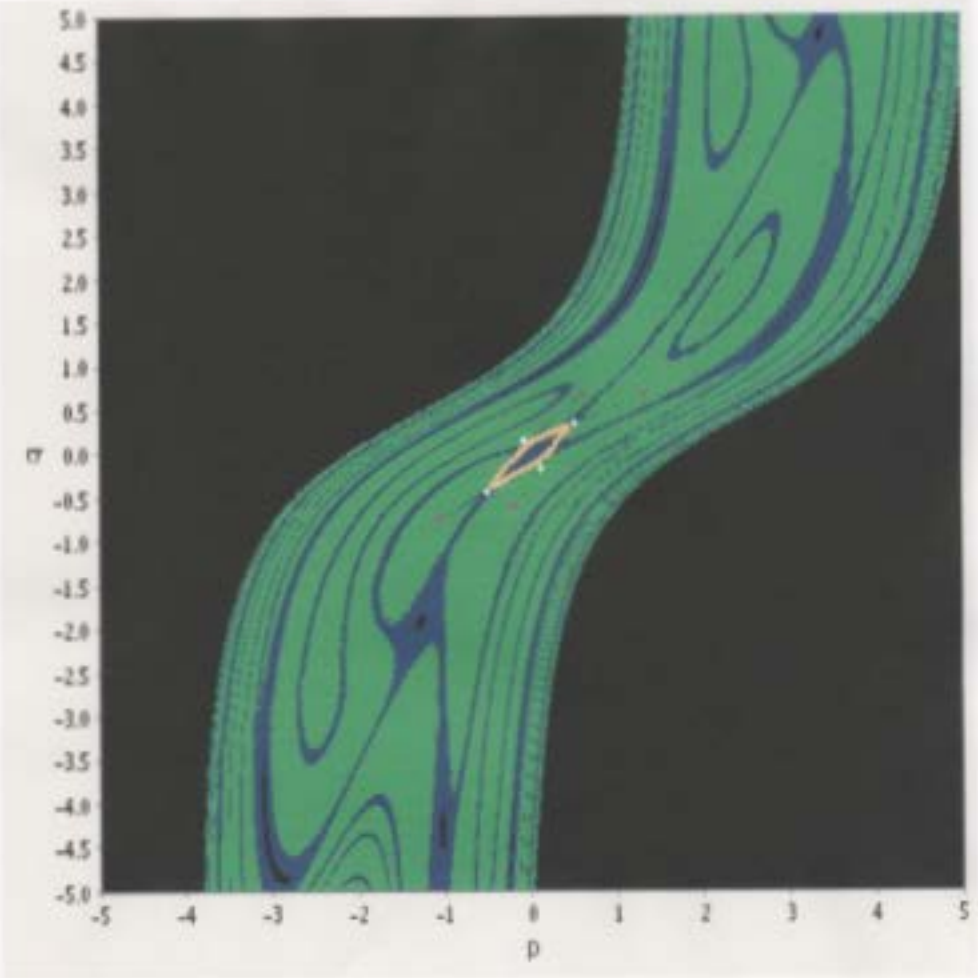

Figure 3.10: Basin Diagram ($c = 0.59$)

The basin for the limit cycle is shown in green, the basin for the period–4 cycle is shown in blue, the basin for infinity is shown in black, the stable period–4 cycle is shown in pink, and the unstable period–4 cycle is shown in white.

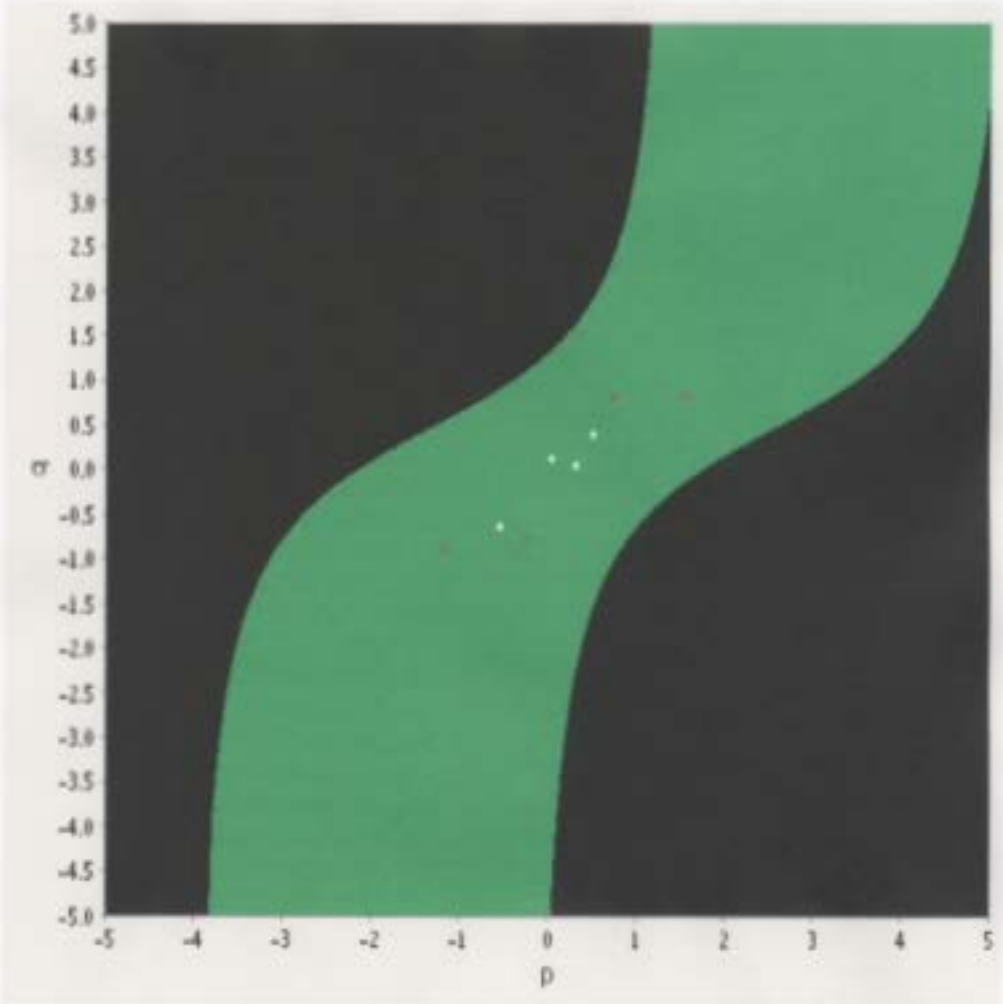

Figure 3.11: Basin Diagram ($c = 0.60$)

The basin for the period–4 cycle is shown in green, the basin for infinity is shown in black, the stable period–4 cycle is shown in pink, and the unstable period–4 cycle is shown in white.

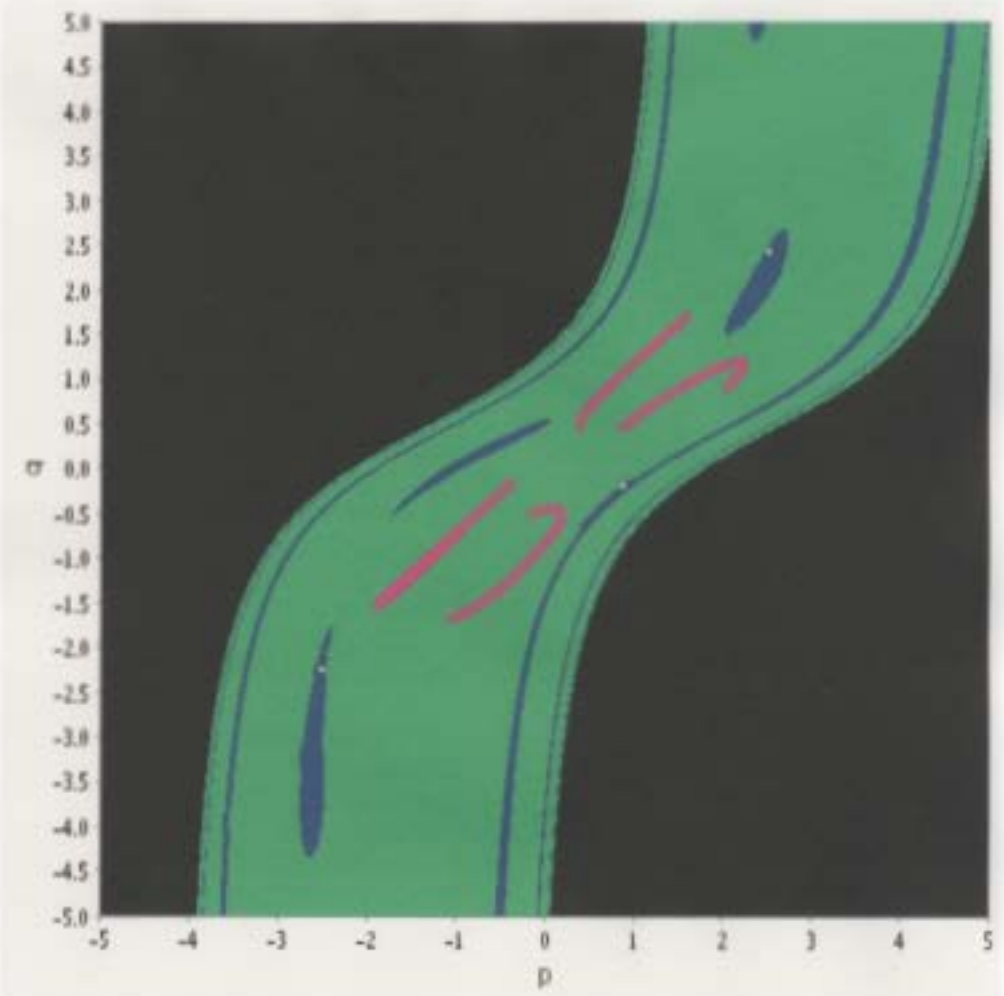

Figure 3.12: Basin Diagram ($c = 0.646$)

The basin for A_4 is shown in green, the basin for the period–3 cycle is shown in blue, and the basin for infinity is shown in black.

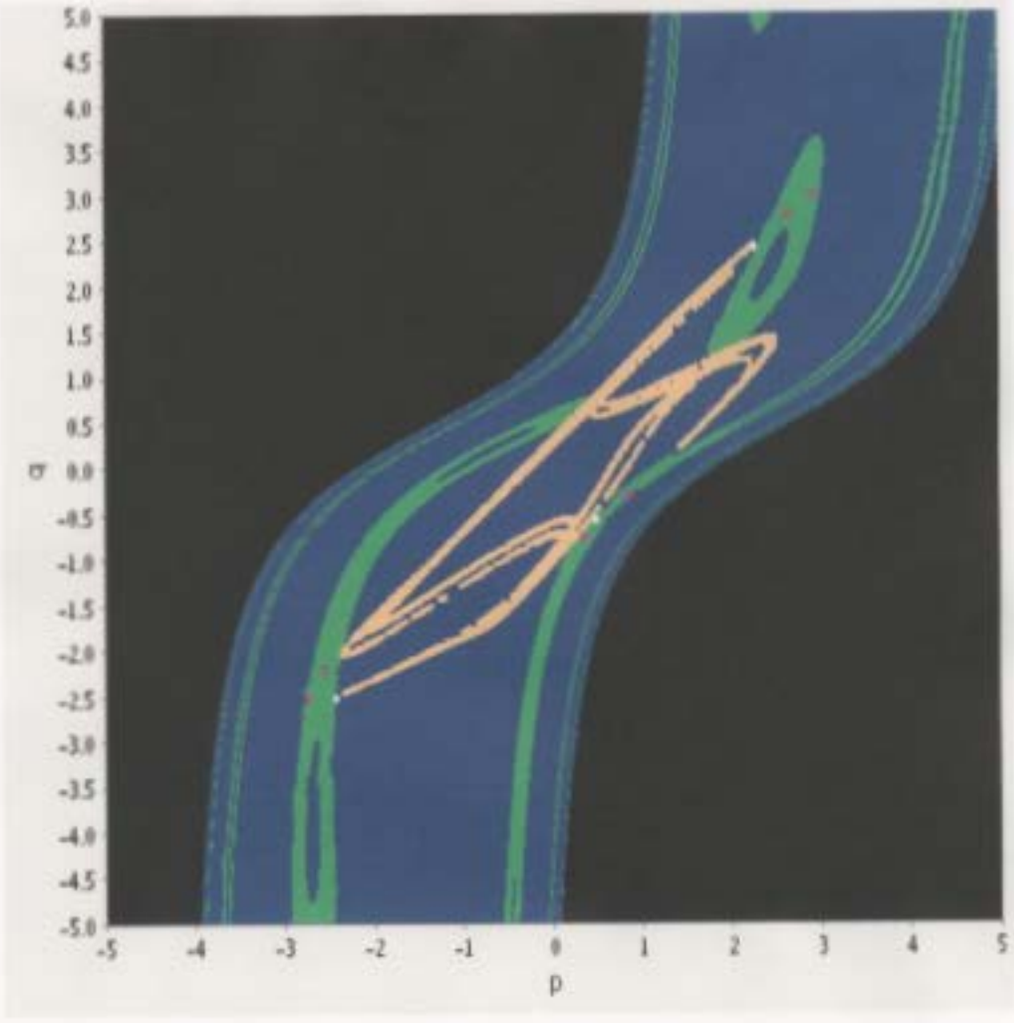

Figure 3.13: Boundary Crisis ($c = 0.675$)

The basin for the period–3 cycle is shown in green, the basin for A_4 is shown in blue, A_4 is shown in orange, and the unstable period–3 cycle is shown in white.

Figure 3.14: Basin Diagram ($c = 0.69$)

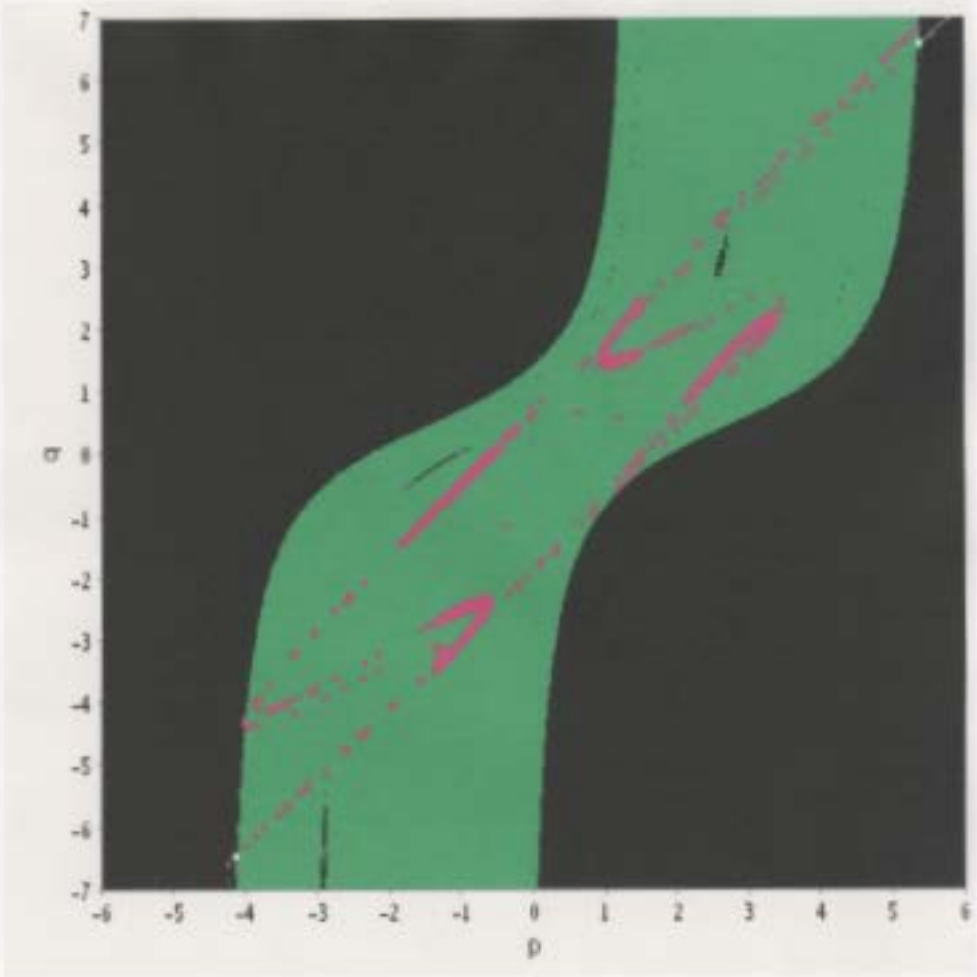

Figure 3.15: Basin Diagram ($c = 0.8149$)
The unstable period–2 cycle is shown in white.

This creates a locally stable period–3 cycle, and an unstable period–3 cycle. The stable period–3 cycle co–exists with the chaotic attractor A_4. The basins of attraction for these attractors are shown in Figure 3.12. As c increases, the period–3 cycle period doubles to create a period–6 orbit, and eventually a period doubling cascade to chaos (A_3).

At $c \approx 0.6775$ a boundary crisis occurs. This time A_4 collides with the unstable period–3 cycle (shown in Figure 3.13). This collision results in the annihilation of A_4. This is shown in Figure 3.7 as A_4 being replaced by A_3, with a corresponding increase in the size of the attractor.

Depending on initial conditions, for values of c slightly greater than $c \approx 0.6775$ an orbit may follow the ghost of A_4 before arriving at A_3. We say that A_4 exists as a transient.

When $c \approx 0.6815$ an interior crisis occurs. The unstable period–3 cycle now collides with the basin boundary of A_3, causing A_3 and A_4 to merge into a single stable attractor. This is shown in Figure 3.14 and can also be seen in Figure 3.7 with the re–emergence of A_4.

Finally, when $c \approx 0.8149$, the chaotic attractor shown in Figure 3.14 collides with the unstable period–2 cycle created from the initial subcritical period–doubling bifurcation. This boundary crisis, along with the unstable period–2 cycle, is shown in Figure 3.15.

3.3 Chiarella and He

A similar process is carried out for the three dimensional model constructed by Chiarella and He [12]. We substitute $y = x_{t-1}$ in system (1.3.34) to obtain

the following three-dimensional map:

$$\begin{aligned} x &\mapsto \frac{d}{R}\frac{(1-m)}{a+1+(a-1)m}x \\ m &\mapsto \tanh\left[\frac{\beta}{2a_1\sigma^2}\left(Rx-\frac{d}{R}\left(\frac{1-m}{a+1+(a-1)m}\right)x\right)\left(Rx+\frac{dy-Rx}{a}\right)-\frac{\beta C}{2}\right] \\ y &\mapsto x. \end{aligned} \tag{3.3.1}$$

To study the dynamics, parameter values are careful chosen for six of seven parameters. The following parameter values are used in the analysis of (3.3.1): $R = 1.1$, $d = 1.2$, $\beta = 3.5$, $C = 1.0$, $\sigma^2 = 1.0$, and $a_1 = 1.0$. The fixed points of (3.3.1) are those $\bar{\mathbf{x}} = (\bar{x}, \bar{m}, \bar{y})$ which satisfy

$$\mathbf{f}(\bar{\mathbf{x}}) = \bar{\mathbf{x}}. \tag{3.3.2}$$

More specifically, the fixed points are

$$\bar{m} = \frac{1-11a}{1+11a} \quad (\bar{x} \neq 0), \tag{3.3.3}$$

$\bar{x}$, where $\bar{x}$ satisfies

$$\tanh\left(\frac{7(11a+1)}{400a}\bar{x}^2 - \frac{7}{4}\right) = \bar{m}, \tag{3.3.4}$$

and

$$\bar{y} = \bar{x}. \tag{3.3.5}$$

When $\bar{x} = 0$, $\bar{m} = \tanh(\frac{-7}{4})$ and $\bar{y} = 0$. The other fixed points, $(\bar{x}_+, \bar{m}, \bar{y}_+)$ and $(\bar{x}_-, \bar{m}, \bar{y}_-)$ can be found explicitly from (3.3.3)-(3.3.5). To determine the stability of these fixed points, the Jacobian matrix is calculated and evaluated at each fixed point in order to find the eigenvalues of this matrix. For the fixed point $(0, \tanh(\frac{-7}{4}), 0)$ the eigenvalues are found to be

$$\lambda_{1,2,3} = 0, 0, \frac{12}{11}\left[\frac{1+\tanh\frac{7}{4}}{a+1-(a-1)\tanh\frac{7}{4}}\right]. \tag{3.3.6}$$

Since λ_1 and λ_2 are both zero (and are hence always less than one in absolute value) this fixed point will be stable for $|\lambda_3| < 1$, and unstable otherwise. Consequently, we find it is unstable if $0 < a < 3.01$ and is stable if $a > 3.01$. Similarly, the other fixed points are both unstable for $0 < a < 1.17$ and stable for $1.17 < a < 3.01$.

Figure 3.16 shows the constructed orbit diagram (x vs. a) of this system. It is evident from this diagram that bifurcations occur at $a = 1.17$ and $a = 3.01$. This is consistent with the stability results obtained above. As well, chaotic behaviour is probable for a range of values less than $a = 1.17$. This is confirmed using Liapunov exponents. Figure 3.17 shows the maximal Liapunov exponent as a is varied. If $0.9 < a < 1.17$ the Liapunov exponent is close to zero, indicating the limit cycle behaviour. If $0 < a < 0.9$, the Liapunov exponent is mainly positive, denoting a chaotic regime. However, for several "windows" of a values in this range, the maximal Liapunov exponent is negative. As in Westerhoff's model, these windows represent stable periodic points.

Figure 3.18 shows the bifurcation diagram corresponding to the model of Chiarella and He. The bifurcation taking place at $a = 1.17$ is a Neimark–Sacker bifurcation. Phase diagrams (Figures 3.19 and 3.20), plotting the x and m coordinates of a single trajectory, are used to illustrate the behavior of the system near the Neimark–Sacker bifurcation. If $a > 1.17$, the limit cycle does not exist and the trajectory approaches a single value (Figure 3.19). If $a < 1.17$, but is close to 1.17, the trajectory converges to the limit cycle (Figure 3.20). As a continues to decrease the limit cycle dissipates and is replaced by chaos. The bifurcation at $a = 3.01$ is a pitchfork bifurcation. Since the stable branches appear around an unstable fixed point at $\bar{x} = 0$, the pitchfork is said

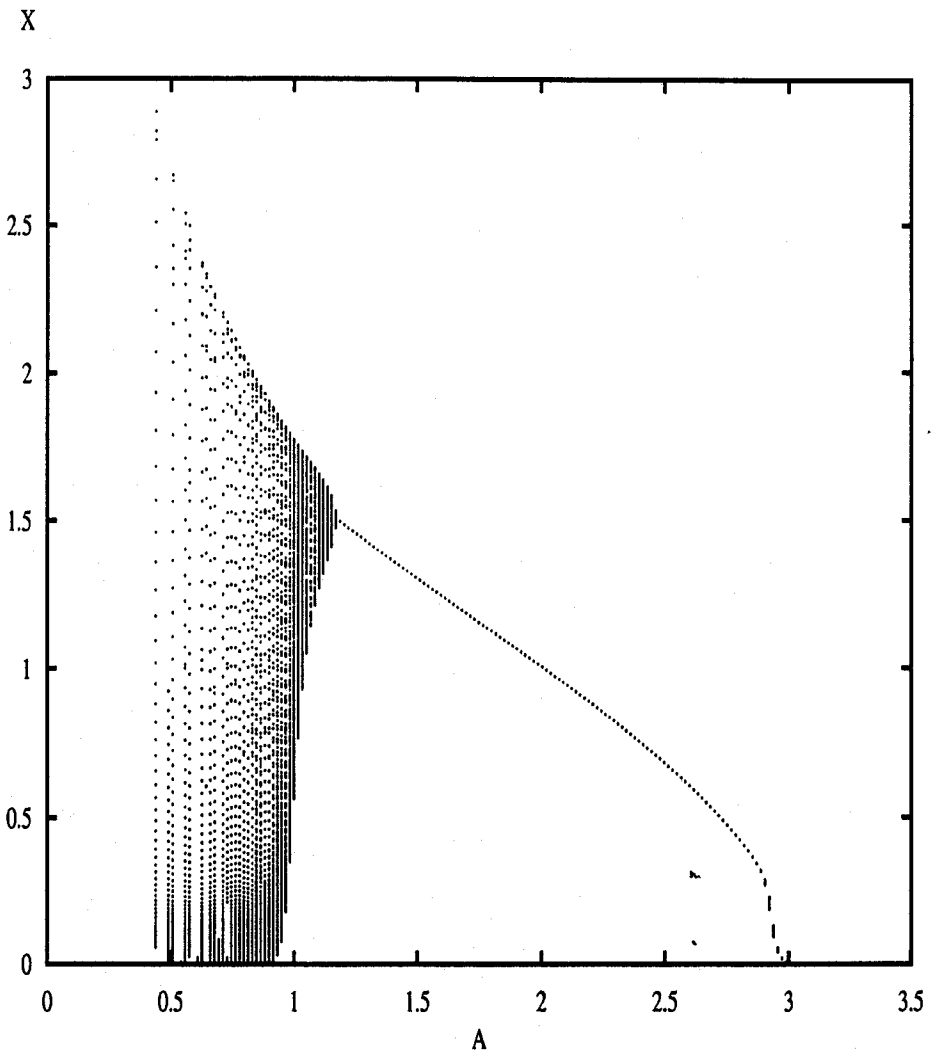

Figure 3.16: Orbit Diagram corresponding to system 3.3.1

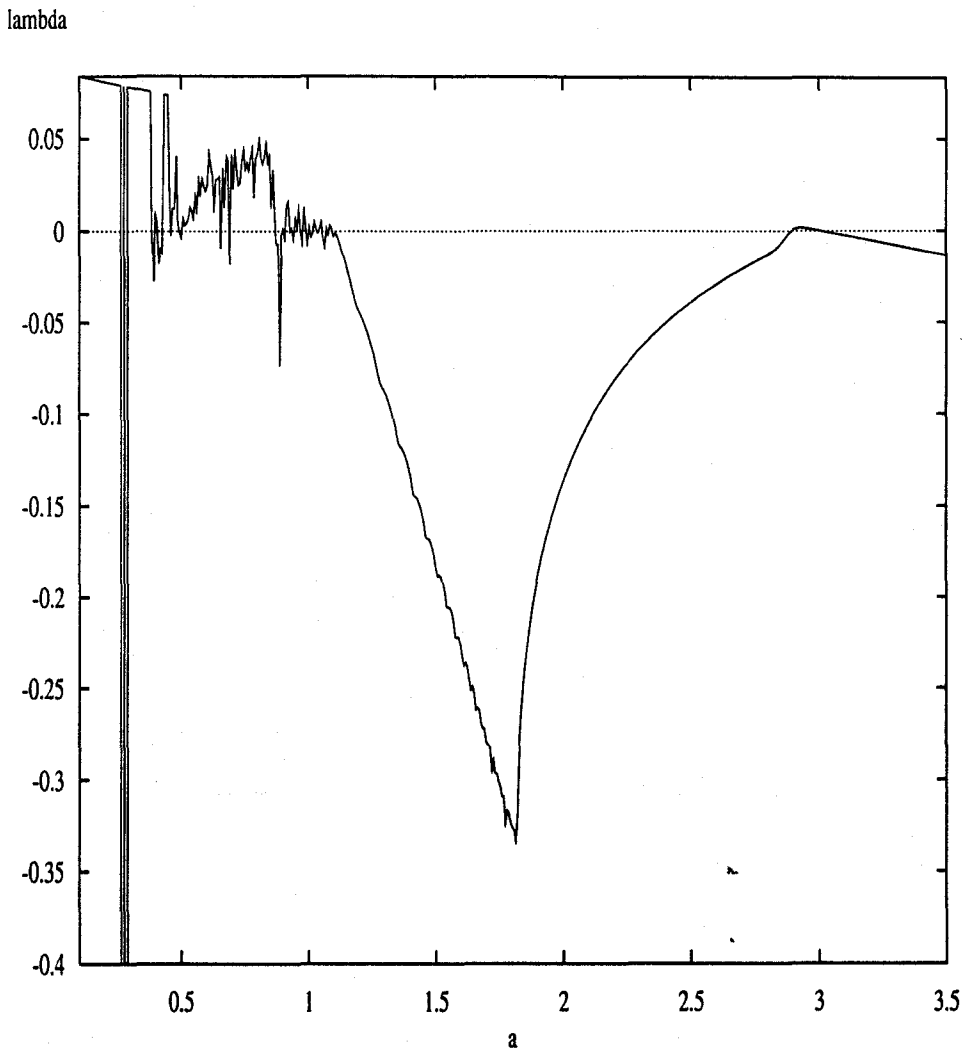

Figure 3.17: Maximal Liapunov exponent as a function of the parameter a

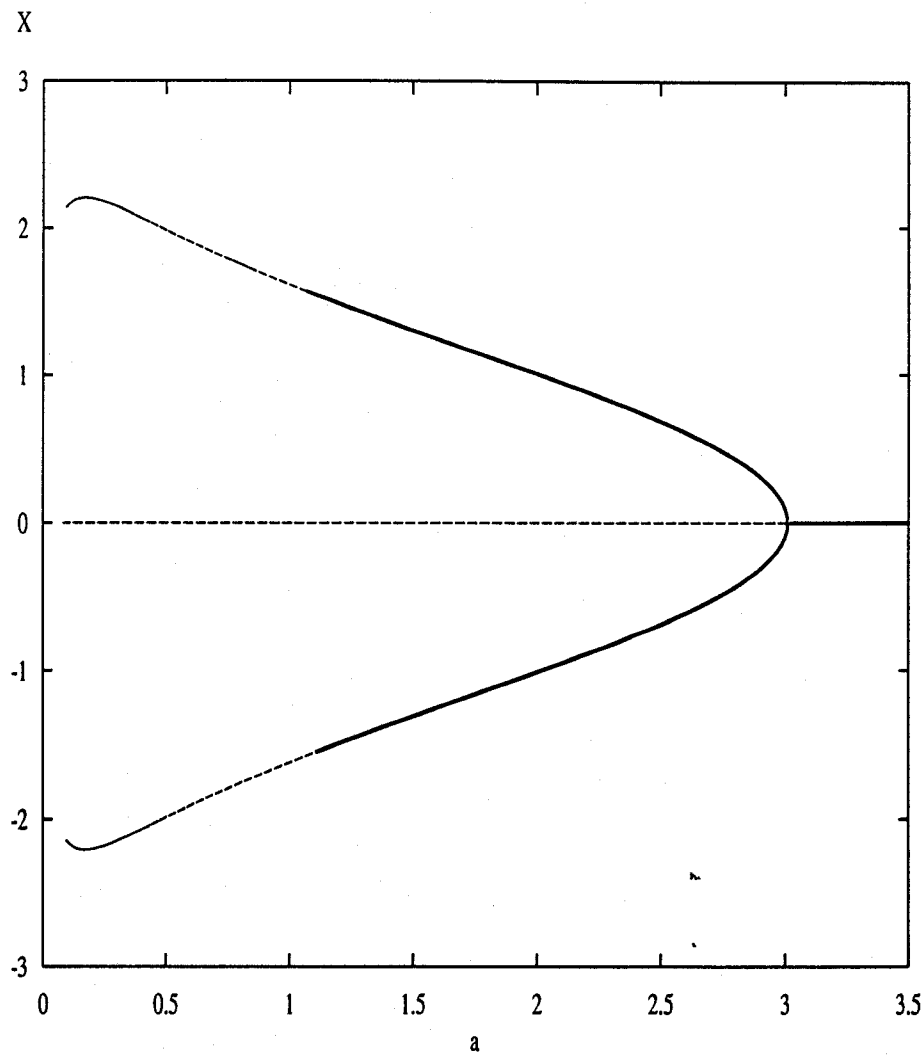

Figure 3.18: Bifurcation Diagram

to be supercritical.

When $a > 3.01$, the chartists are much more risk averse than the fundamentalists. The market is dominated by fundamentalists and prices converge to their fundamental value. When $1.17 < a < 3.01$, the chartists are somewhat more risk averse, and trajectories converge to a positive fixed point $(\bar{x}, \bar{m}, \bar{y})$. When $a < 1$ the fundamentalists are more risk averse. The market is dominated by chartists. Prices converge to a limit cycle rather than to a single value or, if $a < 0.9$, it is impossible for prices to be accurately predicted due to the chaos in the system. It is expected that $a < 1$, and hence the latter is the likely scenario in real markets.

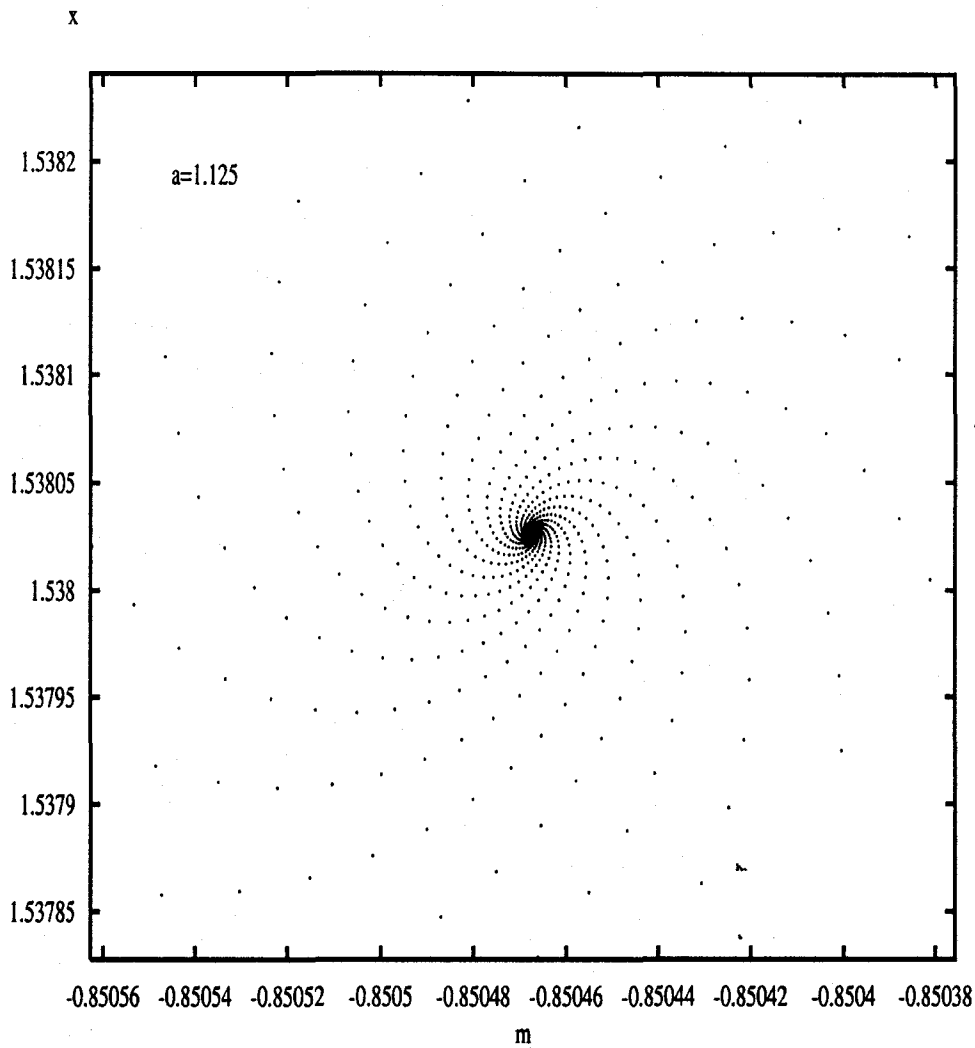

Figure 3.19: Phase diagram before Neimark–Sacker bifurcation ($a = 1.125$)

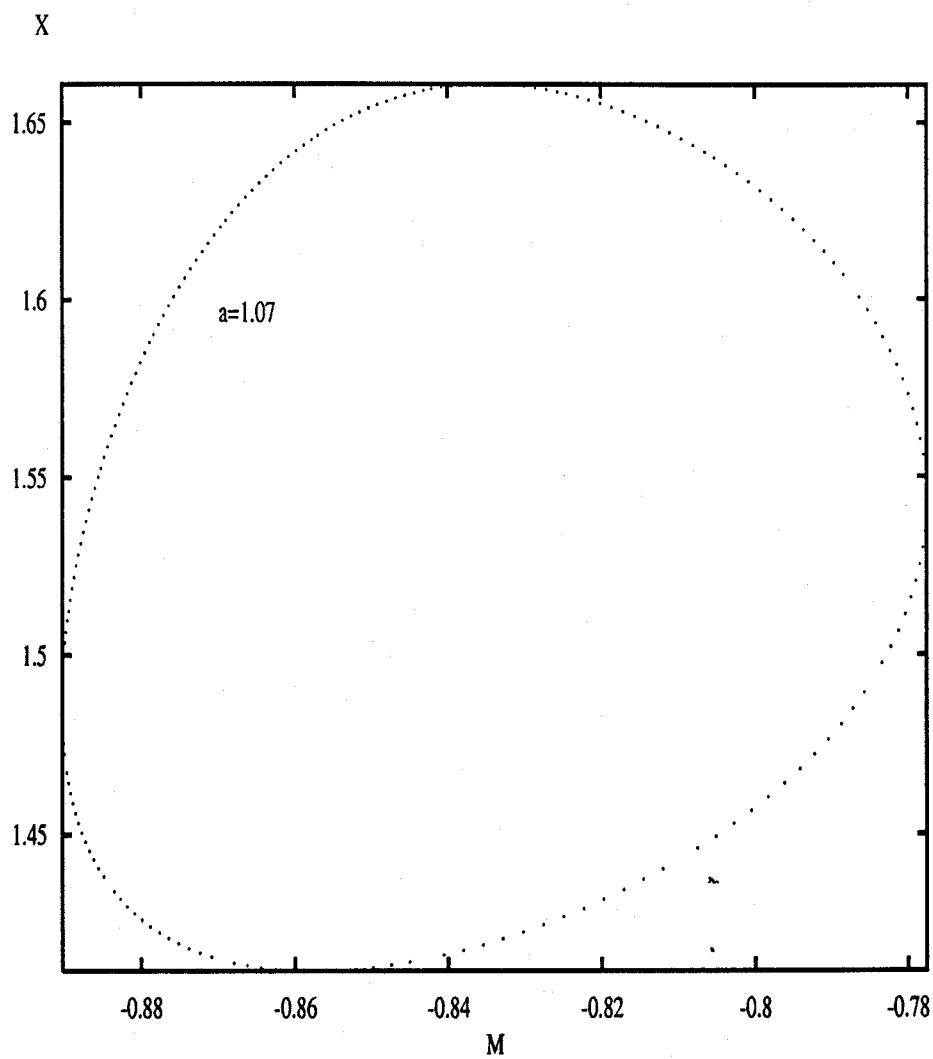

Figure 3.20: Phase diagram illustrating Neimark–Sacker bifurcation ($a = 1.07$)

Chapter 4

New Model

The models presented in [11] and [36] do not account for those chartists known as contrarians. The contrarian approach to investing is quite common in the markets, and the rewards for acting contrary to the majority of investors can be great. Thus, it is natural to include this group in asset pricing models. In this chapter, the contrarian approach to investing is examined, and a new asset pricing model which accounts for this group is introduced. The derivation and analysis of this model are presented in this chapter.

4.1 Contrarian Chartists

Contrarians are those investors who, using trading rules and trends of past prices, choose to take a contrary view of future asset prices at certain times. Thus, although they often have a similar expectation of the price change between the present time and one time period in the future, they sometimes predict prices to change in the opposite direction of "trend–chasing" chartists.

When the price of a stock rises, many investors tend to allocate more of their wealth to that stock because they think the price will continue to increase (*i.e.*, they receive a buying signal). Since investors have purchased the stock at a high price, there is a great amount of risk involved in investing in this stock and there is no guarantee that the price will keep rising. Throughout history, there are countless situations where acting on buying signals has caused investors to lose great deals of money.

A contrarian considers the opinions of other investors, and when this opinion becomes unreasonable or extreme, they invest against it [21]. For instance, they would rather allocate more wealth to a stock when its price is low. The initial risk involved in this investment is much less than the case of a trend–chaser who buys when the price is high. Although this is true, the price of the stock may never reach the level anticipated by contrarians, and thus they may profit very little, if at all, from this investment. It is often the case, however, that a major decrease in price occurs, and after a period of time prices begin to increase to normal levels, or even exceed these levels. In these cases, contrarians can make huge profits.

4.2 Other Models which Include Contrarians

As mentioned in Chapter 1, several dynamical systems models consider contrarian chartists. For instance, [12] incorporates contrarian chartists through the parameter d. If d is negative, but close to zero, then chartists are weakly opposing the current price trends. If d is negative and far from zero then chartists are strongly opposing current price trends.

When trend–chasers and contrarians co–exist and are risk–takers in the markets, asset prices tend to stabilize at the fundamental value. As the level of risk taken by contrarians decreases, and trend–chasers continue to be risk takers, prices exhibit period–2 behaviour, limit cycle behaviour, and prices eventually explode when the risk aversion coefficient for contrarians is low enough.

The approach taken in this thesis allows for all three trader groups to co–exist and to each satisfy their own unique properties. These properties are incorporated into the model by choosing appropriate functions which satisfy the entire set of properties for each trader group.

4.3 The Model

We begin by introducing the notation used in the development of this model. As in [11], let P_t denote the logarithm of the asset price at time t and D_t denote excess demand for the asset at time t. This demand is comprised of fundamentalist and chartist demand. We will denote fundamentalist demand at time t by D_t^f and chartist demand at time t by D_t^c. Since fundamentalists form beliefs concerning the fundamental value of the asset at time t, the demand for the asset by fundamentalists depends on how close the price at time t is to the perceived fundamental value. Thus, we can express this demand as

$$D_t^f = a(F_t - P_t), \tag{4.3.1}$$

where F_t is the logarithm of the fundamental value of the asset at time t. As in [11], the parameter a illustrates how strongly the fundamentalists react to mispricing in the market. Fundamentalists will buy when they believe the

market price is below the fundamental value, and will sell when they believe the market price is above the fundamental value. The extent of the reaction to mispricing affects a fundamentalist's decision to buy or sell, and hence the need for such a parameter. In this model, as in [11], the logarithm of the fundamental value of the asset is assumed known and constant, and hence we can let $F_t = F$.

Chartist demand is composed of trend–chasing chartist demand and contrarian demand, *i.e.*,

$$D_t^c = D_t^{c_1} + D_t^{c_2}. \tag{4.3.2}$$

We will let c_1 represent trend chasers and c_2 represent contrarians. Trend chasers base expectations of future prices on previous price changes, patterns, and the behaviour of other investors. Their expectation of the price change from the current time t to the next period $t+1$, denoted $\gamma_{t,t+1}$ is, by definition, given as

$$\begin{aligned} \gamma_{t,t+1} &= E_t[P_{t+1} - P_t] && (4.3.3)\\ &= E_t[P_{t+1}] - E_t[P_t] && (4.3.4)\\ &= E_t[P_{t+1}] - P_t, && (4.3.5) \end{aligned}$$

where E_t is the expectation at time t. $E_t[P_t] = P_t$ since at time t the asset price is already known.

Chartists allocate their wealth between a risky and riskless asset. This allocation depends on the expected return differential, $\gamma_{t,t+1} - b_t$, where b_t is the return on the riskless asset at time t. The riskless asset could be, for example, a government bond, which has a negligible amount of risk associated with it. The return on this asset, as in [11], is considered constant and hence $b_t = b$.

The demand of each chartist type is given as a function of this differential.

For trend chasing chartists, we write the demand for the risky asset at time t as

$$D_t^{c_1} = g_1(\gamma_{t,t+1} - b). \tag{4.3.6}$$

Strict conditions must be placed on the function g_1 so that for each value of the return differential a realistic value of the excess demand corresponds. For example, if the return differential at time t is positive, more wealth will be allocated to the risky asset and hence the excess demand will obtain a positive value. In other words, if $\gamma_{t,t+1} - b > 0$ then chartists receive a buying signal and hence they increase the number of shares of the risky asset which they own. If the return differential at time t is negative, more wealth will be allocated to the riskless asset and hence the excess demand will obtain a negative value. In other words, if $\gamma_{t,t+1} < 0$ then chartists sell some of their shares of the risky asset.

There are several choices when selecting a function which accurately describes the excess demand of trend–chasers. The choice of a function, g_1, is not as important as the underlying properties of the function. Similar to the properties listed in [11], we reason that the general function g_1 should be twice differential, and have the following restrictions: (where $x = \gamma_{t,t+1} - b$):

1. $g_1(-x) = -g_1(x)$ (*i.e.*, the function is odd). An odd function is symmetric with respect to the origin. Thus, an increase in the return differential from zero will cause the excess demand to shift by the same amount as a corresponding decrease in the return differential from zero. In other words, a trend–chasers idea of the trend is the same for increases and decreases in the return differential.

2. $g_1'(x) > 0 \ \forall x \in \mathbb{R}$. Mathematically this means that the function is increasing for all real numbers. Quite simply, the excess demand increases as the value of the return differential increases.

3. $g_1''(x) > 0 \ \forall x < 0$ and $g_1''(x) < 0 \ \forall x > 0$. Mathematically this means that the function is concave down if $x > 0$ and the function is concave up if $x < 0$ (*i.e.*, the origin is an inflection point). Although the function increases as x increases, the rate at which the excess demand increases actually decreases as the return differential increases from zero. Likewise, the rate at which the excess demand decreases actually decreases as the return differential decreases from zero.

4. $\lim_{x \to \pm\infty} g_1'(x) = 0$. As the absolute value of the return differential gets large, wealth is either allocated completely in the riskless asset or completely in the risky asset. The excess demand for either asset cannot realistically tend to infinity, so this condition bounds the excess demand from above and below.

While these properties are similar to those outlined in [11], one of their properties ($g(0) = 0$) is omitted from those outlined above since it is redundant (an odd function necessarily passes through the origin). Also, the x° discussed in their model (the point of inflection on the graph) is the origin in our case.

Due to the above properties, the choices for the demand function are restricted. A common choice for such a function is

$$g_1(\gamma_{t,t+1} - b) = \alpha \arctan(\gamma_{t,t+1} - b), \alpha > 0, \tag{4.3.7}$$

which is consistent with the function chosen in [11].

We have that

1. $g_1(-x) = \alpha \arctan(-x) = -\alpha \arctan(x) = -g_1(x)$
2. $\frac{d}{dx}(\alpha \arctan x) = \frac{\alpha}{1+x^2} > 0 \ \forall x \in \mathbb{R}$
3. $\frac{d}{dx}\left(\frac{\alpha}{1+x^2}\right) = \frac{-2\alpha x}{(1+x^2)^2}$. Thus, $\frac{d^2}{dx^2}(\alpha \arctan x) > 0 \ \forall x < 0$ and $\frac{d^2}{dx^2}(\alpha \arctan x) < 0 \ \forall x > 0$.
4. $\lim_{x\to\infty} \frac{\alpha}{1+x^2} = 0$ and $\lim_{x\to-\infty} \frac{\alpha}{1+x^2} = 0$.

The properties of g_1 are thus satisfied by our chosen function, and this will be the function used throughout the analysis of the model. However, the analytical results will depend on the properties of g_1 and not the function itself.

The expectation of price change between t and $t+1$ depends on the amount of success that trend-chasers have at accurately measuring the price change in the past. Thus, as in [11] we can further write $\gamma_{t,t+1}$ as

$$\gamma_{t,t+1} = \gamma_{t-1,t} + c[P_t - P_{t-1} - \gamma_{t-1,t}]. \tag{4.3.8}$$

Thus, the difference between the actual change in price from $t-1$ to t and the expected change in price during the same period is examined. If this value is negative (*i.e.*, the expected price change in the previous period was too high), then the expectation of the price change between t and $t+1$ will be less than the expectation of price change between $t-1$ and t. Similarly, if this value is positive, then the expectation of price change between t and $t+1$ will be greater than the expected change between $t-1$ and t. Trend-chasing chartists must constantly adjust their estimates of the changes in future prices. The rate at which they make these changes about current trends is a key factor

when forming expectations of price changes. Thus, as in [11] the parameter c has been inserted into the above equation. This parameter represents the rate at which they update their current estimate of the trend of future price changes, and will realistically take values between 0 and 1.

For contrarian chartists, we write the demand for the asset at time t as

$$D_t^{c_2} = g_2(\gamma_{t,t+1} - b). \tag{4.3.9}$$

Since contrarian chartists may react in different ways, there are several possible options when choosing a demand function for this group. This function depends on the attitude of the investor. Let us consider two possibilities.

4.3.1 Case 1: Pure contrarians

The first case deals with pure contrarians. A pure contrarian always goes against the trend of past price changes. If the majority is buying then they are selling, and if the majority is selling then they are buying. Thus, if the expectation of price change increases from one period to the next then the excess demand for the asset will decrease, and vice–versa.

The demand function for such a group can be characterized by the following properties:

1. $g_2(-x) = -g_2(x)$. As in the case of trend–chasers, the function is symmetric with respect to the origin so that deviations of the return differential from zero shift the excess demand by the same amount in the proper direction.

2. $g_2'(x) < 0 \ \forall \ x \in \mathbb{R}$. Contrary to the function chosen for trend–chasing

chartists, this function is decreasing. If the return differential increases from one period to the next then the excess demand *decreases.*

3. $g_2''(x) < 0 \; \forall x < 0$ and $g_2''(x) > 0 \; \forall x > 0$. Again, the function has a point of inflection at the origin, however in this case the function is concave up when $x > 0$ and concave down when $x < 0$.

4. $\lim_{x \to \pm\infty} g_2'(x) = 0$. As the absolute value of the return differential gets large, wealth is either allocated completely in the riskless asset or completely in the risky asset. The excess demand for either asset cannot realistically tend to infinity, so this condition prevents this from occuring, as in the case for trend–chasers.

An appropriate demand function for such a contrarian could take the form

$$g_2(\gamma_{t,t+1} - b) = \mu \arctan(\gamma_{t,t+1} - b), \mu < 0. \tag{4.3.10}$$

We have that

1. $g_2(-x) = \mu \arctan(-x) = -\mu \arctan(x) = -g_2(x)$
2. $\dfrac{d}{dx}(\mu \arctan x) = \dfrac{\mu}{1+x^2} < 0 \; \forall x$ (since $\mu < 0$)
3. $\dfrac{d}{dx}\left(\dfrac{\mu}{1+x^2}\right) = \dfrac{-2\mu x}{(1+x^2)^2}$. Thus, $\dfrac{d^2}{dx^2}(\mu \arctan x) < 0 \; \forall x < 0$ and $\dfrac{d^2}{dx^2}(\mu \arctan x) > 0 \; \forall x > 0$.
4. $\lim_{x \to -\infty} \dfrac{\mu}{1+x^2} = 0$ and $\lim_{x \to \infty} \dfrac{\mu}{1+x^2} = 0$

The properties of g_2 are thus satisfied by our chosen function, and this will be the function used when analyzing this case of the model.

The model will be analyzed and discussed in Section 4.4.

4.3.2 Case 2: Another Interpretation of Contrarians

Many experts believe that to succeed as a contrarian investor, one must not only disagree with the majority but they must also know when to act on the disagreement. When the right time to buy and sell arises, a contrarian takes action and then waits for the majority to share the same point of view. If this occurs, then a contrarian and a trend chaser are in agreement while the stock price rises or falls, as only a majority can push prices enough to make the initial buy or sell worthwhile to the contrarian.

This second case deals with those contrarians who do just this. They closely monitor the markets and decide when it is a good time to act contrary to prevailing wisdom. For instance, if the price of a certain asset drops substantially over a period of time, the majority of investors may decide to sell their shares of the asset. These contrarians assess the situation carefully, and if they believe that investors have overreacted, they may decide to purchase shares of the asset at the current lower price. They then wait to see if their assessment was correct. If the majority of investors have overreacted, then eventually the trend chasers will change their view, and will side with the contrarian traders. Hence, it is only when the asset price has been beaten down that the two groups differ: when trend–chasers are getting rid of their shares, contrarians are buying them. If an overreaction has occured, the trend–chasers eventually come around, and the two trader types are in total agreement while the asset price rises.

Similarly, when contrarians feel that the price of the asset has peaked and cannot be pushed any further, they may decide to sell, even if the asset price has shown no decrease and other investors are still buying. They think it

is unlikely to continue to profit from owning shares the asset, and that the current price exceeds the actual worth of the asset. Thus, they sell their shares at a much higher price than which they bought them and hence profit from the investment. If the price of the asset has not actually been pushed to the limit, and the price continues to rise, then contrarians may miss out on further profits [21].

In terms of the model, contrarians are buying when the return differential is close to zero, hoping that prices will begin to increase. If this is the case, then trend chasers will see this as an investment opportunity and will also buy. Contrarians are selling when the return differential is far from zero under the impression that prices have peaked and will not continue their upward trend.

1. $g_2(-x) = -g_2(x)$. Again, the function is symmetric with respect to the origin so that deviations of the return differential from zero shift the demand by the same amount in the proper direction.

2. $\exists!\ x^\circ > 0$ such that $g_2''(x) < 0\ \forall\ 0 < x < x^\circ$ and $g_2''(x) > 0\ \forall x > x^\circ$. The value of x° in this case is different from that of trend–chasing chartists (for whom $x^\circ = 0$). This is since, when the return differential is small, contrarians behave similar to trend–chasing chartists. However, for a certain (absolute) value of the return differential, contrarian chartists take a contrary view of future price changes, and hence the excess demand begins to shift in the opposite direction.

3. $\lim_{x\to\pm\infty} g_2'(x) = 0$. As the absolute value of the return differential tends to infinity, investor wealth is all in the riskless asset or all in the risky asset. As this absolute value increases, the rate at which the demand for

the risky asset changes approaches zero so that demand does not reach unrealistic values.

Due to the above properties, the choices for the demand function are again restricted. One such function which satisfies the above properties is

$$g_2(\gamma_{t,t+1} - b) = \frac{m(\gamma_{t,t+1} - b) - (\gamma_{t,t+1} - b)^3}{\sqrt{(\gamma_{t,t+1} - b)^6 + m^2}}, c > 0. \tag{4.3.11}$$

A graph displaying the general shape of such a function is given in Figure 4.1

The total excess demand for the asset at time t is the sum of the fundamentalist demand, the trend chasing chartist demand and the contrarian chartist demand:

$$D_t = D_t^f + D_t^{c_1} + D_t^{c_2}. \tag{4.3.12}$$

More specifically,

$$D_t = \alpha(F - P_t) + g_1(\gamma_{t,t+1} - b) + g_2(\gamma_{t,t+1} - b). \tag{4.3.13}$$

From this equation, the asset price can be determined. The price at time $t + 1$ is given as

$$P_{t+1} = P_t + \beta_p[\alpha(F - P_t) + g_1(\gamma_{t,t+1} - b) + g_2(\gamma_{t,t+1} - b)], \tag{4.3.14}$$

where $\beta_p > 0$ represents the speed at which the price adjusts to the excess demand. This is consistent with [11]. The following system can be used to model the expectation of price change between two consecutive time periods as well as the actual price at the end of the same period:

$$\begin{cases} P_{t+1} = P_t + \beta_p[a(F - P_t) + g_1(\gamma_{t,t+1} - b) + g_2(\gamma_{t,t+1} - b)] \\ \gamma_{t,t+1} = \gamma_{t-1,t} + c[P_t - P_{t-1} - \gamma_{t-1,t}] \end{cases} \tag{4.3.15}$$

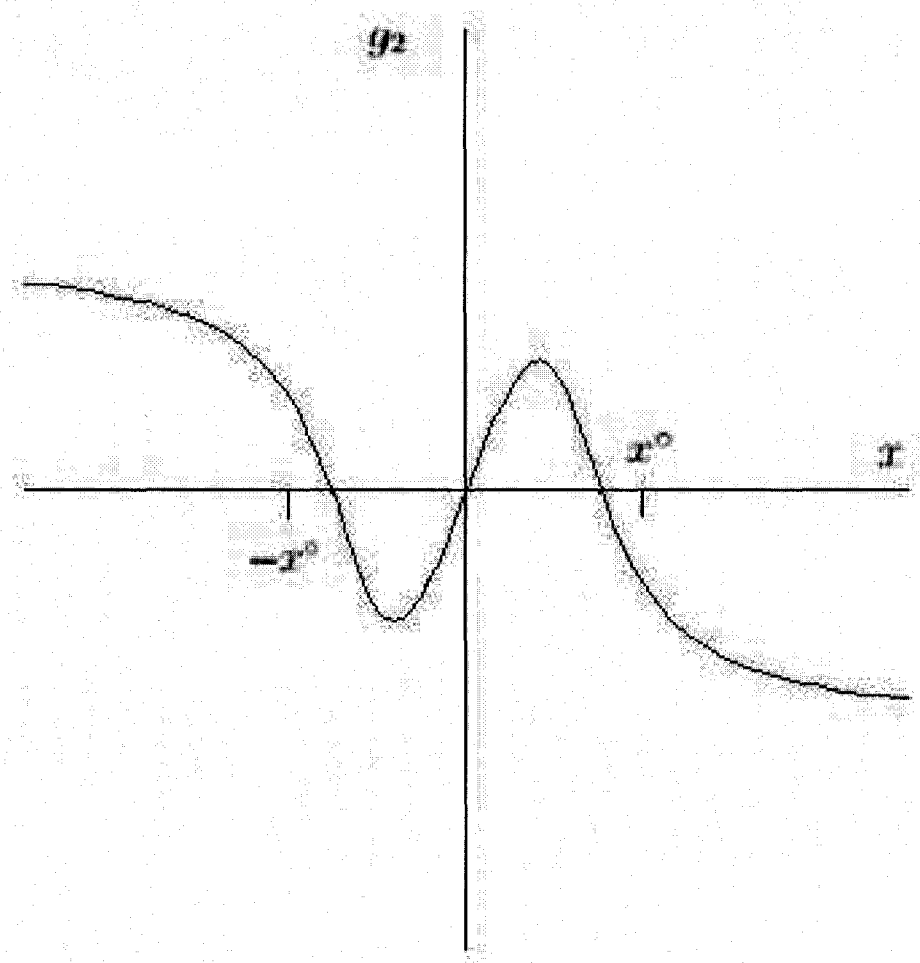

Figure 4.1: Contrarian Demand Function

4.4 Analysis

In this section, the dynamics of both cases will be explored. The results will then be compared to those obtained from the other dynamical systems models discussed in this thesis.

In either case, equation (4.3.15) can be written as the following:

$$\begin{aligned} P &\mapsto P + \beta_p \left[a(F-P) + g_1(\gamma - b) + g_2(\gamma - b)\right] \\ \gamma &\mapsto (1-c)\gamma + c\beta_p \left[a(F-P) + g_1(\gamma - b) + g_2(\gamma - b)\right]. \end{aligned} \tag{4.4.1}$$

Fixed points are found by solving the following system:

$$\begin{aligned} \bar{P} &= \bar{P} + \beta_p \left[a(F-\bar{P}) + g_1(\bar{\gamma} - b) + g_2(\bar{\gamma} - b)\right] \\ \bar{\gamma} &= (1-c)\bar{\gamma} + c\beta_p \left[a(F-\bar{P}) + g_1(\bar{\gamma} - b) + g_2(\bar{\gamma} - b)\right]. \end{aligned} \tag{4.4.2}$$

One fixed point results from solving this system, namely

$$(\bar{P}, \bar{\gamma}) = \left(F + \frac{g_1(-b) + g_2(-b)}{a}, 0\right).$$

As in [11], we introduce the price deviation, p, such that

$$p = P - \left(F + \frac{g_1(-b) + g_2(-b)}{a}\right).$$

Hence, the new map T_1 (in terms of p and γ), given by

$$T_1 : \begin{cases} p \mapsto p - \beta_p \left(ap - [k_1(\gamma) + k_2(\gamma)]\right) \\ \gamma \mapsto (1-c)\gamma - c\beta_p \left(ap - [k_1(\gamma) + k_2(\gamma)]\right) \end{cases}, \tag{4.4.3}$$

where $k_i(\gamma) = g_i(\gamma - b) - g_i(-b)$, has a unique fixed point at the origin.

To obtain stability results, the eigenvalues of the Jacobian matrix corresponding to (4.4.3) are found. The Jacobian matrix is as follows:

$$J = \begin{bmatrix} 1 - a\beta_p & \beta_p \left[k_1'(\gamma) + k_2'(\gamma)\right] \\ -ac\beta_p & 1 - c + c\beta_p \left[k_1'(\gamma) + k_2'(\gamma)\right] \end{bmatrix}. \tag{4.4.4}$$

The Jacobian matrix is then evaluated at $(0,0)$ so that the corresponding eigenvalues can be obtained:

$$J(0,0) = \begin{bmatrix} 1-a\beta_p & \beta_p\left[k_1'(0)+k_2'(0)\right] \\ -ac\beta_p & 1-c+c\beta_p\left[k_1'(0)+k_2'(0)\right] \end{bmatrix}. \tag{4.4.5}$$

We now find the eigenvalues using the characteristic equation, given as $\det(J(0,0)-\lambda I)=0$. More precisely,

$$\begin{vmatrix} 1-a\beta_p-\lambda & \beta_p\left[k_1'(0)+k_2'(0)\right] \\ -ac\beta_p & 1-c+c\beta_p\left[k_1'(0)+k_2'(0)\right]-\lambda \end{vmatrix} = 0. \tag{4.4.6}$$

Simplifying gives

$$\lambda^2-\lambda(2-c+c\beta_p[k_1'(0)+k_2'(0)]-a\beta_p)+1-c+c\beta_p[k_1'(0)+k_2'(0)]-a\beta_p+ac\beta_p=0. \tag{4.4.7}$$

The eigenvalues resulting from the above equation are as follows:

$$\lambda_{1,2} = \frac{2-a\beta_p-c+c\beta_p[k_1'(0)+k_2'(0)]}{2} \pm \frac{\sqrt{a^2\beta_p^2-2ac\beta_p(1+\beta_p[k_1'(0)+k_2'(0)])+c^2(1-\beta_p[k_1'(0)+k_2'(0)]+\beta_p^2[k_1'(0)+k_2'(0)]^2)}}{2}.$$

The unique fixed point $(p,\gamma)=(0,0)$ is stable when $|\lambda_{1,2}|<1$. This occurs when

$$\frac{2(a\beta_p-2)}{2\beta_p[k_1'(0)+k_2'(0)]+a\beta_p-2} < c < \frac{a\beta_p}{\beta_p[k_1'(0)+k_2'(0)]+a\beta_p-1},$$

assuming that no division by a negative number has occured when simplifying the inequality. If either denominator is negative, that particular inequality is reversed in sign. For all other ranges of the parameter c the fixed point $(0,0)$ is unstable.

Bifurcations are found to occur at the following values of the parameter c:

$$c = \frac{2(a\beta_p - 2)}{2\beta_p[k_1'(0) + k_2'(0)] + a\beta_p - 2} \tag{4.4.8}$$

and

$$c = \frac{a\beta_p}{\beta_p[k_1'(0) + k_2'(0)] + a\beta_p - 1}. \tag{4.4.9}$$

We will now look at these bifurcation values for each case of the new model. The results (obtained using orbit diagrams) will be given, and compared to results previously given. Global bifurcations occuring in the system will also be analyzed. This will be carried out in the same manner as in Chapter 3.

4.5 Case 1

In (4.4.3) we have that

$$\begin{aligned} k_1(\gamma) &= g_1(\gamma - b) - g_1(-b) \\ &= \alpha(\arctan(\gamma - b) - \arctan(-b)) \end{aligned} \tag{4.5.1}$$

and

$$\begin{aligned} k_2(\gamma) &= g_2(\gamma - b) - g_2(-b) \\ &= \mu(\arctan(\gamma - b) - \arctan(-b)). \end{aligned} \tag{4.5.2}$$

Thus,

$$k_1'(\gamma) = \frac{\alpha}{1 + (\gamma - b)^2} \tag{4.5.3}$$

and

$$k_2'(\gamma) = \frac{\mu}{1 + (\gamma - b)^2}. \tag{4.5.4}$$

In this case g_1 and g_2 are the same underlying function, and hence

$$k_1'(0) + k_2'(0) = \frac{(\alpha + \mu)}{1 + b^2}. \tag{4.5.5}$$

Thus, (4.4.3) reduces to (3.2.3) in Chapter 3, with the parameter α now being replaced by $\alpha + \mu$, where μ is known to be negative.

4.5.1 $\mu = -1.0$

Using the following parameter values, the numerical values of the bifurcations (in terms of c) can be obtained: $a = 1.8$, $\beta_p = 1.8$, $b = 0.5$, $\alpha = 2.3$, $\mu = -1.0$. To do this we use (4.4.8) and (4.4.9). Figure 4.2 is the orbit diagram corresponding to Case 1 of the new model using the above parameter values.

As c increases through $c^* \approx 0.498$, a period doubling bifurcation occurs. As in (1.3.12), this creates an unstable period–2 cycle when $c > c^*$. When $0.498 < c < 0.788$, prices converge to their fundamental value.

As in (1.3.12), there are a series of local bifurcations occuring in this model. For instance, when $c \approx 0.7249$, a saddle–node bifurcation in period–3 occurs, creating a locally stable period–3 cycle and an unstable period–3 cycle. This is shown in Figure 4.3. For $0.7249 < c < 0.772$, the fixed point at the origin and the period–3 cycle co-exist as local attractors. Thus, for most initial conditions prices will approach their fundamental value, but for some initial conditions prices will tend toward switching between the values in the period–3 cycle. This is similar to the situation in Chapter 3.2, where a saddle–node bifurcation in period–4 occured, and the locally stable period–4 cycle co–existed with the limit cycle for a range of c values. At $c \approx 0.772$, the period–3 cycles start a period–doubling cascade, eventually forming a local chaotic attractor (A_3).

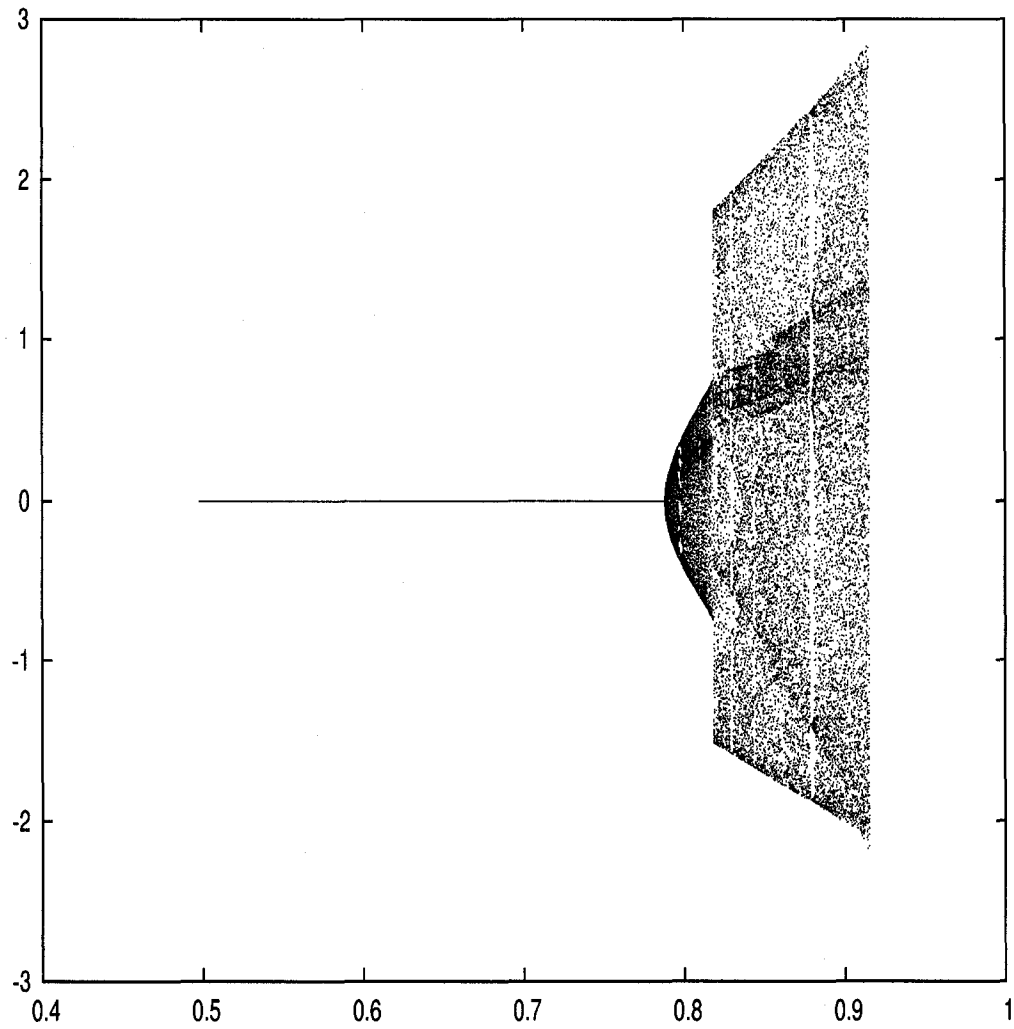

Figure 4.2: Orbit Diagram - Case 1 when $\mu = -1$

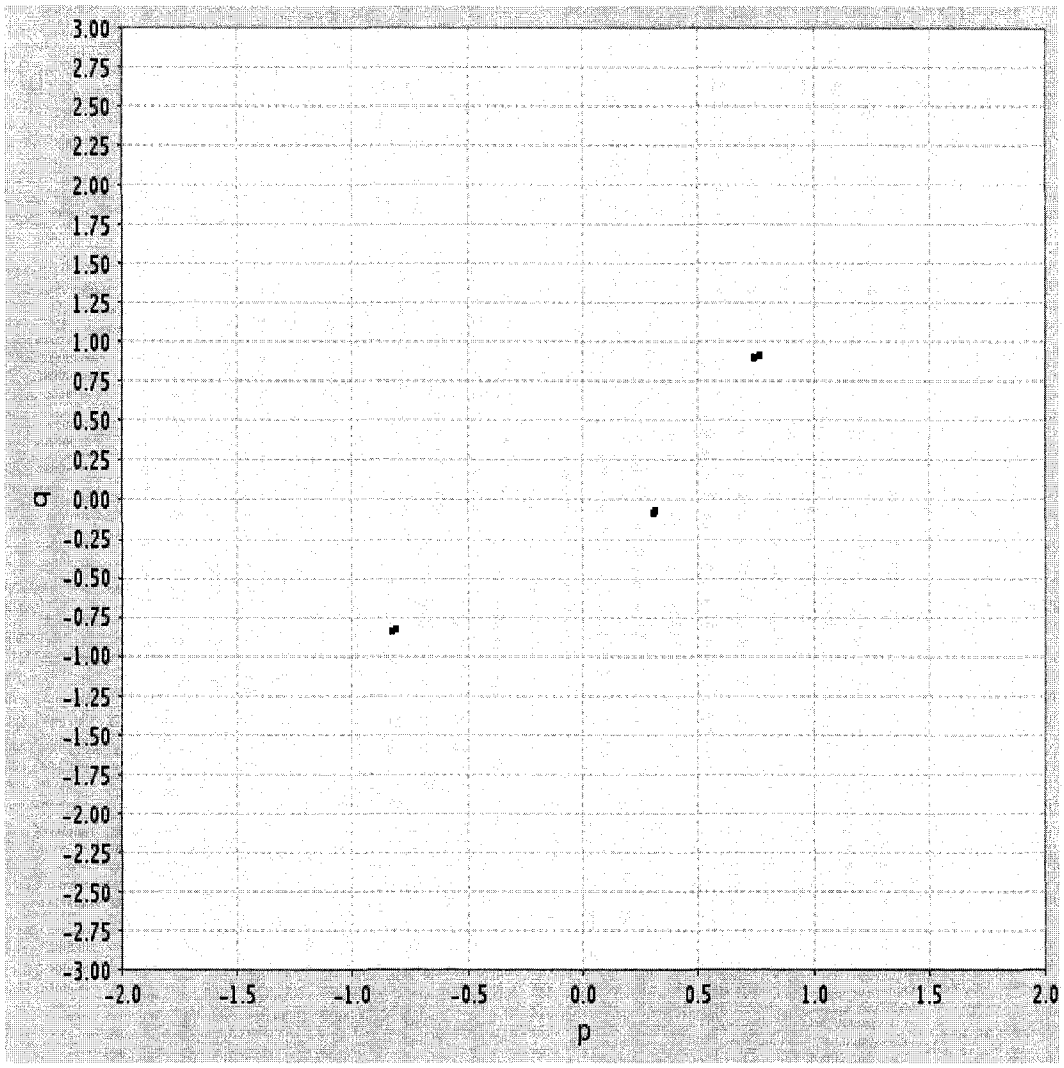

Figure 4.3: Saddle Node bifurcation in Period–3 ($c = 0.7249$)

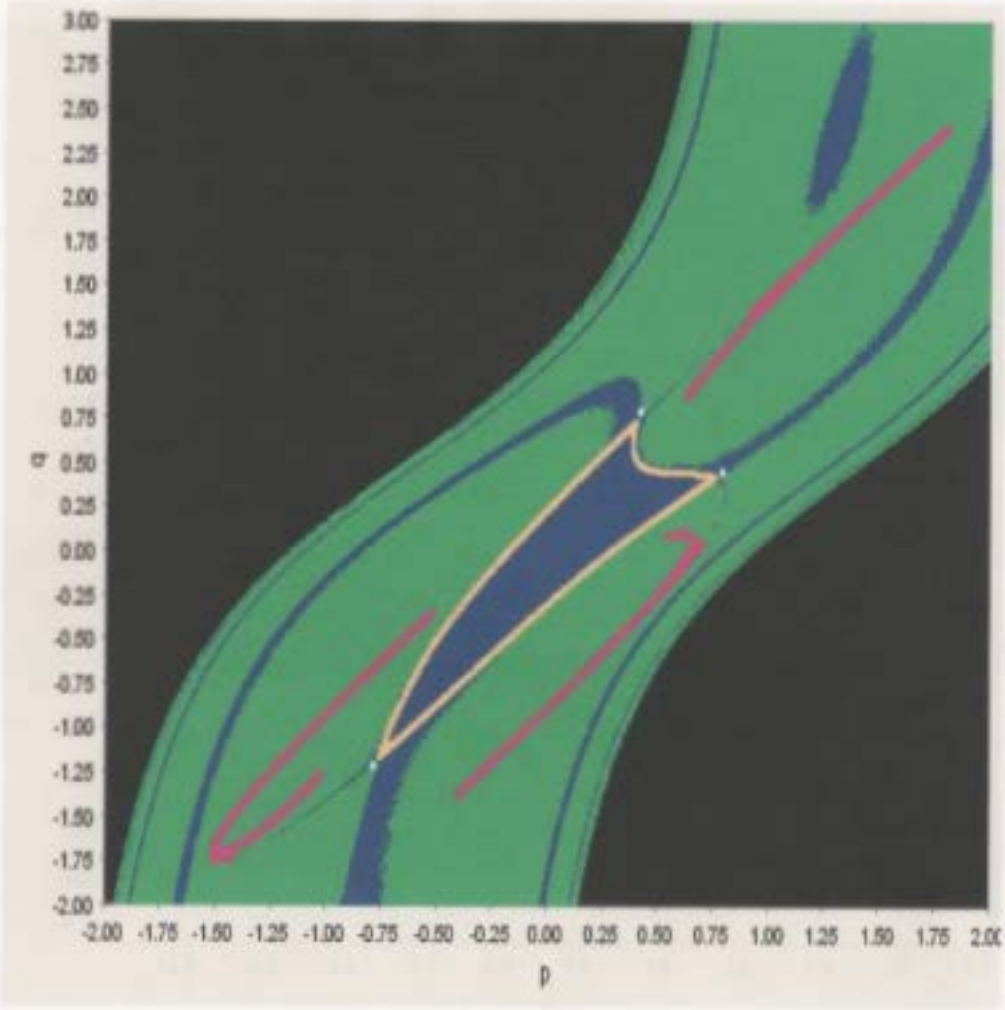

Figure 4.4: Contact Bifurcation ($c \approx 0.81812$)
The basin for the limit cycle is shown in blue, the basin for A_3 is shown in green, and the unstable period–3 cycle is shown in white.

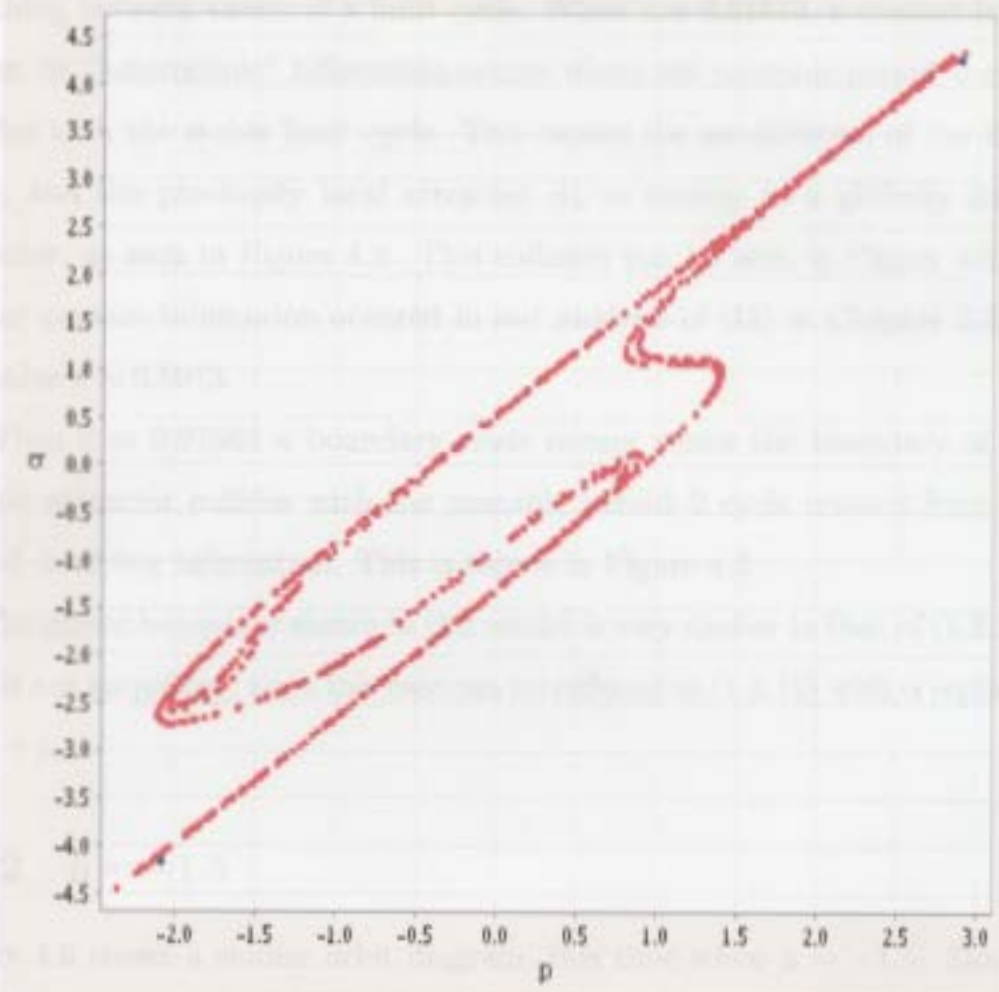

Figure 4.5: Boundary Crisis ($c \approx 0.91562$)
The unstable period–2 cycle is shown in blue.

At $c \approx 0.788$ a Neimark–Sacker bifurcation occurs, and prices are now switching between values of a limit cycle. When $c \approx 0.81813$, a contact bifurcation, or "heteroclinic" bifurcation occurs where the unstable period–3 cycle collides with the stable limit cycle. This causes the annihilation of the limit cycle, and the previously local attractor A_3 to emerge as a globally stable attractor, as seen in Figure 4.2. This collision can be seen in Figure 4.4. A similar contact bifurcation occured in our analysis of [11] in Chapter 3.2, at the value $c \approx 0.5913$.

When $c \approx 0.91562$ a boundary crisis occurs where the boundary of the chaotic attractor collides with the unstable period–2 cycle created from the period–doubling bifurcation. This is shown in Figure 4.5.

The global behaviour shown in this model is very similar to that of (1.3.12). This is not surprising, since this case can be reduced to (1.3.12) with α replaced by $\alpha + \mu$.

4.5.2 $\mu = -1.5$

Figure 4.6 shows a similar orbit diagram, this time when $\mu = -1.5$. Similar behaviour is shown, however the period–doubling bifurcation now occurs when $c \approx 0.6998$ and the Neimark–Sacker bifurcation now occurs when $c \approx 0.9552$. Thus, when contrarians consistently disagree with the majority of investors, and the degree to which they act on this disagreement is large enough, their actions stabilize asset prices.

When $0.6998 < c < 0.95$, prices typically tend to their fundamental value. At $c \approx 0.9362$, a saddle–node bifurcation in period–3 occurs. This creates a locally stable period–3 cycle and an unstable period–3 cycle. This cycle

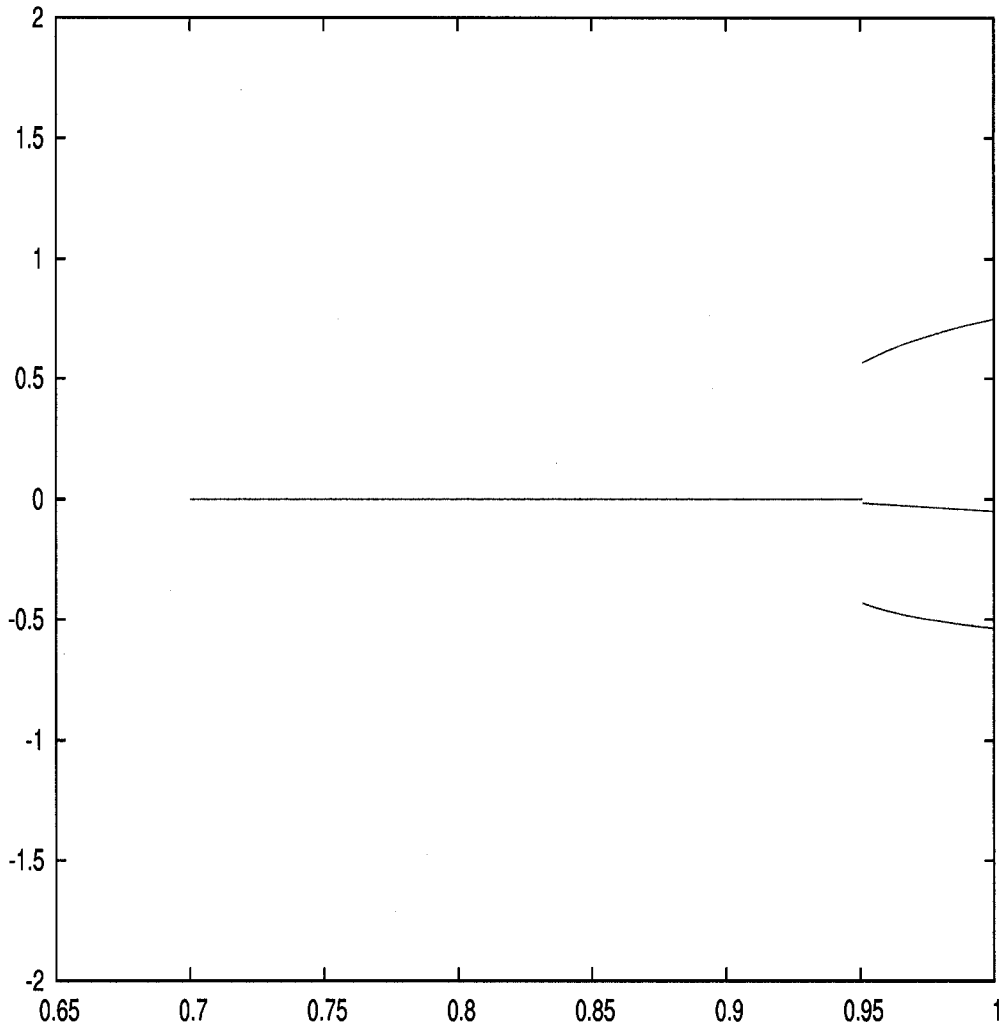

Figure 4.6: Orbit Diagram - Case 1 when $\mu = -1.5$

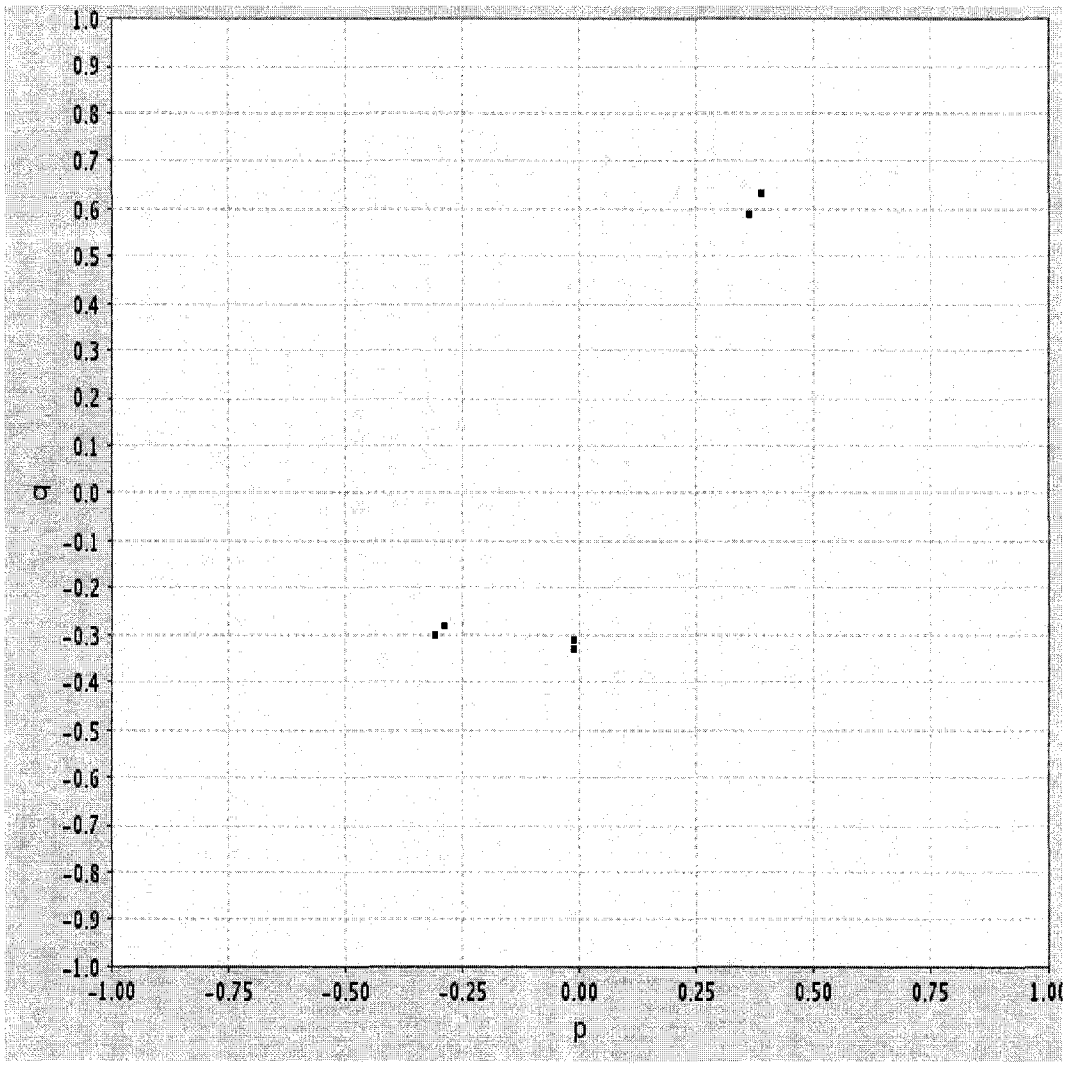

Figure 4.7: Period–3 Cycle ($c = 0.9362$)

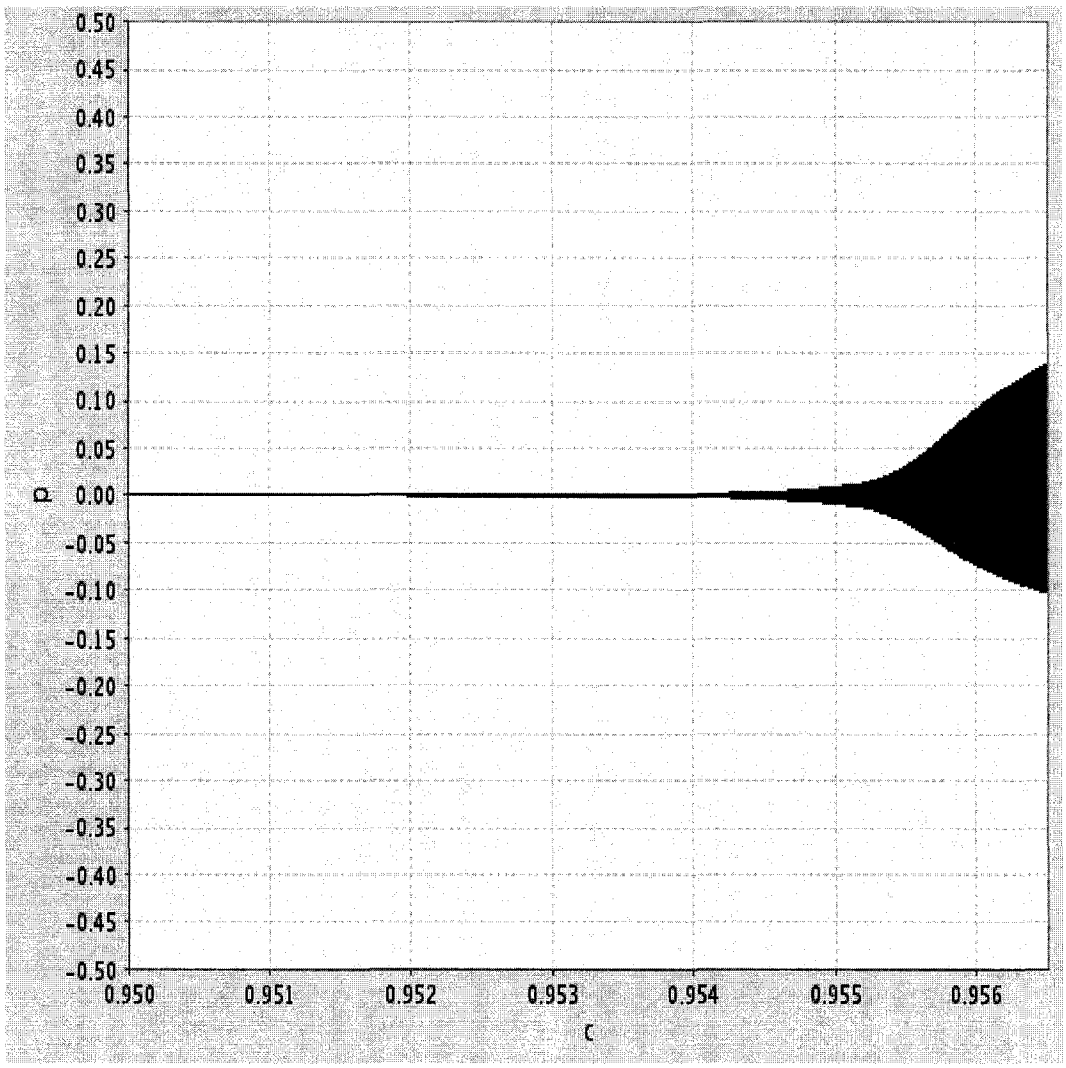

Figure 4.8: Limit Cycle Behaviour

is shown in Figure 4.7. The stable fixed point at the origin and the stable period–3 cycle co–exist as local attractors when $0.9362 < c < 0.95667$.

When $0.9552 < c < 0.95667$, the stable period–3 cycle co–exists with the limit cycle as local attractors. The amplitude of the limit cycle is very small, so for initial conditions which tend toward this cycle, prices are hovering very close to the fundamental price. The limit cycle is shown in Figure 4.8.

When $c \approx 0.95667$ a contact bifurcation ("heteroclinic" bifurcation") occurs where the stable limit cycle collides with the unstable period–3 cycle. A similar situation occurred in the case when $\mu = -1$ at $c \approx 0.81813$. This causes the limit cycle to disappear and the stable period–3 cycle to remain as the only attractor (except infinity). When $c > 0.95667$ prices tend to switch between the values of the period–3 cycle. It is unrealistic to go beyond $c > 1$, since chartists cannot update their estimate of the trend more often than they receive information.

4.6 Case 2

In (4.4.3) we have that

$$\begin{aligned} k_1(\gamma) &= g_1(\gamma - b) - g_1(-b) \\ &= \alpha(\arctan(\gamma - b) - \arctan(-b)) \end{aligned} \tag{4.6.1}$$

and

$$\begin{aligned} k_2(\gamma) &= g_2(\gamma - b) - g_2(-b) \\ &= \frac{m(\gamma - b) - (\gamma - b)^3}{\sqrt{(\gamma - b)^6 + m^2}} - \frac{b^3 - bm}{\sqrt{b^6 + m^2}} \end{aligned} \tag{4.6.2}$$

Thus,

$$k_1'(\gamma) = \frac{\alpha}{1+(\gamma-b)^2} \tag{4.6.3}$$

and

$$k_2'(\gamma) = \frac{m-3(\gamma-b)^2}{\sqrt{(\gamma-b)^6+m^2}} + \frac{3(\gamma-b)^5[(\gamma-b)^3-m(\gamma-b)]}{[(\gamma-b)^6+m^2]^{3/2}} \tag{4.6.4}$$

In this case, $k_1'(0)+k_2'(0)$ is much more complicated:

$$k_1'(0)+k_2'(0) = \frac{\alpha}{1+b^2} + \frac{(m-3b^2)(b^6+m^2)+3b^5(b^3-bm)}{(b^6+m^2)^{3/2}}. \tag{4.6.5}$$

4.6.1 $a = 1.8$, $\beta = 1.8$

Using the following parameter values, the numerical values of the bifurcations (in terms of c) can be obtained: $a = 1.8$, $\beta_p = 1.8$, $b = 0.5$, $\alpha = 2.3$, $m = 2.3$. With the given parameter values inserted into the above equations, (4.4.8) reduces to $c \approx 0.24$ and (4.4.9) reduces to $c \approx 0.48$. The orbit diagram displaying these bifurcations is given in Figure 4.9.

As c increases through $c^* \approx 0.24$ a period–doubling bifurcation takes place. As in the analysis of (1.3.12) and (4.4.3), this bifurcation creates an unstable period–2 cycle when $c > c^*$. This cycle is shown in Figure 4.10, when $c = 0.45$. This Figure shows the basin of attraction for the origin (in blue) and the basin for infinity (in black). The unstable period–2 cycle is given in white. As in the analysis of the basin structures for (1.3.12), the unstable period–2 cycle determines the size of the basin of attraction for the origin.

When $0.24 < c < 0.48$, prices typically converge to their fundamental value. This range of values is less than the range of values for which p tends to zero in (1.3.12). Thus, the impact of fundamental traders on asset prices decreases when trend chasers and contrarian traders both exist in the markets.

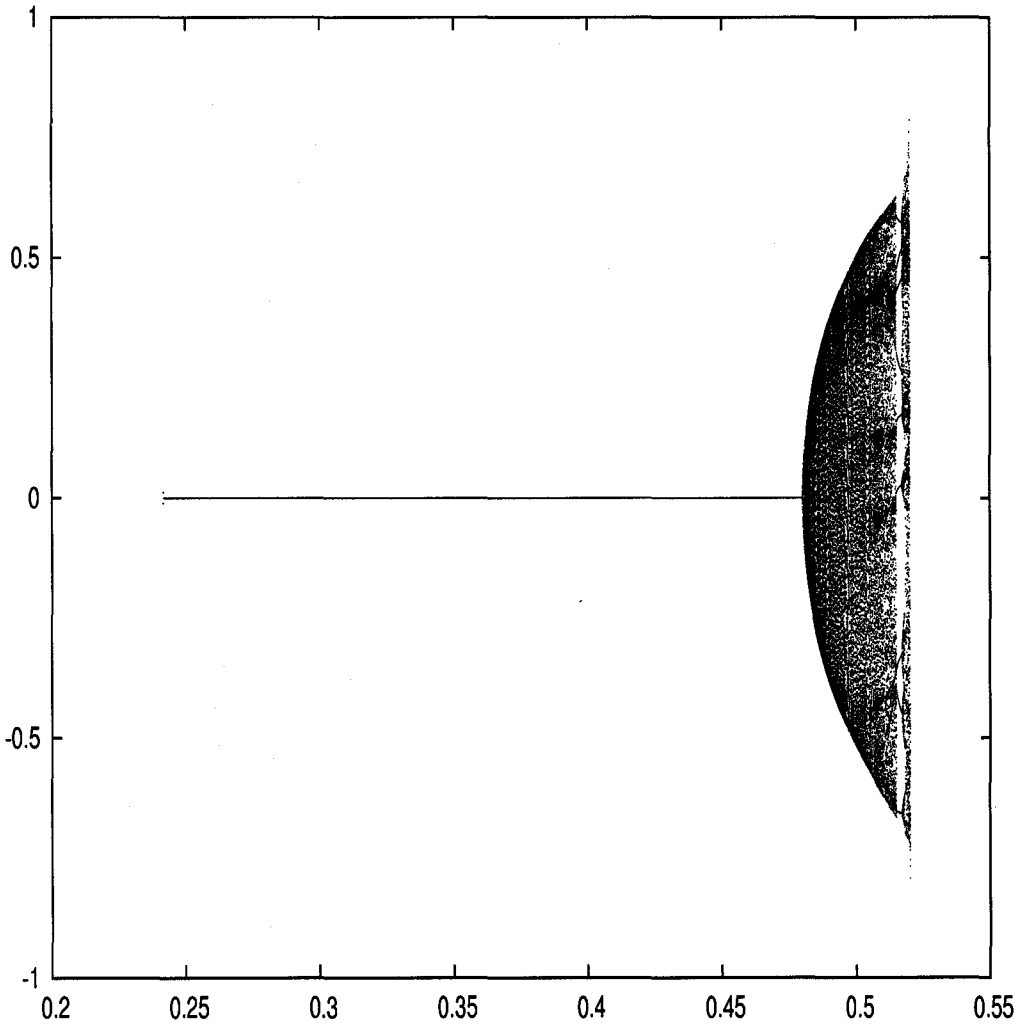

Figure 4.9: Orbit Diagram – Case 2

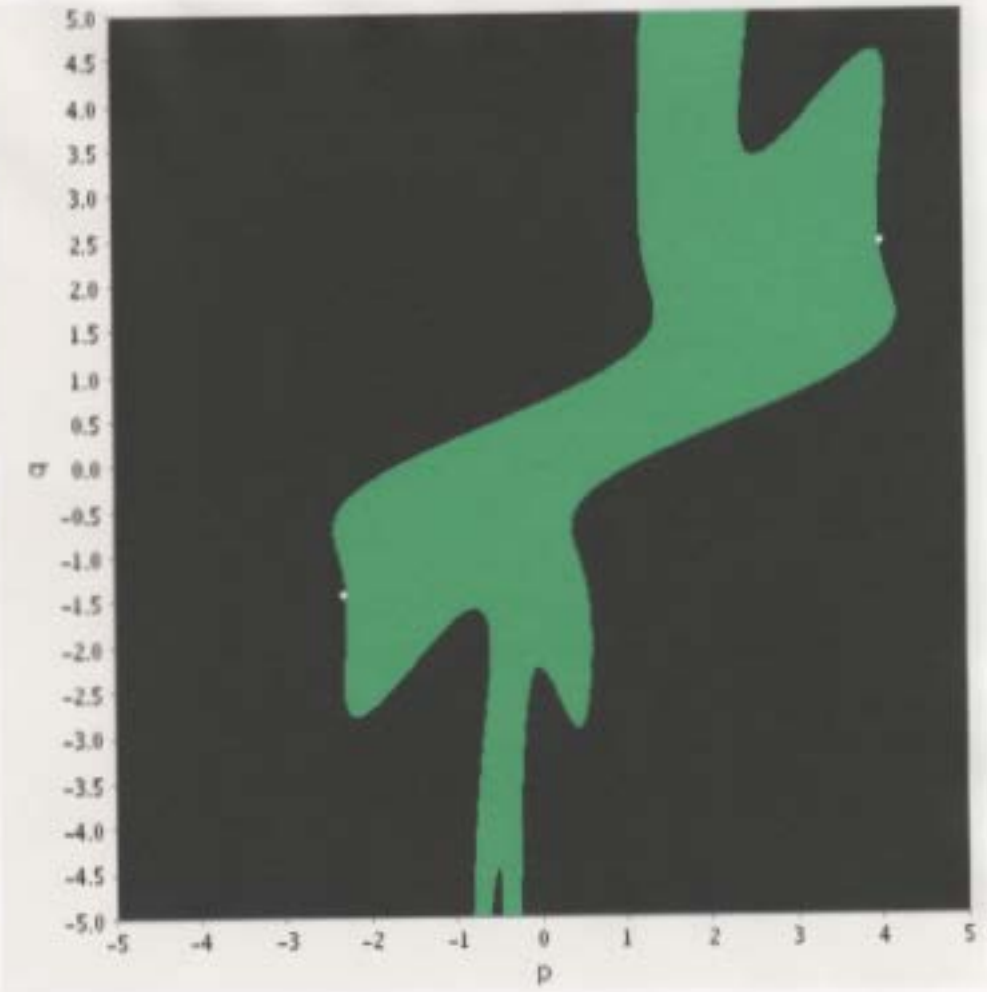

Figure 4.10: Basin Diagram ($c = 0.45$)

When $0.24 < c < 0.48$, various saddle–node bifurcations in several periods occur. For instance, at $c \approx 0.413$, a saddle–node bifurcation in period–3 occurs, in period–4 at $c \approx 0.477$, in period–5 at $c \approx 0.465$, etc. Each of these saddle–node bifurcations creates a locally stable cycle and an unstable cycle, and each typically undergoes a period–doubling cascade to chaos. Each of these generates an attractor (A_n) which is stable for a small set of initial conditions located far from the origin.

As c increases through $c \approx 0.48$ a Neimark–Sacker bifurcation occurs. This bifurcation occurs earlier than in (1.3.12). Although the orbit diagram corresponding to this case of the model appears less complicated than that of 1.3.12, some of the behaviour is similar, while some new behaviour is also observed.

When $0.48 < c < 0.5151$, prices are mainly switching between values of a limit cycle. The limit cycle corresponding to $c = 0.485$ is given in Figure 4.11.

When $c \approx 0.5151$, a saddle–node bifurcation in period–9 occurs. This creates a locally stable period–9 cycle and an unstable period–9 cycle. The limit cycle becomes a "transient" where its stability is replaced by that of the stable period–9 cycle. A close–up of this region of the orbit diagram is given in Figure 4.12.

For $0.5151 < c < 0.5172$ prices are tending to these nine values. When $c \approx 0.5172$, a Neimark–Sacker bifurcation in period–9 occurs. Thus, prices are tending toward values of nine limit cycles, with a single orbit visiting all nine of the limit cycle "islands." These limit cycles are shown in Figure 4.13. Since the amplitudes of the limit cycles are small, price movement will appear similar to that of a period–9 cycle.

When $c \approx 0.5182$ a saddle–node in period–36 occurs on the period–9 limit

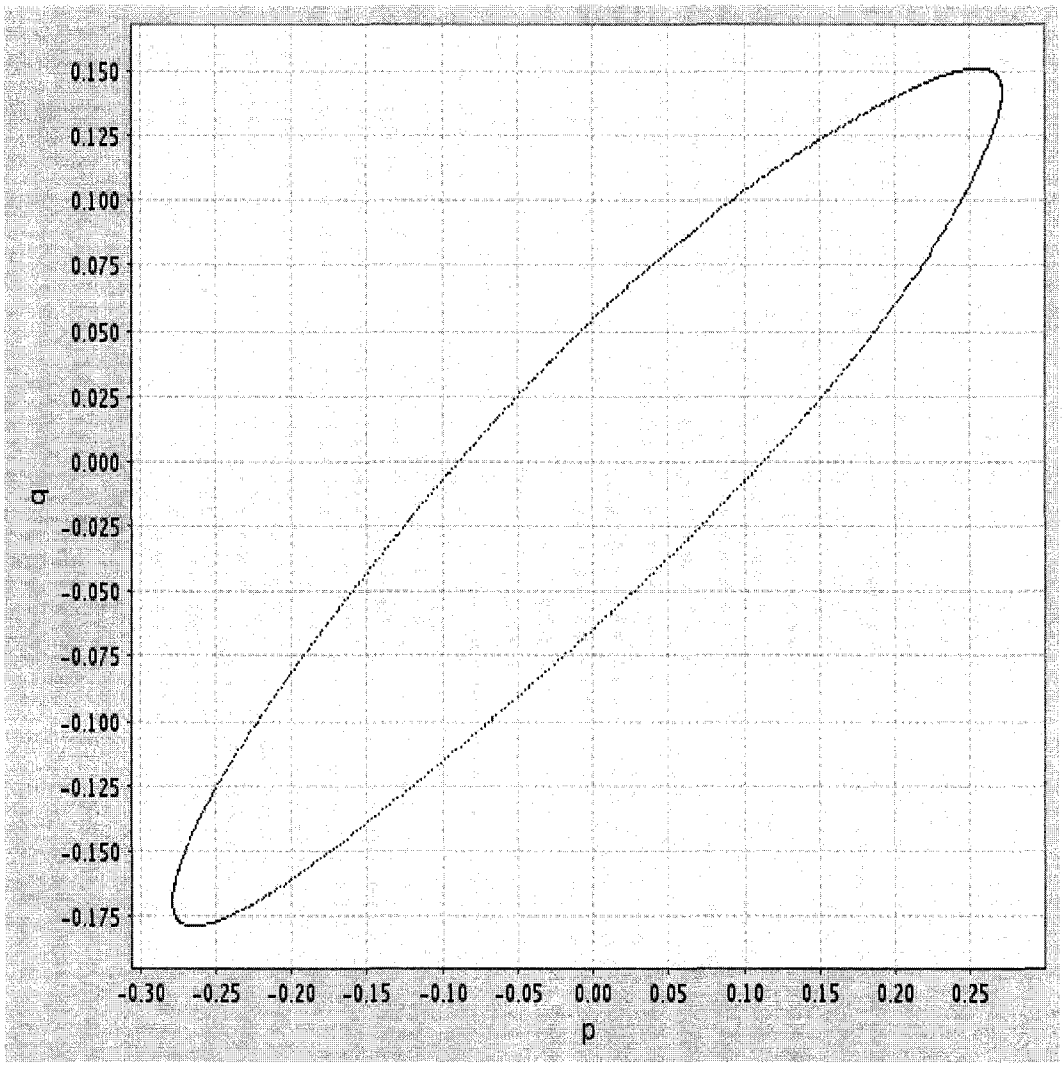

Figure 4.11: Trajectory ($c = 0.485$)

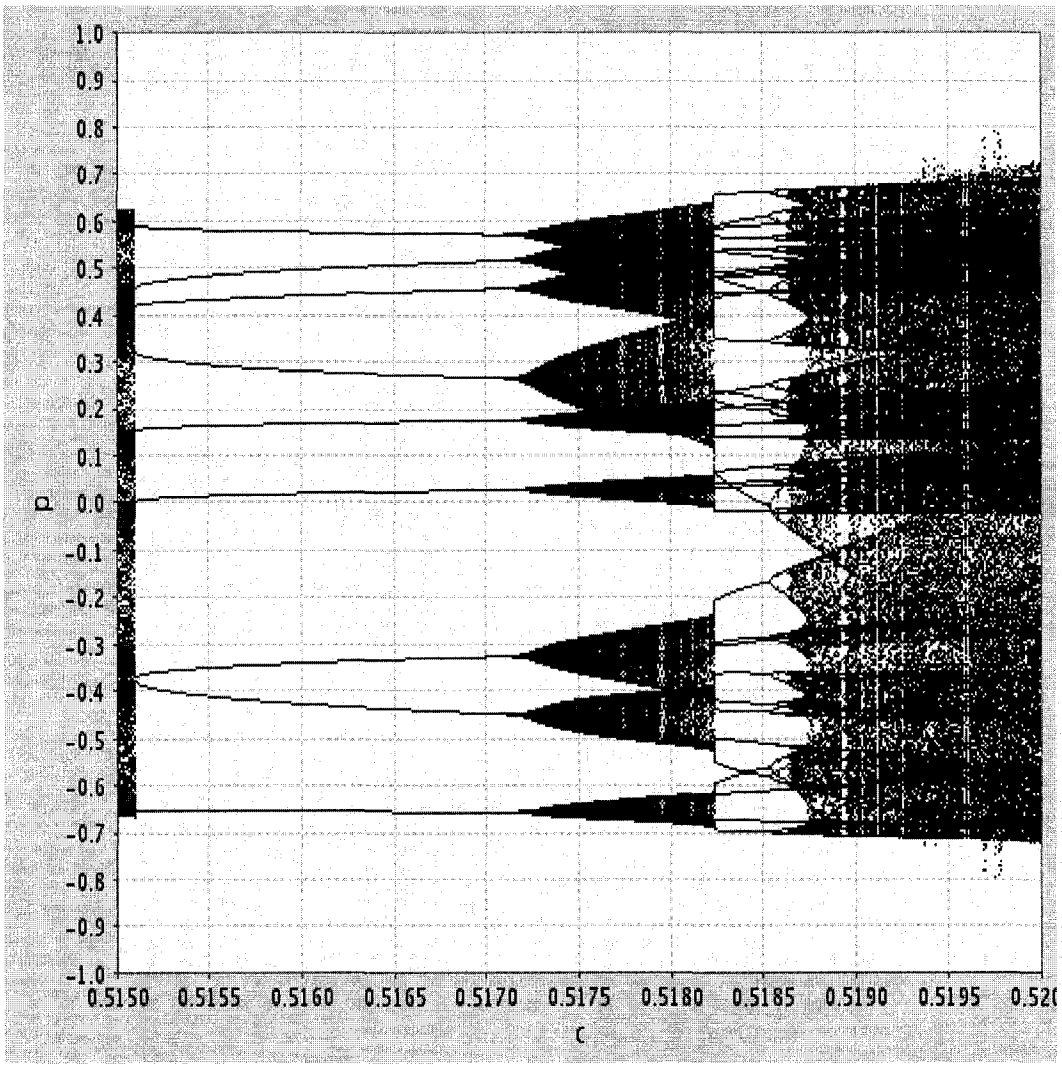

Figure 4.12: Orbit Diagram ($0.515 < c < 0.52$)

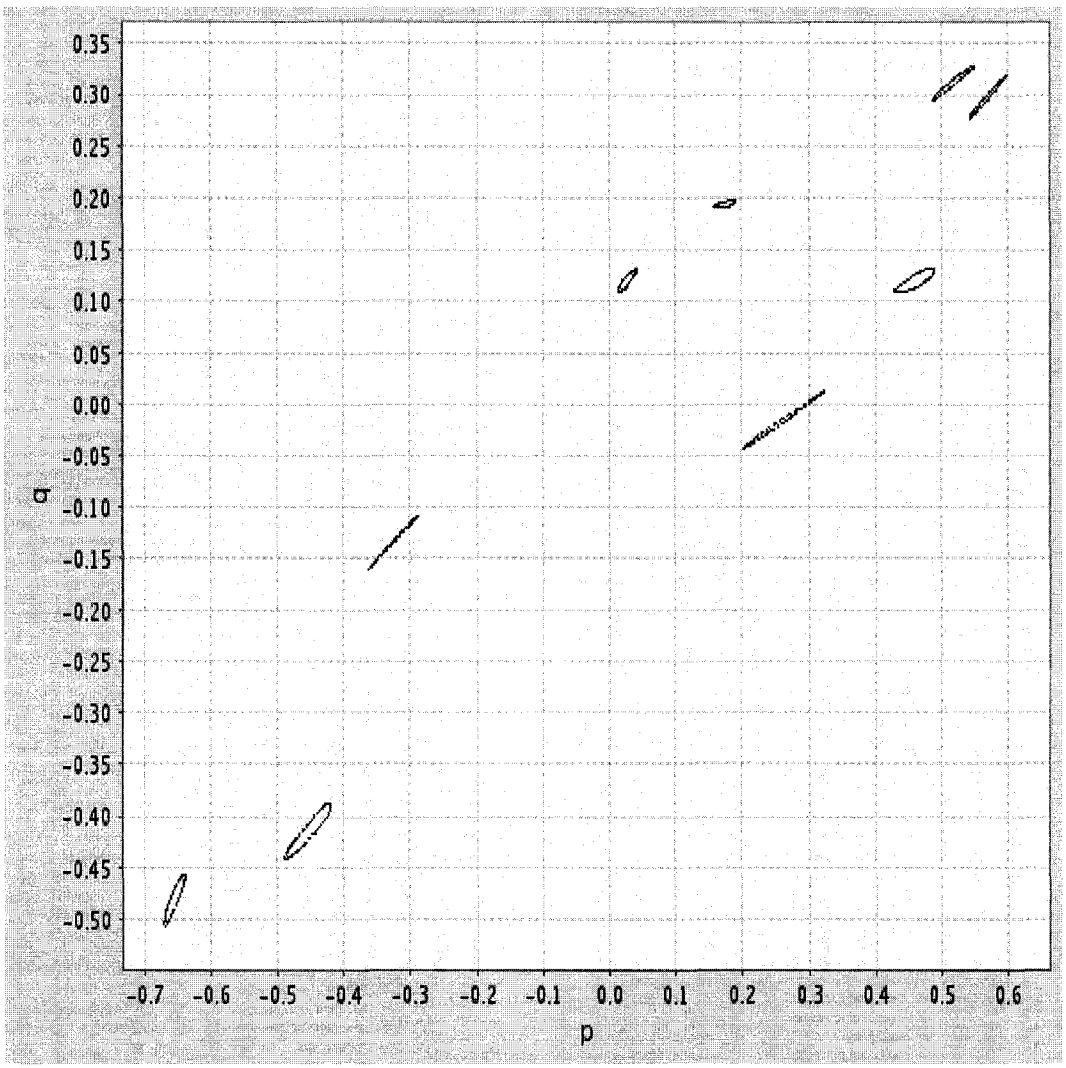

Figure 4.13: Trajectory – Neimark–Sacker bifurcations in Period–9 (c = 0.5175)

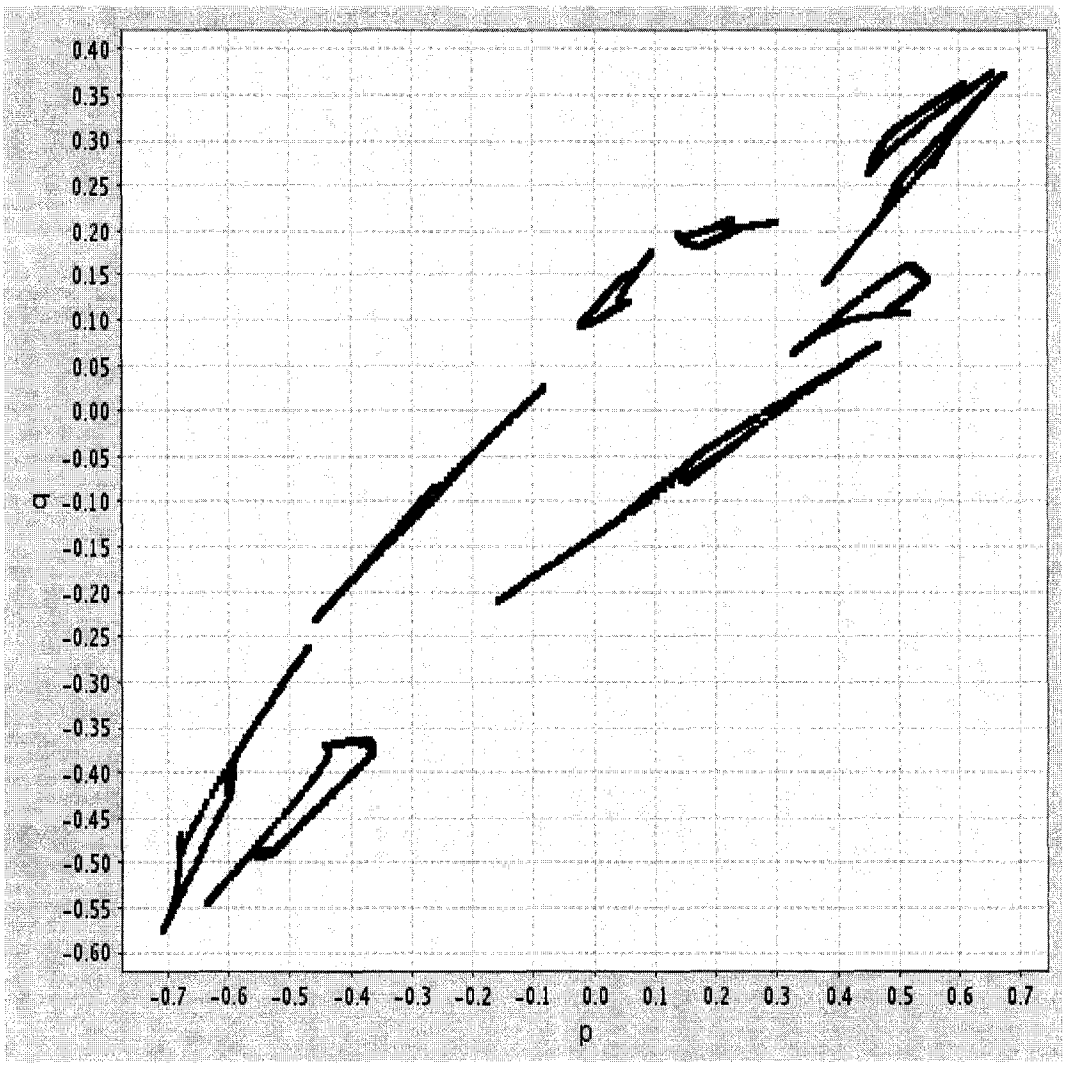

Figure 4.14: Chaotic Attractor (after interior crisis) ($c = 0.519$)

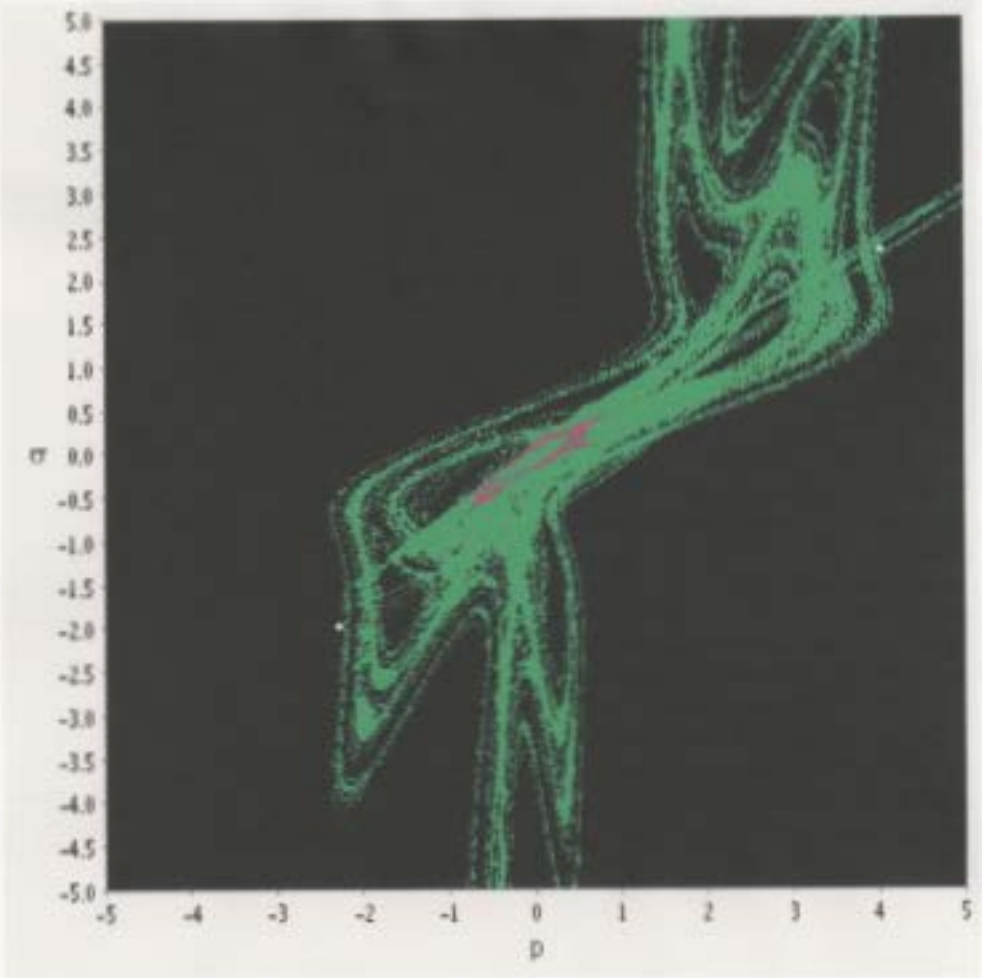

Figure 4.15: Basin Diagram ($c = 0.520283$)

The basin for the chaotic attractor is shown in green, the basin for infinity is shown in black, and the unstable period–2 cycle is shown in white. and the unstable period–2 cycle is shown in white.

cycle, creating a locally stable period–36 cycle and an unstable period–36 cycle. This bifurcation is evident from Figure 4.12. Thus, prices are now tending toward values in the period–36 cycle, causing the period–9 limit cycle to become a transient. The locally stable period–36 cycle period doubles, and a period–doubling cascade to chaos is observed (Figure 4.12). This chaotic attractor is labelled A_{36}.

As c increases through $c \approx 0.5187$ an interior crisis occurs where the unstable period–36 cycle collides with the chaotic attractor A_{36} causing A_{36} and the previous limit cycle attractors to merge into a single chaotic attractor. This attractor is shown in Figure 4.14.

Finally, when $c \approx 0.5203$, a boundary crisis occurs where the chaotic attractor shown in Figure 4.14 collides with the unstable period–2 cycle created from the initial subcritical period–doubling bifurcation. This is shown in Figure 4.15.

4.6.2 $a = 1.5$, $\beta = 1.5$

A final version of Case 2 is discussed with the following parameter values: $a = 1.5$, $\beta = 1.5$, $m = 2.3$, $\alpha = 2.3$. From Figure 4.16 it is obvious that the behaviour occuring when this particular parameter set is used is quite complicated, however the types of bifurcation sequence occuring in this version of the model are similar to those encountered in Chapters 3 and 4. We will focus on a small range of c values, when $c < 0.520$, and discuss the behaviour occuring in this region. The orbit diagram corresponding to $0.445 < c < 0.520$ is given in Figure 4.17.

A subcritical period–doubling bifurcation occurs at $c \approx 0.065$. This can

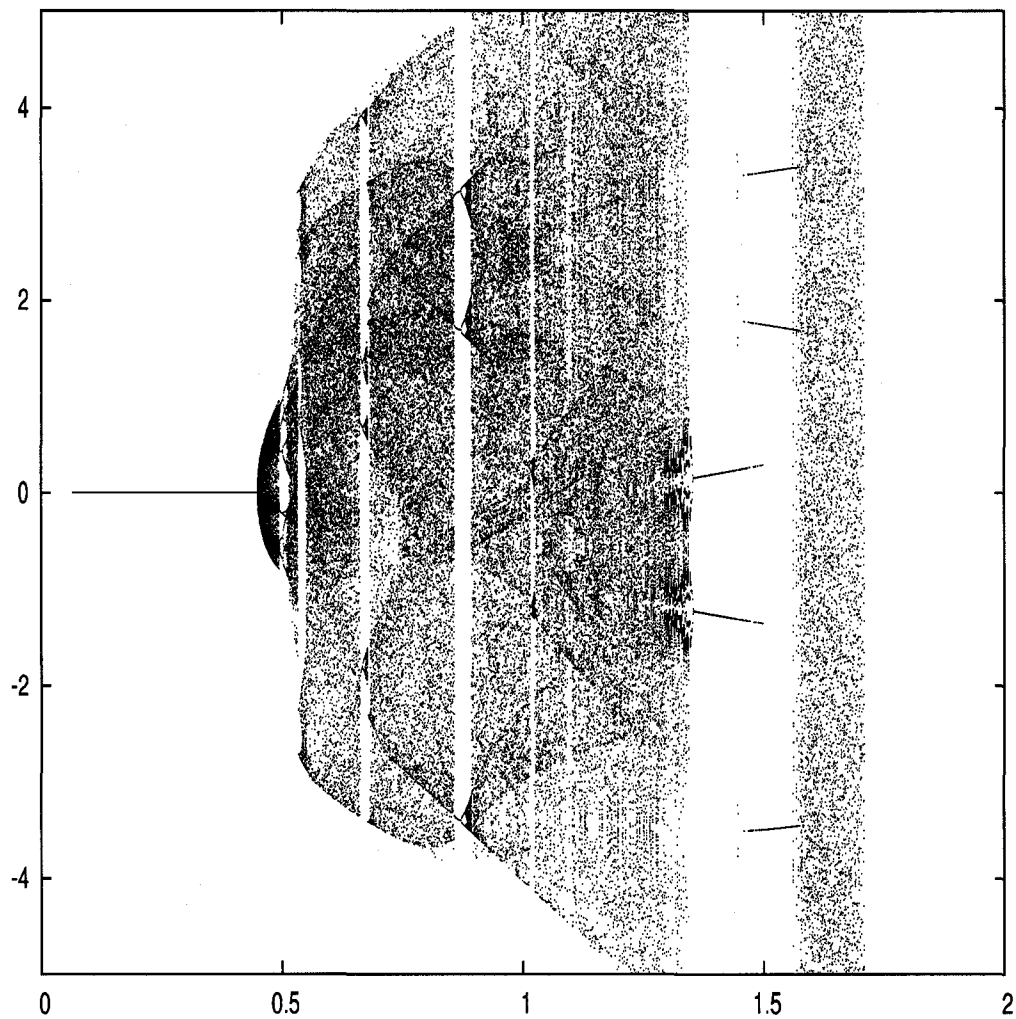

Figure 4.16: Orbit Diagram ($a = 1.5$, $\beta = 1.5$)

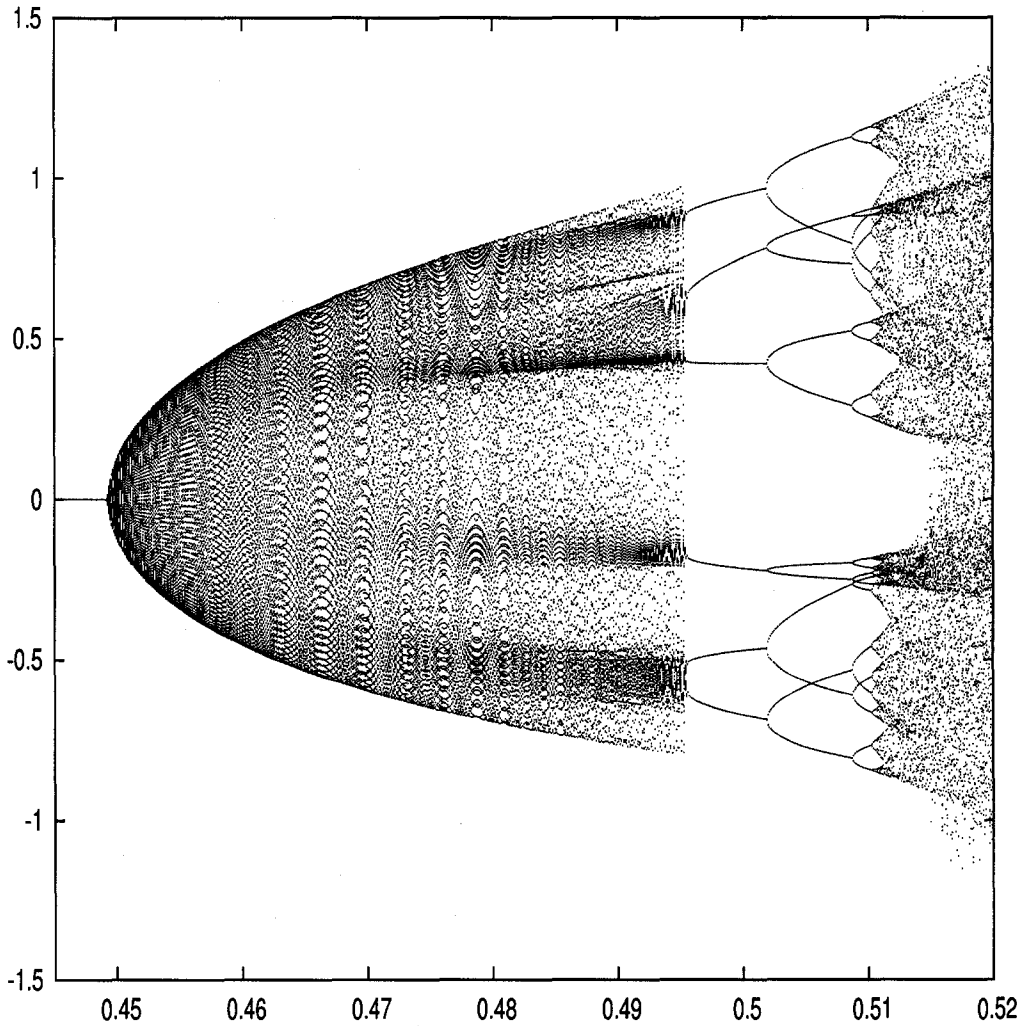

Figure 4.17: Orbit Diagram ($0.445 < c < 0.520$)

be shown using (4.4.8) or by looking at Figure 4.9. This creates a stable fixed point at the origin, and an unstable period–2 cycle. As in the other examples, when initial conditions are close to the origin, orbits will tend to the origin. Orbits from initial conditions far from the origin will tend to infinity.

When $c \approx 0.449$, a Neimark Sacker bifurcation occurs and prices tend to values in a limit cycle. This behaviour occurs for a range of c values, namely when $0.449 < c < 0.496$. When $c \approx 0.492$, a saddle–node bifurcation in period–4 occurs. This creates a locally stable period–4 cycle, and an unstable period–4 cycle. Hence, when $0.492 < c < 0.496$, the period–4 cycle co–exists with the limit cycle. This can be seen in Figure 4.18 when $c = 0.495$.

When $c \approx 0.496$, a saddle–node bifurcation in period–6 occurs on the limit cycle, creating a stable period–6 cycle and an unstable period–6 cycle, and a "window" in the limit cycle attractor. This can be seen in Figure 4.17. Similar to Section 4.6.1, the limit cycle becomes a transient, where its stability is replaced by that of the stable period–6 cycle. The stable period–6 cycle period–doubles and undergoes a period–doubling cascade to chaos. This chaotic attractor is denoted A_6. At $c \approx 0.50640$ a saddle period–doubling bifurcation of the unstable period–6 cycle occurs from the previous saddle–node bifurcation, creating an unstable period–12 cycle and an unstable period–6 cycle.

When $c \approx 0.51484$, the chaotic attractor A_6 collides with the unstable period–12 cycle which was created from the saddle period–doubling bifurcation. This causes an interior crisis, where the chaotic attractor and the previous limit cycle attractor merge into a single larger chaotic attractor. This is shown in Figure 4.17. Figure 4.19 is a basin diagram showing the emergent chaotic

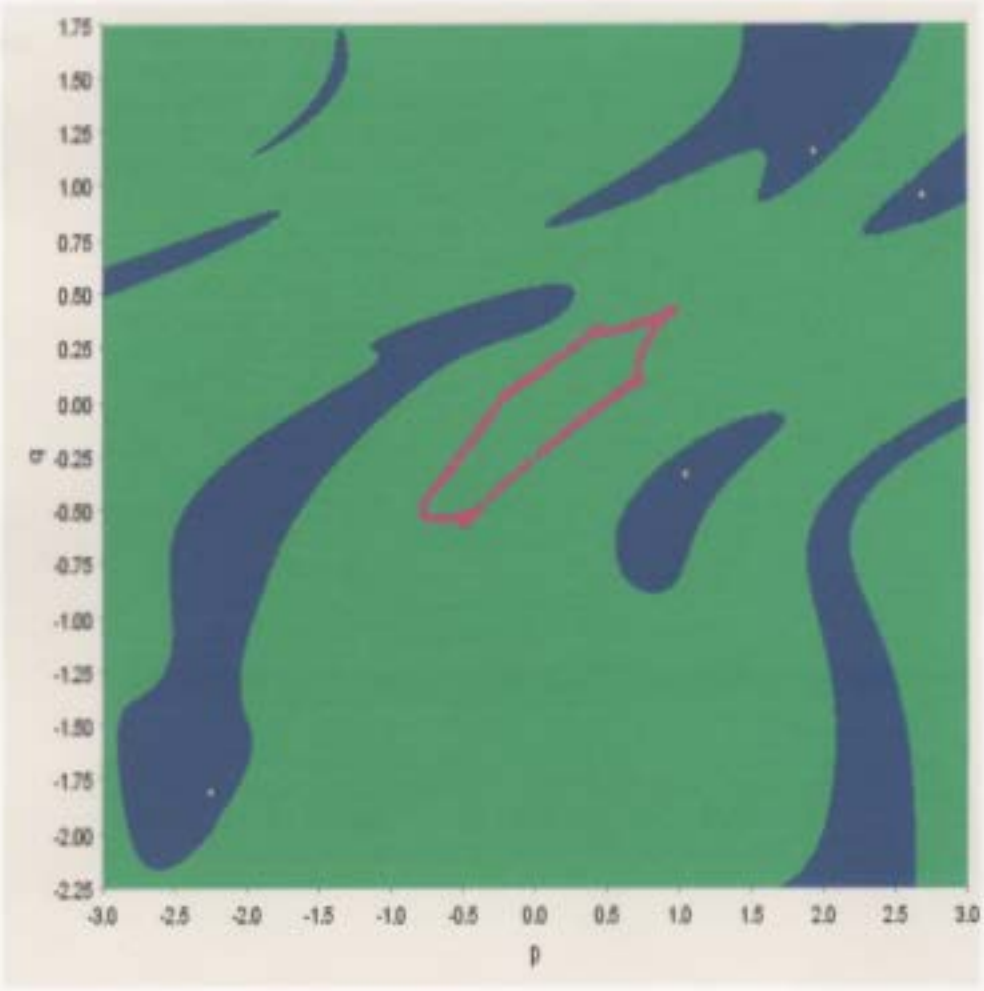

Figure 4.18: Basin Diagram ($c = 0.495$)

The basin for the limit cycle is given in green and the basin for the period–4 cycle is given in blue

attractor when $c = 0.516$, along with the local period–4 attractor which is still present.

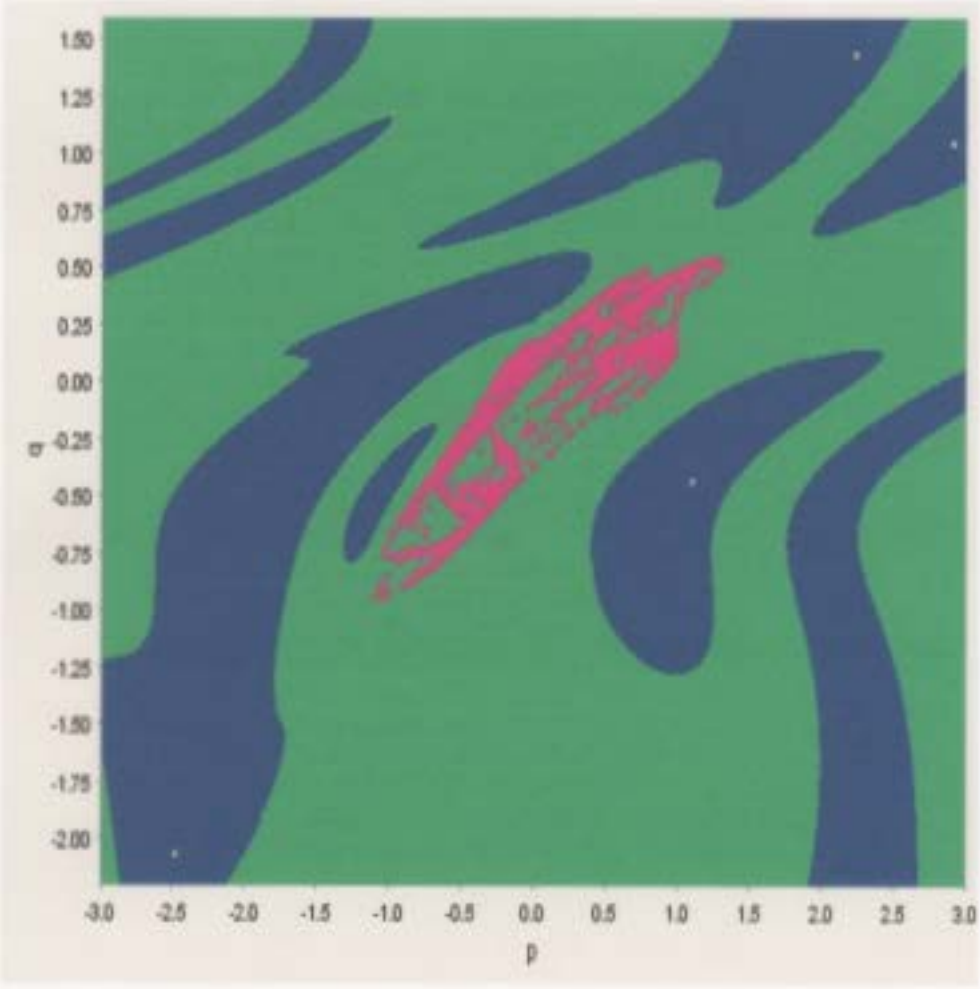

Figure 4.19: Basin Diagram ($c = 0.516$)
The basin for the chaotic attractor is given in green, and the basin for the period–4 cycle is given in blue

Chapter 5

Discussion

In this chapter, some of the main results and ideas of this thesis will be reviewed, and some final conclusions and future research plans will be given.

5.1 Summary and Conclusions

In this thesis, several dynamical systems models of asset pricing were discussed. These models consider heterogeneous beliefs among traders, and are much different from the CAPM and stochastic calculus based models in current use. Two basic trader groups are considered, fundamental traders and chartists.

The main focus was to create a different asset pricing model which considered fundamental traders and two types of chartists. The first type of chartist, called trend–chasing chartists, use trends of past price changes to predict future prices. The second type, called contrarian chartists, use the same ideas to go against the actions of trend–chasers. The model, which is an extension of [11], considers two cases. The first case deals with "pure" contrarians, or

those contrarians who always choose to go against the actions of trend–chasing chartists. When the majority of traders are buying, these contrarians are selling, and when the majority of traders are selling, they are buying. The second case deals with contrarians who, having access to the same information as all other traders, not only decide to go against the majority, but they also attempt to determine when to act on the disagreement in order to make a profit. Thus, they are not simply disagreeing, but rather are waiting for an opportunity to disagree when they believe prices are about to increase rapidly, or have been pushed to their maximum value.

In either case, the model is given in (4.4.3). However, the contrarian demand functions differ. In Case 1 of the model we have the trend–chaser demand function,

$$g_1(\gamma_{t,t+1} - b) = \alpha \arctan(\gamma_{t,t+1} - b),$$

and the contrarian demand function,

$$g_2(\gamma_{t,t+1} - b) = \mu \arctan(\gamma_{t,t+1} - b).$$

The following parameter values were used to analyze this case of the model: $a = 1.8$, $\beta_p = 1.8$, $b = 0.5$ and $\alpha = 2.3$, $\mu = -1.0$. With the given parameter set, the following conclusions regarding asset prices can be made:

1. When c is small, prices converge to their fundamental value.

2. As c increases, prices tend toward the values in a period–3 cycle for a small range of initial conditions. Due to period–doubling bifurcations prices tend toward values of a period–6 cycle, followed by a period–12 cycle, and so on, as c increases. Again, this is only true for a small range

of initial conditions. Otherwise, prices still converge to their fundamental value.

3. When $0.788 < c < 0.81813$ prices switch between values of a limit cycle from most initial conditions. The amplitude of the limit cycle starts out small so, although prices are tending toward values of a limit cycle, prices are hovering around the fundamental value. As c increases, a corresponding increase in the amplitude of the limit cycle occurs, and prices are tending away from the fundamental price.

4. As c continues to increase, the limit cycle behaviour disappears and prices now become chaotic. There is still a distinct range of possible price values. However, there is no determined pattern describing how prices jump from one value to another.

A second parameter set in case 1 is also examined. The parameter μ is set to $\mu = -1.5$. The results, in terms of asset prices, can be summarized as follows:

1. As before, prices tend to their fundamental value when c is small. As c increases, prices tend toward values in a period–3 cycle from certain initial conditions, and tend to the fundamental value from other initial conditions. The location of the period–3 cycle begins close to the origin, so prices are still hovering around the fundamental value, but moves away from the fundamental value as c increases.

2. Prices tend to the period–3 cycle from many initial conditions and to the values of a limit cycle when initial conditions are chosen to be near the

origin, as c continues to increase. The amplitude of the limit cycle is always extremely small, so prices are still hovering around the fundamental value when they are not tending to the period–3 cycle.

3. Prices eventually tend only toward the period–3 cycle as c increases to $c = 1$. Prices do not become chaotic as c increases, and generally stay close to the fundamental price, unlike other cases of the model. Thus, when pure contrarians are highly active in the market, prices typically stay close to their fundamental value, and price dynamics are much less complex. It appears in this case that fundamental traders may be most successful at predicting future prices.

In Case 2 of the model, we have that

$$g_1(\gamma_{t,t+1} - b) = \alpha \arctan(\gamma_{t,t+1} - b)$$

and

$$g_2(\gamma_{t,t+1} - b) = \frac{m(\gamma_{t,t+1} - b) - (\gamma_{t,t+1} - b)^3}{\sqrt{(\gamma_{t,t+1} - b)^6 + m^2}}.$$

The parameter set used in this case is $a = 1.8$, $\beta = 1.8$, $\alpha = 2.3$, $m = 2.3$, $b = 0.5$.

1. Prices tend to the fundamental value for small c values. As c increases, many cycles of varying periods occur, and hence prices are tending to these cycles from certain initial conditions, while still tending to the fundamental value from most initial conditions.

2. As c continues to increase, prices tend to the values in a limit cycle from many initial conditions, while they can still tend to these cycles from

other initial values. As before, the amplitude of the limit cycle starts out small, and as c increases, prices begin to drift from the fundamental value.

3. Prices no longer tend toward values of a limit cycle as c continues to increase, and instead prices switch between values of a period–9 cycle. As c increases slightly, the period–9 cycle dominates and prices are only switching between values of this cycle. These nine values change to nine limit cycles as c continues to increase. The amplitude of these limit cycles is small, so prices are still hovering around the period–9 cycle.

4. Eventually, prices tend toward values of a period–36 cycle, and ultimately, prices become chaotic through period–doubling bifurcations. Prices continue to experience chaos, but with a larger range of values, with the re–emergence of the previous limit cycle behaviour, combined with the chaotic attractor which is already present.

To summarize, two–parameter bifurcation diagrams have been created, shown in Figures 5.1, 5.2 and 5.3. The parameters which are varied in these diagrams are c (on the x–axis) and β (on the y–axis). From this diagram, we can give the location of the important local behaviour (period–doubling and Neimark Sacker bifurcations) occuring in (4.4.3), as well as the boundary crisis which is common to all cases of the model when c gets large. In these diagrams, the parameter a has been kept constant at $a = 1.8$. The black region denotes all of those orbits which go to infinity, the red region denotes those regions where local fixed point behaviour is occuring, and the white region is where the global bifurations and chaos occur. The boundary of the black

and red regions is where the subcritical period–doubling bifurcation occurs for any β and c value in the given ranges. The boundary of the red and white regions is where the Neimark–Sacker bifurcation occurs for any choice of β and c. Finally, the boundary of the white and black regions is where the boundary crisis, caused by the collision of the chaotic attractor with the unstable period–2 cycle, occurs for a choice of β and c values.

5.2 Future Research

There are certain aspects of this modelling approach that were not covered in this thesis. For instance, these models were not tested against actual data. Thus, although they have the capacity to describe complex markets, no tests have been performed to determine their accuracy. In the future, we plan to look at testing several of these models to determine if they accurately describe certain markets. To do this, in depth research on the numerical values for the parameters used in these models must be carried out. Once we are confident that our parameter values are reliable, the behaviour of the models with this certain parameter set can be explored and tested against real markets.

A second future research topic we will consider is if this modelling approach is suitable for derivative assets. Several stochastic models are currently being used to model such assets. The Black–Scholes option pricing model, for instance, is one of the most popular tools for pricing derivative assets, such as European and American call options. We will take a closer look at derivative assets and the possibly of using a dynamical systems approach to determine the value of a derivative asset from time $t = 0$ to maturity.

Figure 5.1: Two Parameter Bifurcation Diagram (Case 2)

Figure 5.2: Two Parameter Bifurcation Diagram (Case 1 – $\mu = -1.0$)

Figure 5.3: Two Parameter Bifurcation Diagram (Case 1 – $\mu = -1.5$)

Finally, another goal for the future is to expand on (4.4.3) to incorporate even more trader groups. In real markets, traders have many different schemes for estimating future asset prices. In this thesis, the contrarian approach to asset pricing was studied, and this group was included in an asset pricing model which already acocunted for fundamental traders and trend–chasers. With more study, other trader behaviours could also be incorporated into dynamical systems models, such as the one given in (1.3.12) or (4.4.3). As well, in [12], the fraction of each trader group existing in the markets at a particular time t was investigated. This is very important in accurately describing market behaviour. However including this into (4.4.3) may make the model less mathematically tractable, and it will also introduce new parameters into the model. Numerical estimates for these new parameters will also have to found. A closer look at trader groups, and the fraction of each trader group existing in the market over time, is indeed an area of interest for future research.

Bibliography

[1] Bjork, T. S. (2004). *Arbitrage Theory in Continuous Time* (2nd edn.). Oxford University Press, New York.

[2] Black, F. (1972). Capital market equilibrium with restricted borrowing. *Journal of Business*, **45**, 444-455.

[3] Black, F., and Scholes, M. (1973). The pricing of options and corporate liabilities. *Journal of Political Economy*, **81**, 637-654.

[4] Brock, W. A. and Hommes, C. H. (1998). Heterogeneous beliefs and routes to chaos in a simple asset pricing model. *Journal of Economic Dynamics and Control*, **22**, 1235-1274.

[5] Brock, W. A. and Hommes, C. H. (1997). A Rational Route to Randomness, *Econometrica* **65**, 1059-1095.

[6] Brock, W. A. and Hommes, C. H. and Wagener, F. (2005). Evolutionary dynamics in markets with many trader types. *Journal of Mathematical Economics*, **41**, 7-42.

[7] Chiarella, C. (1992). Developments in Nonlinear Economic Dynamics: Past, Present and Future. In: *Die Zukunft der Okonomischen Wissenschaft* (Hanusch, H.), Verlag Wirtschaft und Finanzen.

[8] Chiarella, C., Dieci, R. and Gardini, L. (2003). A Dynamic Analysis of Speculation Across Two Markets. Research Paper Series 89, Quantitative Finance Research Centre, University of Technology, Sydney.

[9] Chiarella, C., Dieci, R. and Gardini, L. (2002). Price Dynamics and Diversification Under Heterogeneous Expectations. Computing in Economics and Finance 88, Society for Computational Economics.

[10] Chiarella, C., Dieci, R. and Gardini, L. (2002). Speculative behaviour and complex asset price dynamics. *Journal of Economic Behaviour and Organization*, **49**(1), 173-197.

[11] Chiarella, C., Dieci, R. and Gardini, L. (2001). Asset Price Dynamics in a Financial Market with Fundamentalists and Chartists. *Discrete Dynamics in Nature and Society*, **6**, 69-99.

[12] Chiarella, C., He, H. Z. (2002). Heterogeneous Beliefs, Risk, and Learning in a Simple Asset Pricing Model. *Computational Economics*, **19**, 95-132.

[13] Chiarella, C. and He, H. Z. (2003). Heterogeneous Beliefs, Risk, and Learning in a Simple Asset Pricing Model with a Market Maker. *Macroeconomic Dynamics*, **7**(4), 503-536.

[14] Chiarella, C. and He, H. Z. (2002). An Adaptive Model on Asset Pricing and Wealth Dynamics with Heterogeneous Trading Strategies. Re-

search Paper Series 84, Quantitative Finance Research Centre, University of Technology, Sydney, Australia.

[15] Chiarella, C., Gallegati, M., Leombruni, R. and Palestrini, A. (2002). Asset Price Dynamics among Heterogeneous Interacting Agents. *Computational Economics*, **22**, 213-223.

[16] Chiarella, C. and He, H. Z. (2001). Asset price and wealth dynamics under heterogeneous expectations. *Quantitative Finance*, **1**, 509-526.

[17] Devaney, R. L. (1989). *An Introduction to Chaotic Dynamical Systems* (2nd edn.). Addison Wesley, Redwood City, California.

[18] Ermentrout, B., (2002). *Simulating, Analyzing, and Animating Dynamical Systems: A Guide To XPPAUT for Researchers and Students.* Society for Industrial and Applied Mathematics.

[19] Fama, E. F. and French, K. R. (1992). The Cross–Section of Expected Stock Returns. *Journal of Finance*, **47**(2), 427-465.

[20] Fernandez, P. (2002). *Valuation Methods and Shareholder Value Creation.* Academic Press, Amsterdam.

[21] Gallea, A. M. and Patalon, W. (1998). *Contrarian Investing.* New York Institute of Finance, New York.

[22] Grebogi, C., Ott, E., Yorke, and J. A. (1983). Crises, Sudden Changes in Chaotic Attractors, and Transient Chaos. *Physica D*, 181-200.

[23] Griffiths, D. F., Higham, D.J. (1997). *Learning LaTeX.* Society for Industrial and Applied Mathematics, Philadelphia.

[24] Hale, J. and Koçak, H. (1991). *Dynamics and Bifurcations.* Springer–Verlag, New York.

[25] Harold, J.B., (1993). *Chaotic Mapper: User's Manual.* American Institute of Physics, New York.

[26] Kuznetsov, Y. A. (1995). *Elements of Applied Bifurcation Theory.* Springer–Verlag, New York.

[27] Lintner, J. (1965). The valuation of risky assets and the selection of risky investments in stock portfolios and capital budgets. *Review of Economics and Statistics*, **47**, 13-37.

[28] Markellos, R. N. and Mills, T. C. (2003). Asset Pricing Dynamics. *The European Journal of Finance*, **9**, 533-556.

[29] Medio, A. and Lines, M. (2001). *Nonlinear Dynamics: A Primer.* Cambridge University Press, Cambridge, U.K.

[30] Meyer, M. (2001). *Continuous Stochastic Calculus with Applications to Finance.* Chapman & Hall/CRC, Florida.

[31] Ott, E. (2002). *Chaos in Dynamical Systems* (2nd edn.). Cambridge University Press, Cambridge.

[32] Roll, R., (1977). A critique of the Asset Pricing Theory's Tests: Part I: On past and Potential Testability of Theory. *Journal of Financial Economics*, **4**, 129-176.

[33] Ross, S. A., Westerfield, R. W., Jaffe, J. F., Roberts and G. S. (2003). *Corporate Finance* (3rd Canadian edn.). McGraw–Hill Ryerson, Toronto.

[34] Sharpe, W.F. (1964). Capital asset prices: A theory of market equilibrium under conditions of risk. *Journal of Finance*, **19**, 425-442.

[35] Sydsaeter, K., Strom, A. and Berck, P. (1999). *Economists' Mathematical Manual* (3rd edn.). Springer–Verlag, Berlin.

[36] Westerhoff, F. H. (2005). Heterogeneous Traders, Price-Volume Signals, and Complex Asset Price Dynamics. *Discrete Dynamics in Nature and Society*, **2005**, 19-29.